TURBULENT FLOW OF IRON ORE-WATER SUSPENSIONS

TURBULENT FLOW OF IRON ORE-WATER SUSPENSIONS

BY

JORGE N. CARDENAS

A Thesis

Submitted to the Faculty of Graduate Studies

in Partial Fulfilment of the Requirements

for the degree

Master of Engineering

McMaster University

September 1971

Master of Engineering (1971) McMaster University

(Chemical Engineering) Hamilton, Ontario

TITLE: Turbulent Flow of Iron Ore-Water Suspensions

AUTHOR: Jorge N. Cardenas
Q.I. Universidad Technica Del Estado (Chile)

SUPERVISORS: Dr. M.H.I. Baird
Dr. G.F. Round

NUMBER OF PAGES: vi, 115

SCOPE AND CONTENTS:

This thesis describes the behaviour of iron ore-water suspensions under turbulent flow conditions.

This work is divided into two parts. Part I deals with the regimes of transport under steady state flow conditions in circular and horizontal ducts. The heterogeneous flow regime is extensively analyzed; a sequential discrimination of models with an oriented design of experiments have permitted the determination of the best model to correlate hydraulic gradients for these suspensions. A critical discussion on the limit deposit conditions is also included.

Part II describes the behaviour of clear water under oscillatory flow conditions. The study demonstrates that the quasi-steady state hypothesis, i.e., fully developed flow assumption, applied to pulsatile turbulent flow under the conditions studied. Observations on the behaviour of iron ore-water suspensions under pulsatile flow are also included. The experiments were carried out using a new air-pulsing technique.

ACKNOWLEDGEMENTS

The author expresses his sincere gratitude to his supervisors, Dr. M.H.I. Baird and Dr. G.F. Round. Their interest, enthusiasm and stimulating sense of "what should be looked at" was complemented by a good measure of direction and encouragement.

The author is particularly indebted to the Government of Chile and the Inter-American Development Bank for providing financial support during these studies.

The careful and conscientious work of typing this thesis by Miss Charlotte Traplin is gratefully appreciated.

Finally, the author expresses his acknowledgements to all those who indirectly contributed to this work.

TABLE OF CONTENTS

TABLE OF CONTENTS

FIGURE INDEX

PART I STEADY STATE FLOW STUDIES

1.1 INTRODUCTION

Many industrial processes and natural phenomena involve some form of solid-liquid interaction. The understanding of these interactions is basic to the control of these systems.

Solids movement through pipelines is now a commercial reality and has some advantages over other forms of overland transportation. These are: continuous operation, immunity to adverse weather conditions and relatively low capital and operating costs per unit mass transported. The first part of this thesis deals with one of the main factors which must be considered in the optimization of a solids pipeline design, i.e., the energy requirements for slurry flow under steady state conditions. The main emphasis is focused on the study of the heterogeneous flow regime, because this regime is normally identified with economical operation, that is to say, the amount of material transported per unit power consumption is at a maximum. Due to its importance, great research effort has ben concentrated in this regime, but unfortunately no generally accepted criterion to describe head loss under various flow conditions within this regime has yet been established as the following analysis of this thesis will show. For this reason, the author has carried out a statistical discrimination between the most-used models which describe this regime using the Bayes theorem, and a design of experiments using the Roth criterion for the optimal choice of experimental conditions, on the basis that this is the best strategy for efficient experimentation.

All tests were carried out with aqueous slurries of hematite (size passing 30 mesh and specific gravity 5.17) in concentrations of solid up to 25% by volume.

1.2 BASIC ASPECTS

Two phase solid-liquid flow has been analyzed theoretically and experimentally by many investigators, and most of these investigations are concerned with the pressure drop of the two phase flow in a pipe using the same methods as in ordinary hydraulic research, that is, of one-dimensional treatment with simple assumptions regarding the flow pattern. However, general conclusions on this subject have not been obtained, because the nature of this flow depends on many complicated factors such as particle size, particle form, concentration, pipe diameter, density of solid and fluid, flow velocity and so on. Nardi (1959) has indicated eight physical characteristics of the solids, ten physical characteristics of the slurry and about fourteen factors in the design data, all of which should be considered in the design of a slurry pipeline.

The theoretical study of the behaviour of a particle in turbulent flow poses immense difficulties. Ayukawa (1968) et.al. indicate that the motion of a solid particle in a pipe is governed by a drag force caused by the difference of velocity between fluid and the particle, a friction force at the pipe wall, a gravitational force, a force resulting from collisions of particles or between a particle and the wall, and a lift force caused by asymmetry of pressure distribution on the surface of the particle. Because the ratio of the density of solid to that of water is in general comparable with unity, these forces have about equal significance in determining the motion of a particle. On the other hand, the physico-chemical forces acting between pairs of particles also depend on particle size and shape but, more important, they arise because of the electro-chemical nature of the particle surface, the chemical environment in the suspending liquid and the physical interaction arising out of collisions of two or more particles. It is outside the scope of the present thesis to detail the exact nature of the inter-particle forces, except to mention that they vary from material to material and are very sensitive to small changes in ionic and surfactant concentrations in the liquid surrounding the particles. While it is convenient to distinguish between the factors considered above, in practice, further interactions between them are possible. Thus, a large particle may be supported by the mass of smaller particles held together by the inter-particle forces as if it were a homogeneous flow. Or the aggregates of particles, flocculated by the interparticle forces, will immobilize the suspending liquid within the flocs and the electrical double layer outside, and behave as larger particles. And again, when the relative velocities between the liquid flow and particle movement are large, the drag and lift experienced by the particles may overcome the gravitational pull and suspend the particles which would otherwise settle.

Therefore, each particle moves along very complicated trajectory with mutual interferences, and the pressure drop may be affected by these circumstances. Only a small number of significant contributions to this theoretical problem appear to have been made since the pioneering studies of Tchen (1947). Whether the solution has been via analytical, numerical or stochastic methods it has generally been necessary to make numerous simplifying assumptions, which may be unrealistic in many practical situations involving the transport of solids.

In view of the immense difficulties, it is customary to resort to alternative semi-empirical theories in order to model slurry behaviour. This aspect is discussed in the following sections of this thesis.

1.3 REGIMES OF MOTION OF PARTICLES IN HYDRAULIC CONVEYING

From the point of view of behaviour during flow, solid-liquid mixtures may be divided into two groups. Some mixtures can be transported successfully even in laminar flow without appreciable deposition of solid on the pipe bottom. On the other hand, there are mixtures from which solid particles separate rapidly unless the flow is highly turbulent. It is convenient to refer to the mixtures in these two groups as "non-settling" and "settling" mixtures or slurries.

According to Brebner (1962), mixtures with low settling velocities of the order of roughly 0.005 feet per second behave as "non-settling" pseudo homogeneous fluids at almost all velocities, whereas mixtures with settling velocities greater than the mentioned value behave as "settling" mixtures. Williams (1953) and other authors have noted that "non-settling" mixtures with particle diameters less than 10 microns exhibit a clear non-Newtonian behaviour. The behaviour of these "non-settling" mixtures will not be considered further here: information concerning them is given by Gay (1969).

The present thesis deals with the flow in horizontal pipes of "settling" mixtures. Because of the interaction between the tendency of the solid particles in a "settling" mixture to settle out and the drag and lift exerted by the flowing liquid on them, four different flow patterns are possible in horizontal pipes. These are shown in Figure (1.1), where a plot of the hydraulic gradient versus the mean flow velocity,

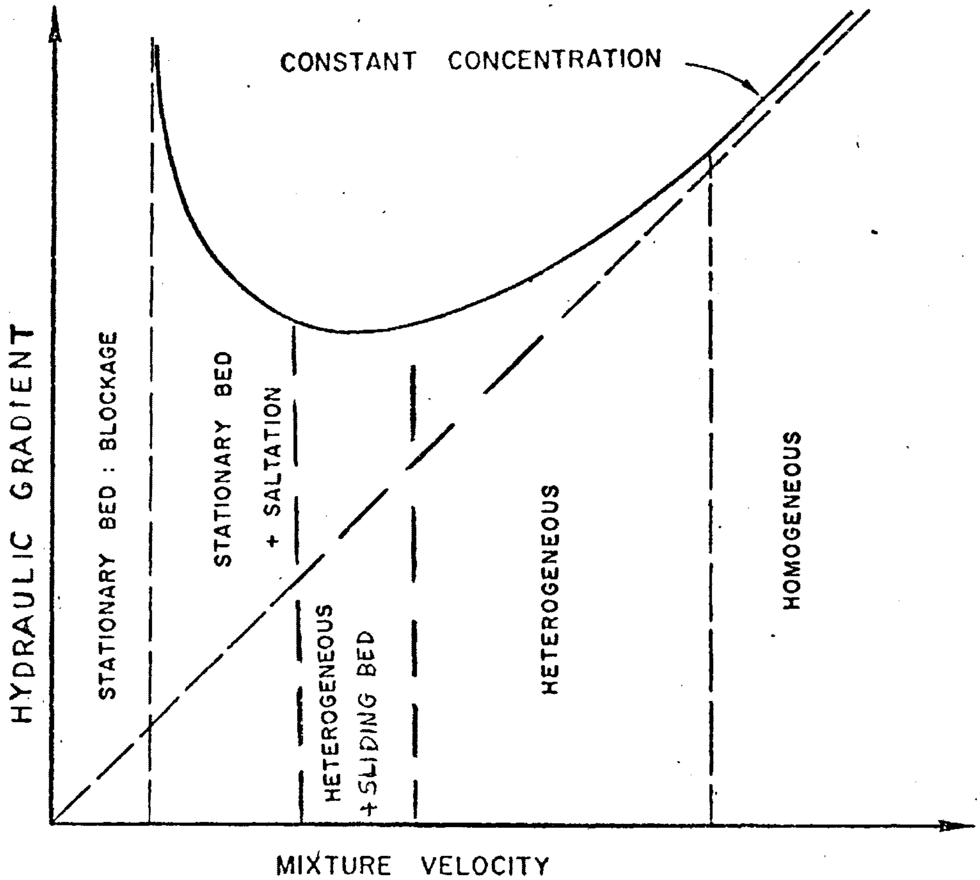

Fig. 1.1 Typical head loss curve. Modified from Brebner (1962).

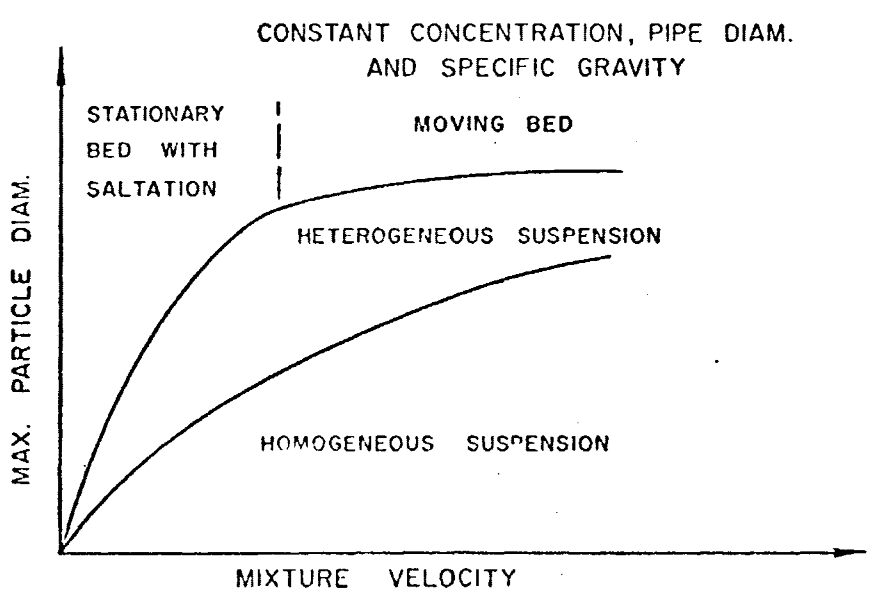

Fig. 1.2 Flow regimes for a given system after Durand. Modified from Brebner (1962).

on double logarithmic paper, yields a straight line, in pure water for a pipe with the same relative roughness in the turbulent flow regime. When the hydraulic gradient obtained with a liquid-solid mixture of a given concentration is plotted on Figure (1.1), the divergence decreases as the transportation velocity decreases. Or, in other words, for a given particle size and concentration, a certain flow velocity of the mixture is necessary to assure flow. But the flow of the mixture takes place in various forms, as shown in Figure (1.1). At very high velocities the solid particles can be more or less uniformly mixed with the carrier liquid and this results in a "homogeneous" flow pattern; thus, the vertical distribution of solid particles is nearly uniform. At somewhat lower velocities the vertical particle concentration gradient is not uniform, but all solids are in suspension. This flow pattern is termed "heterogeneous" suspension and this is probably the most important regime of hydraulic conveying because it is normally identified with economical operation. At still lower velocities, some of the solid particles move as a sliding bed on the bottom of the pipe. This flow pattern is termed "sliding bed with heterogeneous suspension". At still lower velocities, part of the pipe area is occupied by solid particles which do not move. Above these, there may be particles which slide, although most of the solid movement is by saltation. This flow pattern is termed "stationary bed with saltation" and will not be discussed in this thesis because it is essentially a rigid boundary problem not pertinent to solid transportation in pipes. The relative extent of each of these flow regimes in any pipeline flow situation depends on many factors such as particle size, particle form, concentration, pipe diameter, density of fluid and solid, flow velocity, configuration of pipes and so on; however, the solid-fluid flow interactive mechanisms are sufficiently different from regime to regime that this classification is really justified.

Durand (1952) proposed a classification of solid-liquid mixtures based on the particle size. Mixtures with particles less than 25 microns were considered intermediate; and particles greater than 50 microns, heterogeneous. The variation of flow characteristics with particle size and mean velocity are shown diagrammatically in Figure (1.2).

1.3.1 THE HOMOGENEOUS FLOW REGIME

Zandi (1968) has indicated that this type of flow occurs when solid particles are fine and light, or the mean velocity of the flow is high enough to keep the particles uniformly in suspension throughout the pipe cross-section. The mixture usually, but not necessarily, exhibits a shear stress-shear strain relationship different from that of the conveying liquid. When water is used as the conveying fluid, the behaviour of the slurry may become non-Newtonian, as indicated by Clarke (1967). This non-depositing, non-stratified flow is encountered in the transport of many materials as indicated by Metzner (1964), Newitt (1962), Durand (1953), etc.

However, the homogeneous regime comes into being as the result of the combination of particle size, solid and liquid densities, and the mean velocity of the flow. The only criterion is the uniformity of solids' distributions in the cross-section of pipe. Newitt (1955) proposed the following relationship for this regime,

$$\frac{1800\ g\ D\ w}{U^3} > 1 \tag{1.1}$$

where g is the acceleration of gravity in ft./sec.^{2}, D is the diameter of the pipe in feet, w is the free settling velocity of particles in ft./sec., and U is the mean velocity of suspension in ft./sec. Unfortunately, this criterion has not been tested extensively against experimental work, therefore it should be used only as a guideline rather than a hard and fast rule.

The homogeneous flow may be further subdivided into those regimes in which the particle-liquid interactions do not alter the rheological properties of the conveying liquid, and those in which it does. It is becoming more and more apparent that water carrying a small amount of fine particulate matter produces less pressure-gradient than when water alone is flowing, all other conditions being the same. Under certain conditions the supression of head loss may be considerable and increased efficiency of pumping may be realized. Publications pointing to this unexpected phenomenon are now many. A recent paper by Zandi (1967) indicates that this phenomenon is observed when low concentrations of either fine coal, fine charcoal, or fine ash is added to the flowing water, however, this effect cannot be predicted quantitatively in the present state of knowledge.

When the solid-liquid system is such that because of the combination of concentration, particle size and mean velocity the flow is still homogeneous but not of the type of decreasing head loss and when the slurry does not exhibit strong non-Newtonian characteristics, the energy loss can be computed with the following formula which is due to Newitt (1955):

$$\phi = s - 1 \tag{1.2}$$

where

$$\phi = \frac{h_m - h_w}{h_w C_v} \tag{1.3}$$

h_m is the hydraulic gradient due to the slurry in feet of water per foot of pipe, h_w is the hydraulic gradient due to pure water, s is the specific gravity of solids and C_v is the volumetric concentration of solids.

It should be emphasized that there is no way to differentiate a priori between those suspensions which may exhibit pressure gradient suppressing action and those which would not. Those homogeneous suspensions which exhibit non-Newtonian behaviour will not be considered further here.

1.3.2 HETEROGENEOUS FLOW REGIME

This type of flow occurs when the concentration of solids varies from a minimum at the top of the pipe to a maximum at the bottom due to the tendency of the particles to settle at a velocity proportional to their fall velocity, or in other words, there is a concentration distribution across the pipe cross-section. It is, however, important to note that as defined by most of the investigators in this regime there is no deposit on the bottom of the pipe and the particles do not interact chemically with the conveying fluid. Examples of heterogeneous flow can be found in the transport of sand (Bonnington, 1958), nickel (Round, 1963), coal (Durand, 1954). This non-depositing flow regime has wide application in industry. Therefore, it has been the subject of many experimental, theoretical and review studies. Despite all these investigations, however, the main useful body of available knowledge is still empirical and in many aspects not internally consistent. The theoretical work, because of the complexity of the phenomenon, has been mainly directed toward very dilute suspensions, which are not of great industrial significance. On the other hand, the flow of concentrated suspensions, which is of industrial significance, is treated experimentally for the most part, and mainly aimed at developing some kind of correlation for the prediction of pressure gradients. In addition, most available data are for slurries consisting of uniform particles. Figure 1.1 shows a typical variation of pressure gradient with velocity when the concentration of solids is constant. From this figure it is apparent that as the mean velocity decreases, the head loss of the suspension decreases and then increases, passing through a minimum point. Through observation it is established that this minimum coincides with the appearance of a bed load on the bottom of the pipe indicating a change of the regime from heterogeneous to saltation. The velocity associated with the minimum point is defined as critical velocity or minimum deposit velocity.

Many attempts have been made to develop a relationship for the prediction of the head loss when the velocity is above the critical point. In general, the investigators have assumed that the pressure gradient required to maintain the flow of a slurry is composed of two parts. First, the pressure gradient required to maintain turbulent flow of conveying liquid, and second, the pressure gradient required to keep particles in suspension. Consequently the total press. gradient is:

$$h_m = h_w + h_s \tag{1.4}$$

where h_m is the press. gradient for suspension, h_w is the head loss for pure water flowing with the average velocity of suspension, and h_s is the excessive amount of energy loss as a result of suspended matters; all in feet of water per foot of pipe.

Several equations have been proposed to correlate pressure gradients in the heterogeneous regime. By far the most extensive experimental work has been carried-out in France by Durand (1952, 1953) and his co-workers. They used particles up to 1 inch in diameter in concentrations up to 22% by volume in horizontal and vertical pipes varying in diameter from 1½ to 22 inches. They found that all their results could be correlated with reasonable accuracy by the formula,

$$\frac{h_m - h_w}{C_v\, h_w} = \theta_1 \left[\frac{g\, D(s-1)}{U^2} \times \frac{w}{\sqrt{g\, d(s-1)}}\right]^{1.5} \tag{1.5}$$

where U is the mean velocity of the mixture, C_v is the volumetric concentration of solids, s is the specific gravity of solids, w is the terminal falling velocity of a particle, g is the acceleration due to gravity, d is the diameter of the particle, D is the pipe diameter and θ_1 is a constant evaluated by experiments. The value of this constant reported by Durand, op. cit., in his original paper is 121. However, values of θ_1 = 60, 120, 150, 180 and 380 have been reported in the literature. With a little algebra equation (1.4) can be expressed in terms of friction factors,

$$h_m = (f + \lambda_1)\,\frac{U^2}{2gD} \tag{1.6}$$

where f is the friction factor of pure water and

$$\lambda_1 = f\,C_v\,\theta_1 \times \frac{(s-1)^{0.75}}{F_r^{\,1.5}} \times \left(\frac{w}{\sqrt{gd}}\right)^{1.5} \tag{1.7}$$

and F_r is the Froude Number defined as

$$F_r = \frac{U^2}{gD} \tag{1.8}$$

Charles (1969) indicated that Durand's equation tends to underestimate the hydraulic gradient due to slurry h_m in the homogeneous flow regime. In a plot of the parameter ϕ versus U or the Froude Number, in double logarithmic paper for a given value of θ_1 and s, for both equations (1.5) and (1.2), the line representing equation (1.5) has a negative slope, while the line representing equation (1.2) is horizontal with the value of ϕ directly dependent on s. The intersection of equations (1.2) and 1.5) suggest that there is a sudden transition from a regime in which equation (1.5) applies to one in which equation (1.2) applies. In fact, this sharp transition is physically unrealistic and is not supported by experimental data. (See figure 1.13 or 1.14)

According to Charles, op. cit., a much improved relationship is obtained by combining equations (1.2) and (1.5) to give,

$$\frac{h_m - h_w}{C_v\, h_w} = \theta_2 \left[\frac{gD(s-1)}{U^2} \times \frac{w}{\sqrt{gd(s-1)}}\right]^{1.5} + (s-1) \qquad (1.9)$$

and thereby providing for a smooth relationship between ϕ and U throughout the heterogeneous and homogeneous regimes. Charles, op. cit., has summarized about 500 individual tests in this way and has also indicated that equation (1.9) should be valid for concentrations up to 25% by volume. Equation (1.9) is known as the Charles equation while equation (1.6) is known as the Durand-Condolios equation. θ_2 should be identical to θ_1 according to the original paper of Charles.

Newitt et.al. (1955) using an energy approach developed the following expression to describe the head loss for heterogeneous flow,

$$\frac{h_m - h_w}{C_v h_w} = \theta_3\ (s-1)gD \times \frac{w}{U^3} \qquad (1.10)$$

where θ_3 is a constant evaluated by experiments. Newitt, op. cit., conducted tests with sediment diameters ranging from 0.005 to 0.235 inches and sediment concentrations ranging from 2% to 35% by volume, specific gravity of solids ranging from 1.18 to 4.60, but all his experiments were carried out in a 1 inch diameter pipe. The value of θ_3 reported by Newitt, op. cit., is 1100. It should be noted that both equation (1.10) and Durand's equation (1.6) indicate that the parameter ϕ, as defined in equation (1.3), is inversely proportional to the cube of the mean velocity U. With a little algebra, equation (1.10) can be expressed in terms of friction factors,

$$h_m = (f + \lambda_3) \frac{U^2}{2gD} \tag{1.11}$$

where

$$\lambda_3 = f\, C_v \theta_3 (s-1) (F_r)^{-1.5} \times \frac{w}{gD} \tag{1.12}$$

Kriegel and Brauer (1966) have studied theoretically and experimentally the hydraulic transport of solids in horizontal pipes for some suspensions of coke, coal and ore granulates. They used particles from 0.115 to 1.67 mm in diameter in concentrations up to 42% by volume, and specific gravity of solids ranging from 1.38 to 4.62. This investigation was especially concerned with the conveying mechanism in the turbulent fluid. By means of a semi-theoretical model for the turbulent mixing of mass the friction factor caused by mixing of materials could be derived and was experimentally confirmed up to volumetric concentrations of 25%.

$$h_m = (f + \lambda_4) \frac{U^2}{2gD} \tag{1.13}$$

where

$$\lambda_4 = \theta_4 C_v (s-1) \left(\frac{w^3}{gv}\right)^{1/3} (F_r)^{-4/3} \tag{1.14}$$

v is the kinematic viscosity of the carrier fluid and all other symbols have the same meaning as explained before. The value of θ_4 reported by Kriegel and Brauer, op. cit., is 0.282 and the settling velocity w should be multiplied by a form factor, which depend on particle size and kind of material, whose value ranges from 0.5 up to 1.0. For concentrations higher than 25% by volume, equation (1.14) was extended empirically. According to Kriegel and Brauer equation (1.14) would be also valid for multi-particle size suspensions if a mean diameter of the grains is used. The effect of kinematic viscosity was not checked since all experiments were carried out with clear water as carrier fluid.

Ayukawa and Ochi (1968) derived a formula for the pressure drop in a flow with a sliding bed of particles through a horizontal straight pipe by equating the dissipation of energy of solid particles caused by sliding on a pipe wall to the work done by the additional pressure drop due to the conveying of solid particles. However, the range of velocities covered by these investigators indicates clearly that this equation should be valid for the entire heterogeneous regime, not only for velocities near the limit deposit velocity. The total pressure drop is expressed as

$$h_m = (f + \lambda_5) \frac{U^2}{2gD} \tag{1.15}$$

where λ_5 is the additional friction factor caused by mixing of materials, which is given by

$$\lambda_5 = \eta\, \theta_5 \frac{2.0g\ (s-1)\ D\ C_v}{w^2} \tag{1.16}$$

where θ_5 represents a coefficient of friction due to a friction between a pipe wall and particles, which could eventually be determined using a plate of the same quality as the pipe. η is the modification factor which is determined as a function of parameters obtained from the similarity conditions for particle motions and is a compensating factor to the effect of the existence of floating parts of solid particles caused by their complicated motions. According to the experiments carried out by Ayukawa, op. cit., this modification factor is given by,

$$\eta = 0.90 \left(\frac{d}{D}\right)^{-0.707} (F_d)^{-2.72} \left(\frac{U}{w}\right)^{2} \tag{1.17}$$

where F_d is a modified version of the particle Froude Number defined as,

$$F_d = \frac{U}{\sqrt{gd(s-1)}} \tag{1.18}$$

The critical velocity U_c or the limit deposit velocity for solid liquid-mixture is the velocity below which solid particles settle out and form a stationary bed (not a sliding bed). It is important to note that some authors appear to be confused with this definition and indicate that the limit deposit velocity is that at which solids begin to settle to the bottom of the pipe forming a moving bed. However, Durand (1952), Carstens (1969) and most other authors consider that this velocity is that at which the solids form a stationary bed, and they hydraulic gradient due to slurry can be fairly well correlated by any of the equations indicated in this section at velocities greater than the limit deposit velocity. From the practical point of view, this velocity is not precisely defined and usually corresponds to a "region" whose boundaries can be determined experimentally.

There have been many attempts to present a generalized correlation of limit deposit velocities. Perhaps the best known is that due to Durand (1952), which can be expressed as follows:

$$U_c = F_L \sqrt{2.0 \ gD(s-1)} \tag{1.19}$$

where F_L is a function of particle size and slurry concentration. Spells (1955) determined the following relationship from literature data;

$$U_c = 0.075 \ [(s-1)gd]^{0.816} \ [1 + \frac{C_v(s-1)^D}{\mu}]^{0.633} \tag{1.20}$$

where μ is the viscosity of the fluid. Recently, Charles (1970) recommended the following expression as an estimate of critical velocity,

$$U_c = \frac{4.80 \ C_v^{1/3} \sqrt{gD(s-1)}}{C_D^{1/4}[C_v(s-1) + 1]^{1/3}} \tag{1.21}$$

where C_D is the drag coefficient for the largest particle present. Finally, the simplest relationship is the one proposed by Newitt (1955),

$$U_c = 17\ w \tag{1.22}$$

Unfortunately, this equation has not been verified extensively.

1.3.3 STATIONARY BED WITH SALTATION

Generally, head losses in transportation pipelines with a stationary bed are greater than those associated with the limit depost velocity. The scatter of data in this regime is considerable. According to Condolios and Chapus (1963) Durand's equation can predict the head loss in this regime if D is replaced by the hydraulic diameter. This equation appears to be the most suitable one but it could be used only as a guideline. Since in all applications under steady state flow conditions the systems are designed to prevent occurrence of this regime, this topic is outside the scope of this thesis and will not be discussed further here.

1.4 THE DISCRIMINATION OF MODELS AND THE DESIGN OF EXPERIMENTS

The most important problem in designing a hydraulic haulage system to transport solid materials is the prediction of the head loss and subsequent power consumption. For settling slurries, heterogeneous flow is the most important mode of solid conveying because it is always the most economical regime in which to operate, i.e., it gives the maximum amount of solid transported per unit energy expended. The models introduced in the previous section of this thesis, represent the most widely used to correlate pressure gradients in the heterogeneous regime, but there are many others such as the ones proposed by Wilson (1942), Worster (1954), Wayment (1962), Toda (1969), etc. However, the scatter between the predictions of the models is well known and indeed was so from the very beginning. This fact has not been overlooked by most of the previous authors. Now the obvious question is: how should a researcher who has to analyse many alternatives, determine beforehand the "best" model for a determined system? The question has no answer, a priori. The solution can be found only using an adequate strategy for efficient experimentation, with special emphasis on the analysis of those levels of the independent variables which show up differences between the models. On the other hand, it should be noted that for a given model the agreement between the values of the coefficients determined experimentally and those given by that model, does not necessarily mean that it is the best functional model. The mechanism for determining the "best" model requires a sequential discrimination between rival models. For these and other reasons, the author of this thesis has been strongly urged to perform a statistical design of experiments. The Bayesian Approach has been selected for the discrimination of models because of its proved capability. The Roth Criterion was chosen for the optimal selection of experimental coordinates to improve ulterior discrimination by Bayesian Analysis. A lucid description of these techniques is given by Reilly (1970) and only a brief summary is presented here. The models to be discriminated are presented in Figure 1.5

The Bayesian Approach

The models can be represented in the form

$$y_i = f_k(\underline{\theta}_k, x_i) + e_i \qquad \begin{array}{l} i = 1,2 \ldots i \text{ observations} \\ k = 1.2 \ldots k \text{ models} \\ j = 1.2 \ldots j \text{ parameters} \end{array} \tag{1.23}$$

where y_i is the response or the value of the dependent variable at the i^{th} measurement, x_i is the vector of the independent variables at the i^{th} trial, θ_j is the vector of the parameters for model k, e_i is the error associated with the i^{th} measurement, and $f_k(\underline{\theta}_k, x_i)$ represents the "true" value of the dependent variable at θ_j and x_i.
It is possible to linearize around $\underline{\alpha}_j$ for the k-th model (Box et.al., 1967) as follows:

$$\underline{\mu} = \underline{X}(\underline{\theta}_k - \underline{\alpha}_j) + \underline{e} \tag{1.24}$$

where $\underline{\alpha}_j$ is a prior estimate of $\underline{\theta}_k$, the vector of the unknown parameters, and $\underline{\mu}$ is a vector whose i^{th} element is

$$\underline{\mu} = y_i - f_k(\underline{\alpha}_j, \underline{x}_i) \tag{1.25}$$

$\underline{X}$ is a matrix defined as

$$\underline{X} = \left[\frac{\partial f_k(\underline{\theta}_k, \underline{X}_i)}{\partial \theta_k} \right]_{\theta_k = \alpha_j} \tag{1.26}$$

and $\underline{e}$ is the error vector, assumed to have the multivariate normal distribution with mean 0 and covariance matrix $\underline{V} = I\sigma^2$, where 0 and I are the null and identity matrices respectively. The application of Bayes theorem requires however some prior information, such as the estimated variance of the experimental errors σ^2, the parameters covariance matrix $\underline{U}_j$ considering the possible range of the parameter values reported in the literature and, also, an initial estimate of the parameters. The initial model probability could be taken as 1/k, where $\Sigma\, Pr(M_k) = 1$, showing no initial preference for any model.

Bayes' Theorem states:

{Posterior model probability} α {Prior model probability} x $D_f(\underline{\mu}/M_k)$

$$\text{or} \qquad Pr(M_k/\underline{\mu}) \;\alpha\; Pr(M_k) \times D_f(\underline{\mu}/M_k) \tag{1.27}$$

where $Pr(M_k)$ is the known prior probability of model k and $D_f(\underline{\mu}/M_k)$ is the likelihood density function for $\underline{\mu}$ given the model k, which can be evaluated as follows:

FIGURE 1.5

MODEL 1 $\phi = \theta_1 \left[\frac{gD(s-1)}{U^2} x \frac{w}{\sqrt{gd(s-1)}}\right]^{1.5}$ DURAND (1952)

MODEL 2 $\phi = \theta_2 \left[\frac{gD(s-1)}{U^2} x \frac{w}{\sqrt{gd(s-1)}}\right]^{1.5} + (s-1)$ CHARLES (1968)

MODEL 3 $\phi = \theta_3 \; x \; \frac{0.282}{f} (s-1) \left(\frac{w^3}{g\nu}\right)^{1/3} F_r^{-4/3}$ KRIEGEL BRAUER (1966)

MODEL 4 $\phi = \theta_4 \; x \; \frac{1.80}{f} g(s-1) \; D \left(\frac{U}{gd(s-1)}\right)^{-2.72} x \left(\frac{d}{D}\right)^{-0.707} x \; \frac{1}{w^2}$

AYUKAWA-OCHI (1968)

$$D_f(\underline{\mu}/M_k) = \frac{1}{(2\pi)^n \left|v(\underline{\mu})\right|^{1/2}} \exp\left(-\frac{1}{2}\, \underline{\mu}^T \left[v(\underline{\mu})\right]^{-1} \underline{\mu}\right) \qquad (1.28)$$

where n is the number of experimental points and $v(\underline{\mu})$ is the covariance matrix given by

$$v(\underline{\mu}) = \underline{X}_j\, \underline{U}_j\, \underline{X}_j^T + \underline{V} \qquad (1.29)$$

Note that the superscript T indicates the transpose of $\underline{X}_j$ and $\left|v(\underline{\mu})\right|$ is the determinant of $v(\underline{\mu})$. The posterior model probability is then calculated with equation (1.27).

After the initial set of experiments, the known posterior model probabilities become the prior model probabilities for the next experiment. Also, the posterior parameter distribution becomes the prior parameter distribution for the next run. The posterior estimate of $\underline{\theta}_j$ is given by

$$(\underline{X}_j^T\, \underline{V}^{-1}\, \underline{X}_j + \underline{U}_j^{-1})^{-1} (\underline{X}_j^T\, \underline{V}^{-1}\, \underline{X}_j\, \underline{B}_j + \underline{U}_j^{-1}\, \underline{\alpha}_j) \qquad (1.30)$$

where $\underline{B}_j$ is the least squares estimate of θ_j and $\underline{\alpha}_j$ is the prior estimate of θ_j. Similarly

$$(\underline{X}_j^T\, \underline{V}^{-1}\, \underline{X}_j + U_j^{-1})^{-1} \qquad (1.31)$$

becomes the new prior estimate of $\underline{U}_j$. The sequential application of these equations allow to determine posterior model probabilities and to compute new estimates of the parameters.

The Roth Criterion

After the initial set of experiments the problem is how to select the new set of experimental conditions, i.e., the values of the independent variables, to achieve maximum discrimination. This objective can be attained using the Roth Criterion (Roth, 1965), which gives a weighted average of the total separation among the models, the weights being the Bayesian posterior model probabilities. That is, once the point defined by the independent variables (x_1, x_2) is chosen, the amount of separation Z is computed as follows:

$$Z(x_1, x_2) = \sum_{1}^{k} Pr(M_k) \cdot C_k \tag{1.32}$$

$$C_k = \prod_{\substack{j=1 \\ j \neq k}}^{k} \left| y_j(\underline{x}) - y_k(\underline{x}) \right| \tag{1.33}$$

where $Y_j(\underline{x})$ and $y_k(\underline{x})$ are the predicted responses of model j and k under the experimental conditions (x_1, x_2) using the current best least squares estimates of the parameters. A grid search is defined for which sets of (x_1, x_2) are taken and the corresponding Z values are calculated. The set (x_1, x_2) that defines a maximum value for $Z(x_1, x_2)$ is selected as the new experimental condition for the next run.

For the present case the two independent variabels are obviously the volumetric concentration of solids and the mean velocity of the mixture.

1.5 EXPERIMENTAL

1.5.1 APPARATUS

A schematic diagram of the actual experimental apparatus is presented in Figure 1.3.

The fluid was circulated from the reservoir R through the pipeline system, and then back to the reservoir by a rotary, positive displacement, Moyno pump type CDR, serial S-56275, equipped with a Lovejoy #3225 variable speed Pulley Drive, with a speed range from 227 to 687 r.p.m. The pump capacity vs. 75 PSI is 50 USGPM (min.) and 150 USGPM (max.). A Brooks Mag Electromagnetic flowmeter model 7300 was used to measure the flow rate. It consists of two basic and separate components; a flowhead which develops an electrical signal proportional to flow rate, and a signal converter which amplifies and converts the ac output signal into a dc signal. This dc signal is used to drive a meter on the signal converter that indicates percent of maximum flow. Also, this signal is used with a recorder for registering the instantaneous mean flow. The flow rate was doubly checked for the experiments with slurries by counting the revolutions of the pump wheel with a Strobocat stroboscope type 6310B1, serial 29213. Calibration charts are presented in appendix 1.10.2

The pipeline system consists of a 80 foot loop of 2 inch internal diameter steel pipe. The U section with a radius of curvature 1.33 feet is, however, only 1½ inch diameter in order to prevent the partial blockage of the system. The test section was situated in the upper part of the loop and for the investigation with slurries it was 20 feet long

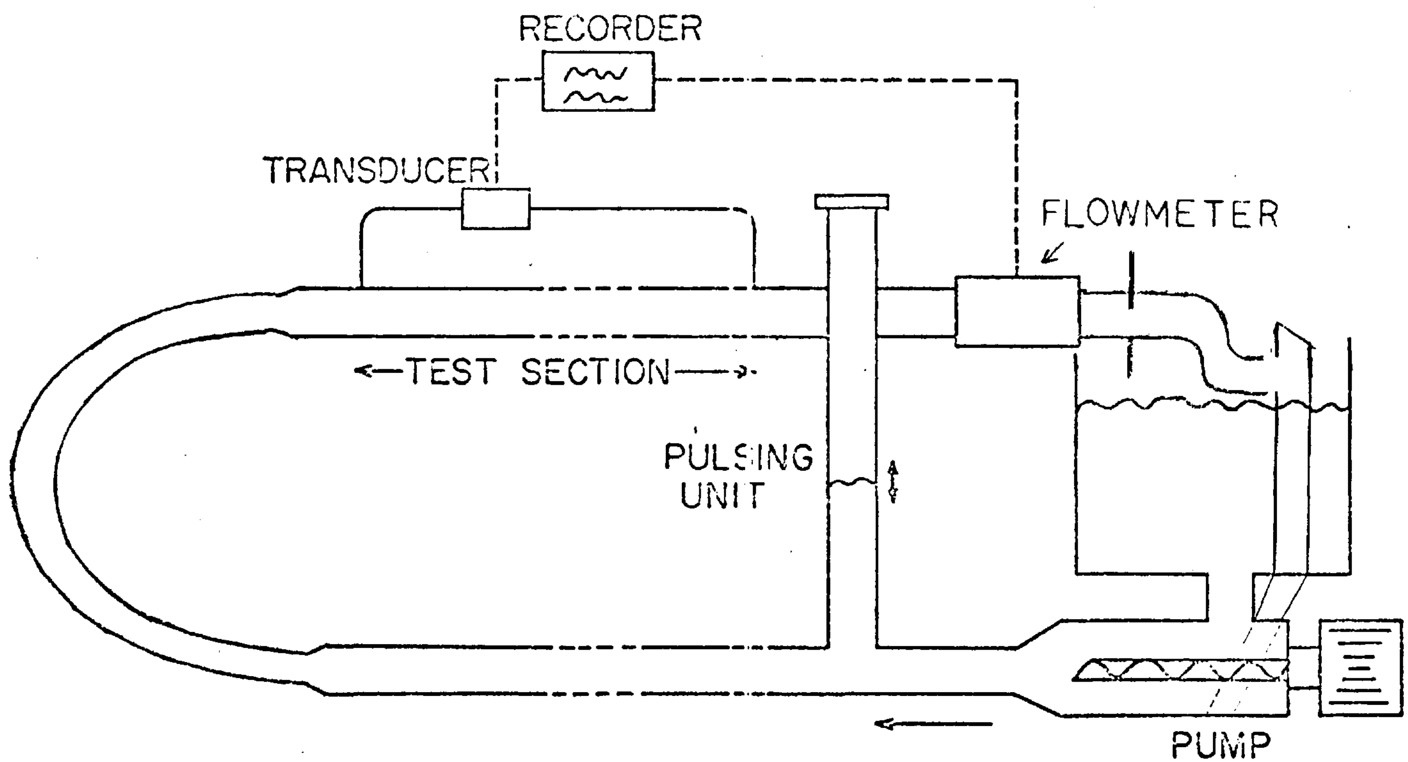

FIG. 1.3 Experimental setup.

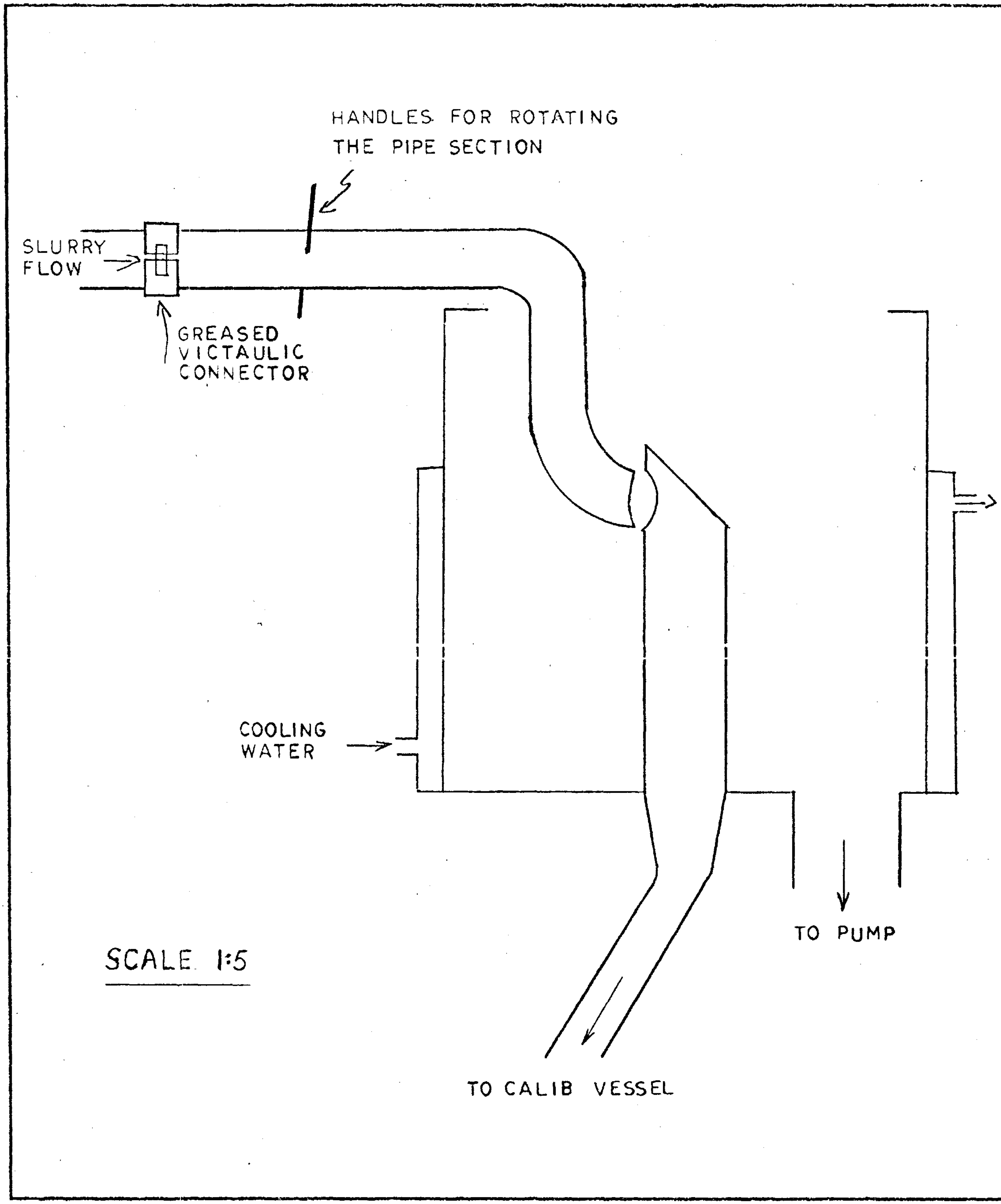

FIG. 1.3.a SLURRY RESERVOIR.

but for the experiments with clear water it was 31.66 feet long. The instantaneous pressure drop in the test section was measured with a Pace Transducer model P7D. This transducer operates with a Pace Carrier-Demodulator model CD10 whose output signal is registered by the recorder. The recorder is a Rikadenki model B-241 with two independent input and pen systems and was used for registering simultaneously the flow rate and the pressure drop in the test section. This recorder uses the principle of a null balancing servo potentiometer and the limit of error is less than ± 0.3 % of full scale. The pen speed is 1 sec. travel full scale and the chart speed used in the experiments was 400 mm/min.

The reservoir (see Figure 1.3.a) is provided with a cooling jacket to keep a uniform slurry temperature. It also contains a sampling system for determining the delivered volumetric concentration of solids of the upper section of the loop (test-section). This is done by rotating an adjustable section of the pipeline in such a manner that a sample of the flowing mixture is collected in a calibrated vessel through a connecting line fixed to the reservoir. Two high-power stirrers were located in the reservoir in order to maintain a uniform distribution of solids and to prevent the partial deposition of particles on the bottom at low flow rates.

1.5.2 PROCEDURE

The initial set of experiments under steady state flow conditions was carried out with tap water. The pressure drop in the test section was measured at different water velocities, from 7.0 ft./sec. up to 15.4 ft./sec. The purpose of these initial experiments was to ascertain the reliability and accuracy of the pressure measuring equipment and consequently to establish a correlation between friction factor and Reynolds number which represents the "true" behaviour of water flowing in the test section. The experimental data is presented in Table I.1.

The second part of the experimental work was concerned with the pressure drop under steady flow conditions with hematite slurries of different volumetric concentrations at different flow rates. The slurries were prepared by adding a determined weight of hematite mineral to water circulating in the system and allowing it to circulate for approximately half and hour in order to achieve constant distribution of solids and constant temperature. Visual observations were made in a 2 ft. long glass tube of 2 in. internal diameter, which formed part of the test section. This made it possible to determine whether solid particles were fully suspended or in the bed transport regime. When the system achieved stability, the pressure drop and the mean mixture velocity were both recorded using the electronic device mentioned in the previous section. Almost simultaneously, samples of slurry were collected in a calibrated vessel to determine the true delivered volumetric concentration of solids. The flow rate was doubly checked by counting the speed of the pump using a stroboscope. See table 1.12.

The procedure indicated above was repeated for different flow rates with a constant overall concentration of solids in the system. When the complete range of velocities was covered, the total concentration of solids was increased by adding hematite to the system and the entire process repeated.

The above experiments with slurries permitted the determination of the modes or regimes of transport for hematite-water mixtures at different experimental conditions. The limit deposit velocity was estimated for five different concentrations of solids. The plane of the independent variables U and Cv was divided in a rectangular grid pattern having equally spaced length. The range of velocities was limited to 10.5-16. ft./sec. to make certain that the design of experiments covers only the non-deposition transport regime. The range of concentrations was 0.-0.25 on a volumetric basis. The procedure in the Bayesian analysis was started-up using the subjective prior information that the probability of each of the proposed models was 0.25. The initial parameter covariance matrix was estimated considering values of parameters reported in the literature. The variance associated with experimental errors was selected on the basis of previous measurements. Four experimental points were chosen initially and the procedure for discrimination of models and design of experiments was started-up. The Roth criterion selected the vector of experimental conditions for the following run. The procedure indicated above was then repeated for 5 experimental points. The sequential procedure continued until one model probability reached a value that caused acceptance of the model by a logic criterion.

1.5.3 Estimation of experimental errors.

The estimated errors of the principal variables or their uncertainities are:

- Pipe diameter. The nominal diameter of the pipe is 2.0 inches. Taking into account the deviations from roundness, caliper error, etc. the uncertainity in the pipe diameter is about ± 0.04 inch.
- Water density. The estimated uncertainty in the water temperature is ± 6° F corresponding to a density variation of less than 0.2%.
- Length of the test section ± 0.5 inch.
- Frequency. The frequency was determined simply by measuring the time required for ten oscillations. This reproduced to within less than 1. %.
- Amplitude ± 0.25 inches.
- Suspension troughput. Approximately 1.02 % (flow in U.S. Gallon per minute) . The determination of the pump speed using the strobo-light gives a reproduction to within less than 1. %.
- Particle settling velocity ± 0.0113 feet/sec.
- Delivered volumetric concentration of solids ± 3 %. However, for very low concentration of solids, say 2-5 % by volume, the error could be considerably large.
- Pressure drop. Replication of experiments indicated that pressure drop is reproduced within 0.018 feet of water/foot of pipe (over the test section of 20 feet) using the electronic device mentioned in section 1.5.1. This corresponds to an error of approximately 5 %. The relationship between the pressure drop and the signal

in the recorder chart was of the type

$$y = 2.267\ x^{0.9539} \qquad (1.33.1)$$

where y is the pressure drop in inches of mercury and x is the reading in recording units. This type of equation changes slighly with the span and/or the diaphragm of the transducer, however, in all cases a slight non-linearity was noted in this relationship.

1.6 DISCUSSION OF RESULTS

Pressure drop with clear water

Pressure drop was measured for different fluid velocities under steady-state conditions. The experimental data is presented in table 1.1. The friction factor was calculated from the data of table 1.1 using the well-known Darcy-Weisbach equation,

$$\Delta P = f\left(\frac{L}{D}\right)\left(\rho\frac{U^2}{2g_c}\right) \tag{1.34}$$

Friction factors and Reynolds numbers were fitted according to the Blasius model and the Prandtl model (Streeter, 1966) using a least squares technique. The estimated regression equations were:

Blasius model

$$f = 1.5233\ (Re)^{-0.3844} \tag{1.35}$$

Prandtl model

$$\frac{1}{\sqrt{f}} = 4.021\ \log(Re\sqrt{f}) - 9.195 \tag{1.36}$$

In table 1.2 are tabulated the set of friction factors calculated from equation 1.34 and those predicted by equations 1.35 and 1.36 along with the residuals associated with these models, as well as the corresponding

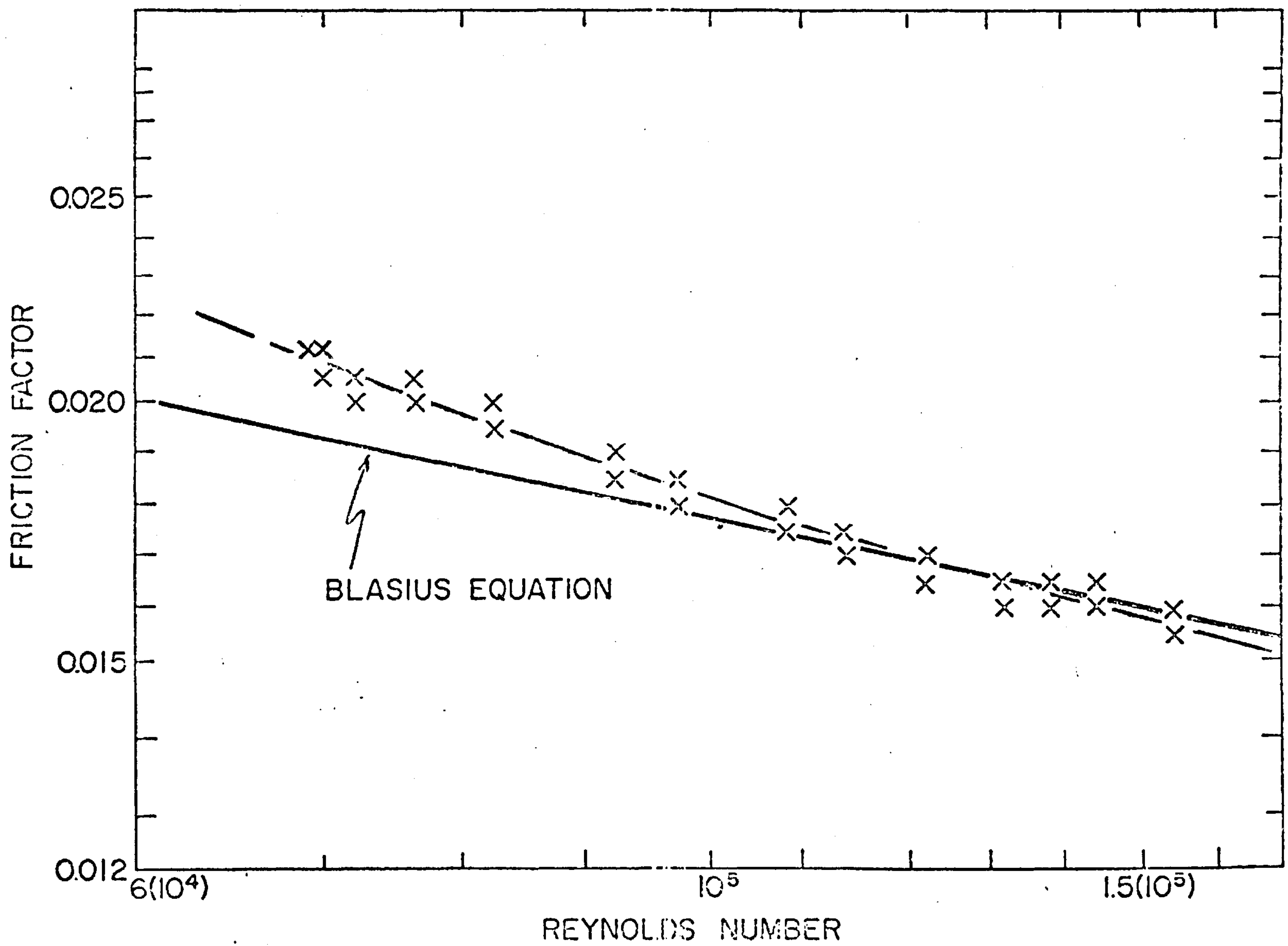

FIG. 1.4 Friction factors under steady state conditions.

Reynolds number. Figure 1.4 shows the experimental friction factor as a function of Reynolds number on double logarithmic paper. The scatter of the data points is consistent with the experimental accuracy of the individual determinations of f. A slight difference is observed between the numerical values of Prandtl and Blasius parameters given by standard references and those obtained with the present experimental data. However, this fact is not really significant because very similar responses are given by these models when using the present parameters or those given by the standard references.

Particle Size Distribution and Settling Velocity of Hematite

The mineral used in the experiments with slurries was hematite whose specific gravity is 5.17. From previous experiments it was noted that the effect of particle attrition, due to prolonged recirculation of the slurry, tended to proceed towards a quasi-equilibrium size distribution after a few hours of recirculation. The mineral used in the pressure drop studies had at least ten hours of recirculation and the results of the screen analysis of this material is presented in table 1.3. The cumulative particle size distribution curve is shown in figure 1.6. The characteristic particle shape is shown in figure 1.7 and it can be appreciated that the solid particles are not nearly spherical. However, as is customary in this type of work, the "mean diameter" of particles found on any screen is expressed as a mean length between the openings in the screen above and that on which the particles rest. The "equivalent diameter" of the mixture was calculated

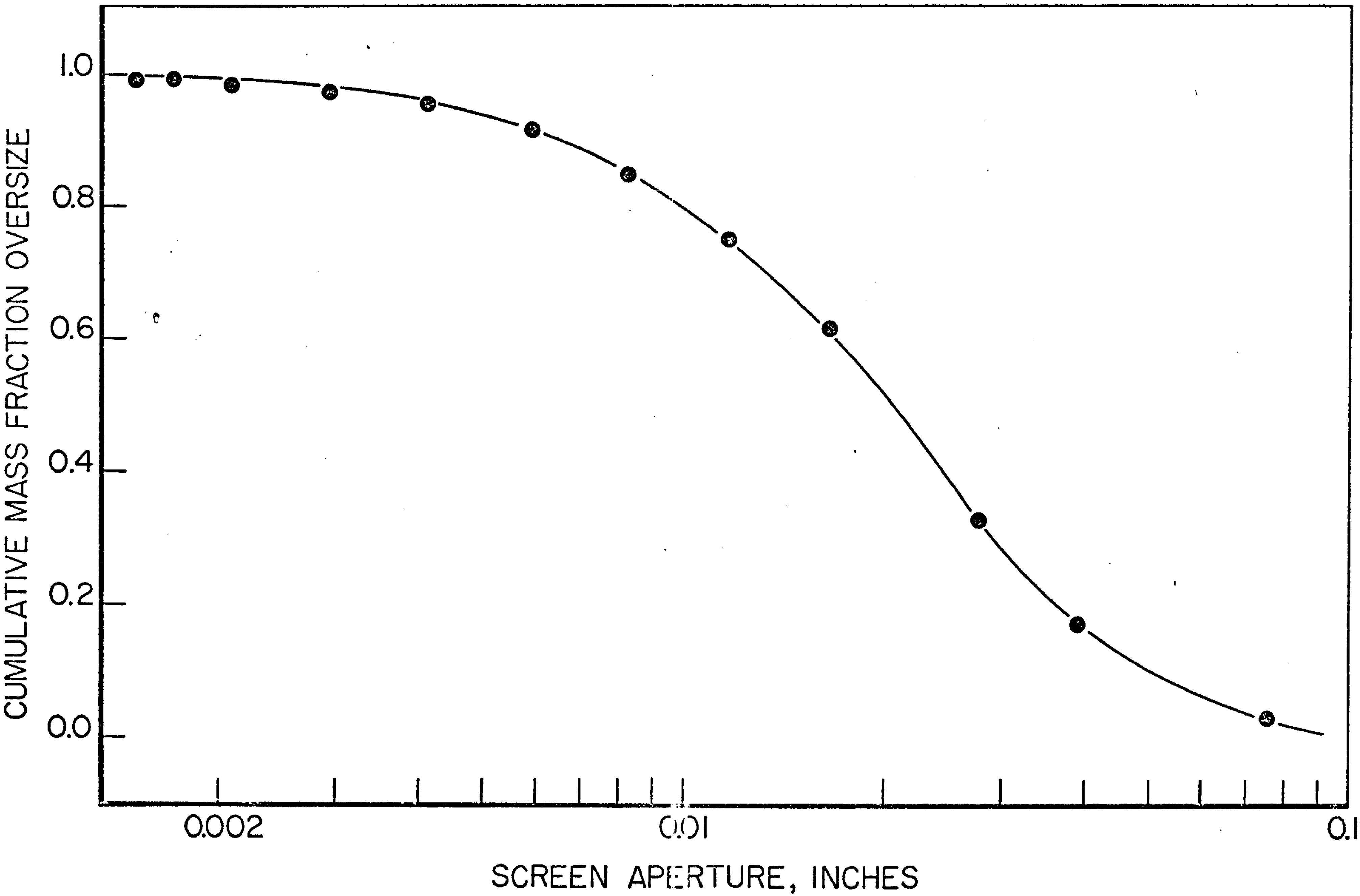

FIG. 1.6 CUMULATIVE PARTICLE SIZE DISTRIBUTION FOR HEMATITE

according to the Sauter mean diameter definition

$$d = \frac{\sum \omega_i}{\sum \omega_i/d_i} \tag{1.37}$$

where ω_i is the fraction by weight of particles with diameter d_i, and d is the equivalent diameter of the mixture. The terminal settling velocities in still water were measured in a five-foot-long, six inch diameter, vertical glass tube, by timing the descent of particles selected at random from each screen. These results are presented in table 1.4. On figure 1.8 the terminal settling velocity has been plotted against the mean diameter on double logarithmic scale. The shape of the curve is similar to that of spheres of similar diameters. This curve has been taken from Perry (1969). The functional relationship between settling velocity and mean diameter was determined using the IBM Share-Program SD3094 for non-linear least squares curve fitting. It was found that data is represented well by the equation

$$w = 6.8916\ (d)^{0.7037} - 0.0552 \tag{1.38}$$

where w is the settling velocity in feet/sec and d is the mean particle diameter in inches. This equation can be used for hematite particles within the range 0.002-0.06 inches with an standard deviation of 0.0113.

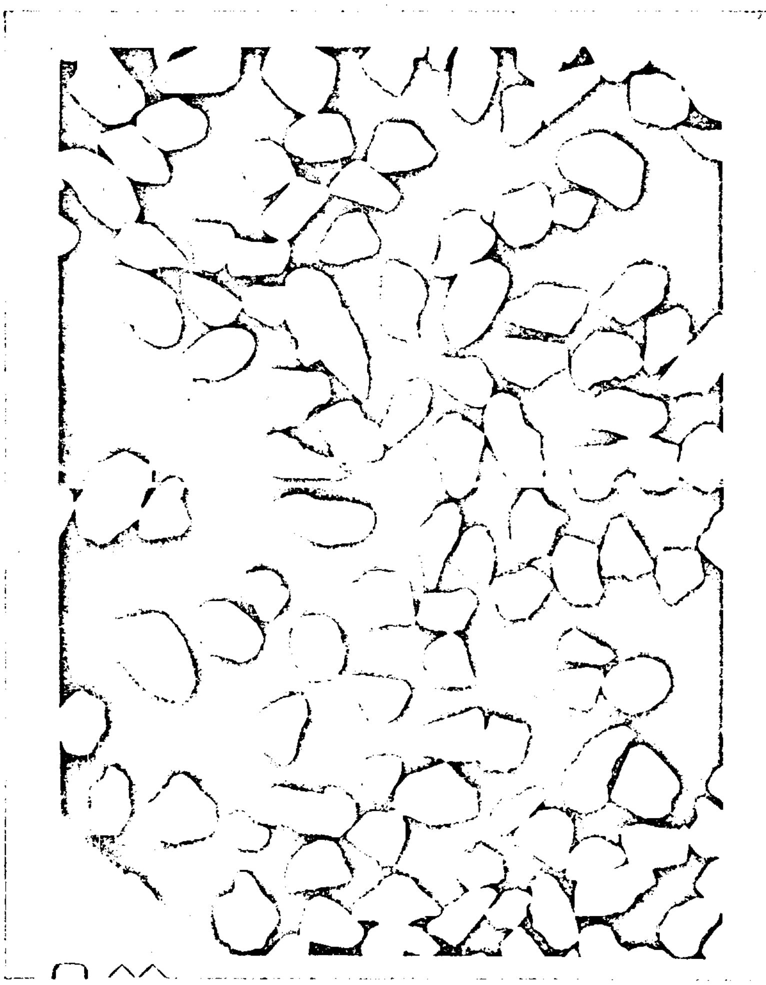

FIG. 1.7 Photograph of hematite particles. Courtesy of Dr. K. Chan, McMaster University.

Delivered Concentration of Solids

The delivered volumetric concentration of solids C_v, defined as the ratio of volume of solids to the volume of slurry, was determining by weighing the collected samples of slurry in a calibrated vessel. It was noted that the delivered concentration of solids was a function of mixture velocity and it was not equal to the overall concentration of solids in the mixture loaded into the system. While the difference is quite small at high flow rates, it is appreciable at low flow rates especially those below the limit deposit velocity, at which a substantial portion of the solids is held-up in the pipe and particularly in the reservoir. This aspect can be observed on figure 1.9, where the delivered volumetric concentration of solids has been plotted against the average velocity of the mixture. There is a systematic decrease in C_v as the average mixture velocity decreases, especially when the total concentration of solids in the system is higher than 10%. However, the error in the determination of C_v is relatively high when the mean velocity is in the neighborhood of the limit deposit velocity, mainly due to the unstable characteristics of the flow pattern in this region.

Pressure Drop with Slurries

Three flow patterns were observed for the flow of hematite-water mixtures in the range 5.0-16.0 ft./sec.

(a) Continuous and discontinuous stationary bed with saltation.

(b) Intermediate flow regime.

(c) Non-depositing transport regime or heterogeneous flow regime.

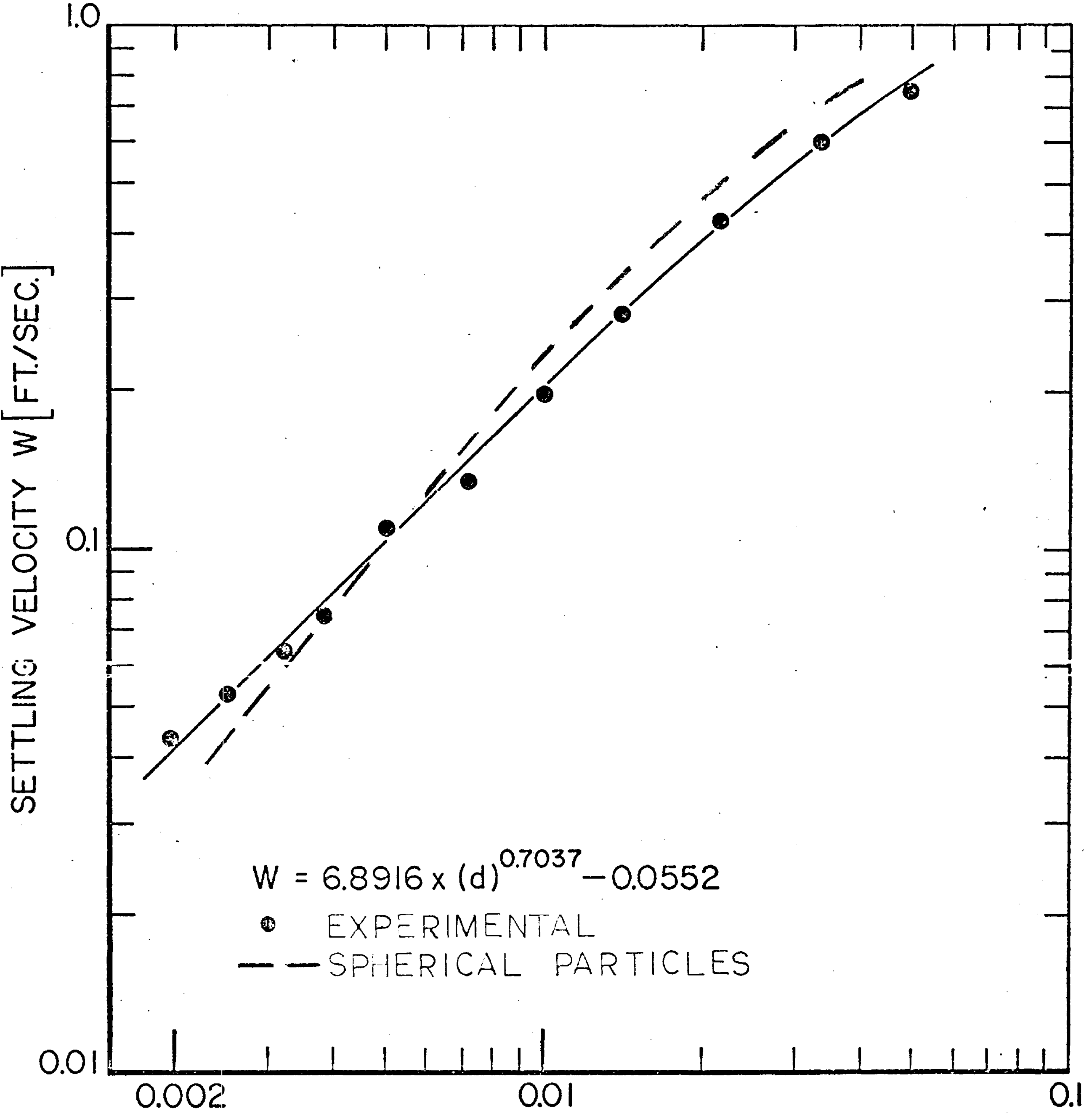

FIG. 1.8 SETTLING VELOCITY OF HEMATITE PARTICLES AT 22°C

These flow regimes are indicated in figure 1.10, where the hydraulic gradient due to slurry h_m (feet of water per foot of pipe) is plotted versus the mean mixture velocity U (the total rate of discharge per cross-sectional area of the pipe, ft./sec.) on linear paper. The points indicated on this figure are, of course, experimental values and the coordinates of most of these are presented in tables 1.5. The clear-water-line has been also included on figure 1.10 for reference. The lines of constant delivered concentration (figure 1.10) have been drawn as the better representations of the experimental coordinates and consequently do not represent the responses of any specific model. The tendency of these curves is similar to those given by most of the authors in the sense that for a given concentration of solids, as the mean mixture velocity decreases from a rather high value, first the hydraulic gradient decreases and then increases, passing through a minimum point. At high velocities the hydraulic gradient lines are approximately parallel to the clear-water-line and the deviation from the slope of this curve increases with concentration. The heterogeneous flow regime is characterized by the full suspension of the particles and it occurs at any velocity greater than 10.5 ft./sec. when the concentration of solids is not greater than 25% by volume.

The transition flow regime is characterized by the tendency for bed formation and the flow in this zone is unstable mainly due to incipient formation of a stationary bed. When deposition of particles occurs there is a reduction in the free area available for flow, and the velocity in the free area is therefore greater than the apparent

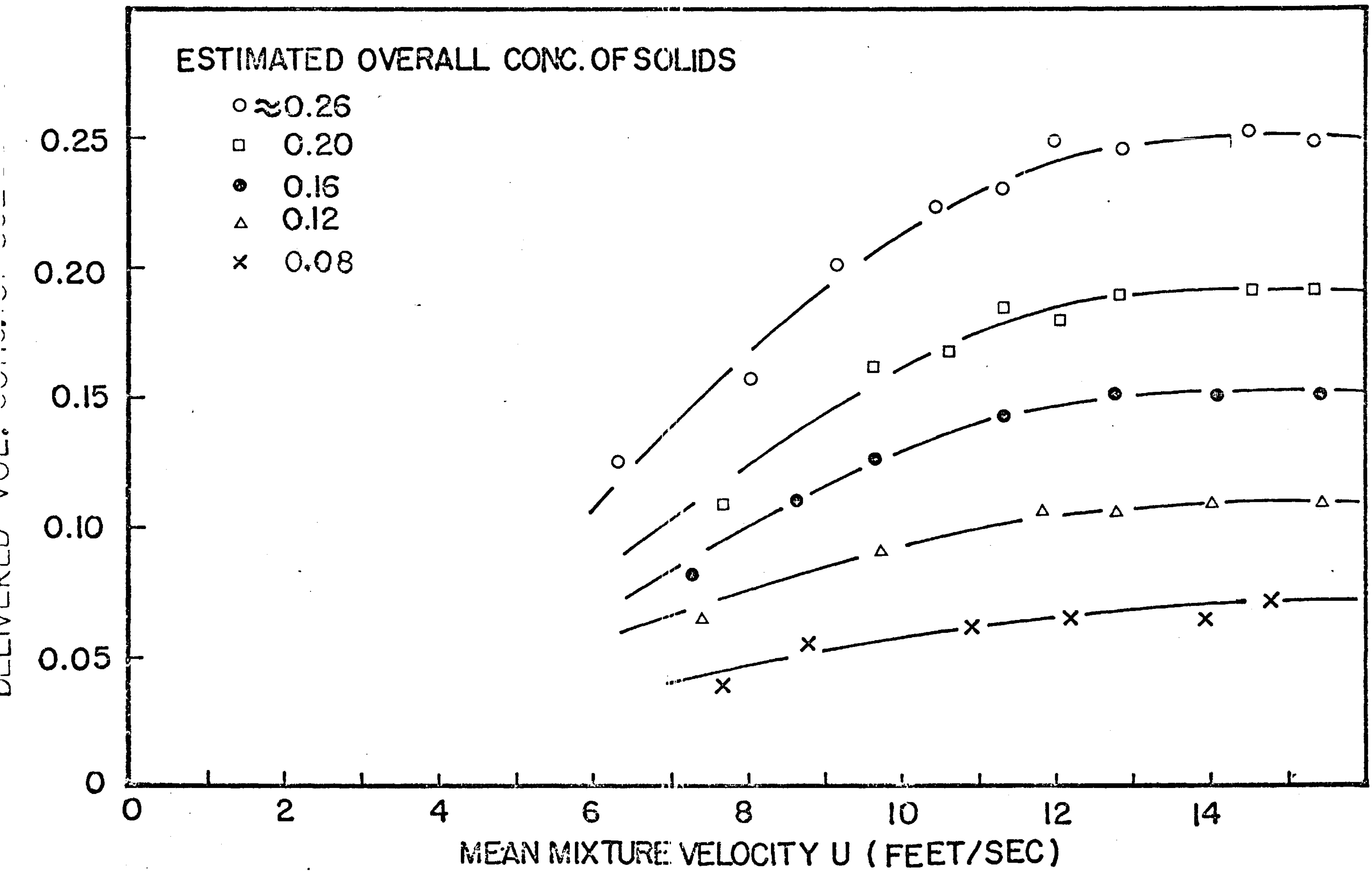

FIG. 1.9 Variation of delivered concentration of solids with mean velocity.

mean velocity; consequently, the shear forces exerted by the flowing water are greater than the frictional forces at the pipe wall and the bed slides along the bottom of the pipe. Associated with this unstable regime is the limit deposit velocity or the critical velocity U_c. As a consequence of this, the pressure behaves erratically and data is not reliable. The velocity U_c does not correspond to a unique number, it is essentially a "region" whose boundaries can eventually be determined experimentally. In the present case, the limit deposit velocity shows a sensitivity to the volumetric concentration of solids, which is not always the case. For example, Round (1963) in his study on nickel (specific gravity   8.9) slurries observed no dependency between U_c and C_v.

Several correlations have been proposed to determine the limit deposit velocity and some of these models were discussed in section 1.3.2. Figure 1.11 represents the critical Froude number versus the volumetric concentration of solids on double logarithmic scale, on which the predicted values of U_c due to different models are presented along with the estimated experimental values of U_c. The scatter among the different responses is very great indeed; however, all models with exception of the one proposed by Newitt show a dependency of the limit deposit velocity with the concentration of solids. Durand's equation appears to correlate best the experimental data, even if the shape of the curve predicted by Charles' model seems to be very similar to the one projected by the experimental data. About this, Charles (1970) recommended using his correlation considering the drag coefficient of the

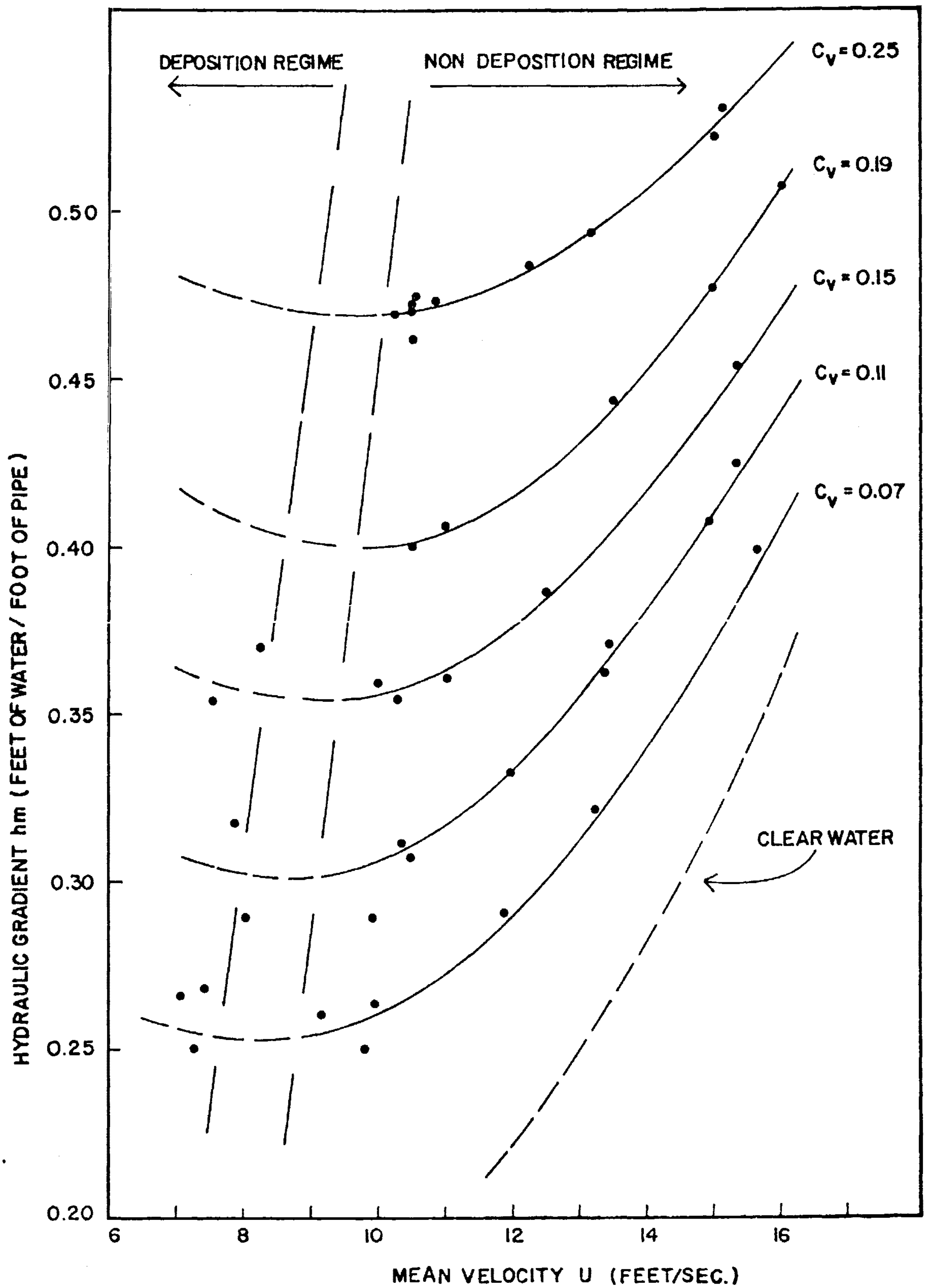

FIG. 1.10 Relationship between h_m-U-C_v for hematite-water mixtures in a 2-inch pipe.

largest particle present. In the present case, a mean diameter of 0.05 inches with an equivalent drag coefficient 0.55 was considered in using equation 1.21, but it seems better to use the drag coefficient of a particle with the equivalent diameter of the mixture rather than the original proposal. The equation proposed by Spells, which considers most of the characteristics of the system, including the viscosity of the carrier fluid, predicts values of U_c considerably in error, and no definite reason for this effect can be advanced. Aside from the possibility of differences in the experimental data used to develop these empirical correlations, the wide deviations in their predictions suggest that the correlations themselves are in error. At the present time no comprehensive theory of the limiting deposit condition, in circular pipes, exists. Shen (1970) has developed an interesting approach, using the Shield's criterion for incipient sediment motion, which is only valid for rectangular closed conduit turbulent flow.

There is no consistent data on hematite-water slurries published in the literature, with exception of some incomplete information given by Castro (1963). He determined the pressure gradients for slurries only 57% by weight of hematite and concluded that Durand-Condolios equation correlated the data well if the value of the constant is taken as 120. No attempt was made to determine the general characteristic of the system over a whole range of concentration. Some results on iron ore have been reported hy Watanabe (1958), Thomas (1961), Sinclair (1960) and Linford (1969). However, the physical and chemical properties of the solids studied are entirely different from author to author, consequently the present data cannot be compared with the information

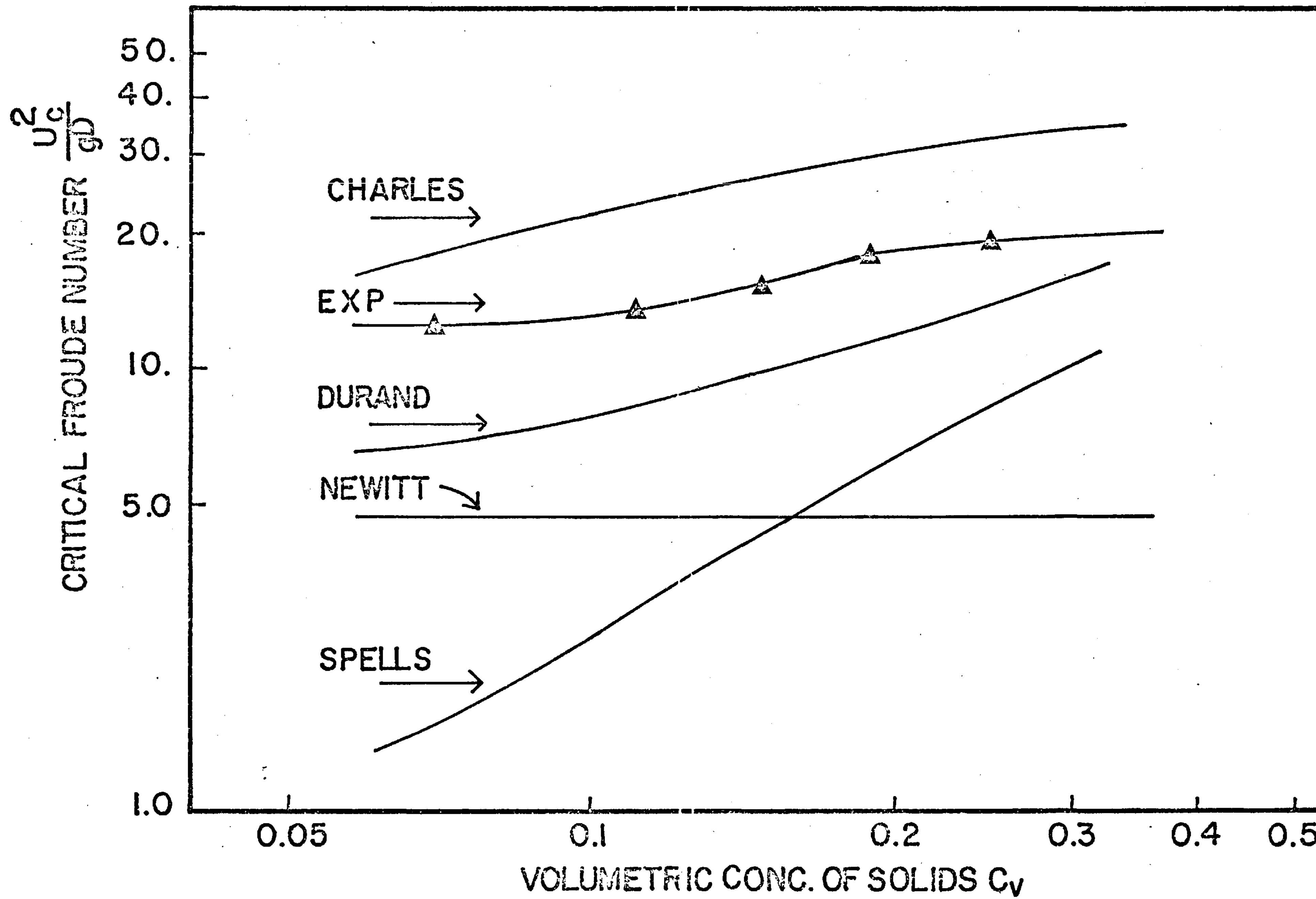

FIG. 1.11 Comparison between experimental and predicted critical Froude Number according to different authors for hematite-water suspensions.

already published.

Discrimination of Models

The purpose of this work was to determine in a scientific manner the best correlation for the heterogeneous flow of hematite-water slurries, as well as to obtain the best estimation of the parameters of each model. The regions of maximum separation between models and experimental data have been determined along with a critical discussion of the alternatives available at different levels of concentration and mixture velocity.

The entire process of sequential discrimination of models with design of experiments was performed using a computer program (see Appendix 1.1) written in single precision Fortran IV language. The process is summarized as follows:

1. Four experimental points were chosen initially. These are indicated in table 1.5 from sequence 1 to 4 and they represent the wide spectrum of possibilities for the heterogeneous flow regime, i.e., low and high concentrations along with maximum and minimum velocities permitted by the constraints of this flow regime. Also, the initial probability for each of the 4 models was taken as 0.25, showing no specific preference for any model. The parameter covariance matrix was selected considering values of the parameters reported in the literature. The variance of the experimental errors was evaluated on the basis of previous experiments.

2. A first estimation of the parameters is carried out using a least squares technique. Subroutine LEASQ repeats this operation for each model, considering initially only the 4 experimental points.

3. The Bayesian Analysis procedure is started. Subroutine Bayes computes the posterior model probabilities and the maximum likelihood estimates of the parameters. However, it should be noted that for the first iteration, in which 4 points are being considered, the values of the maximum likelihood estimates are identical to the least squares values as a condition imposed by the technique. Also, the parameters covariance matrix is updated for the next iteration.

4. The new set of experimental conditions, i.e., the values of the valumetric concentration of solids and the mean velocity of the mixture, is determined by Subroutine Roth.

The process was then repeated at step 2 with 5 experimental points. The sequential procedure was continued until sequence 16, where the probability of Ayukawa-Ochi model reached the value 70%. The posterior model probabilities for each sequence are presented in table 1.17 and figure 1.12 is a graphical representation of this data. It is important to note that the Roth Criterion gave always the coordinates of experimental conditions at the maximum value of concentration (25 % by volume) and at the minimum or the maximum velocity impossed by the boundaries of this flow regime. However, it was not always possible to run an experiment at

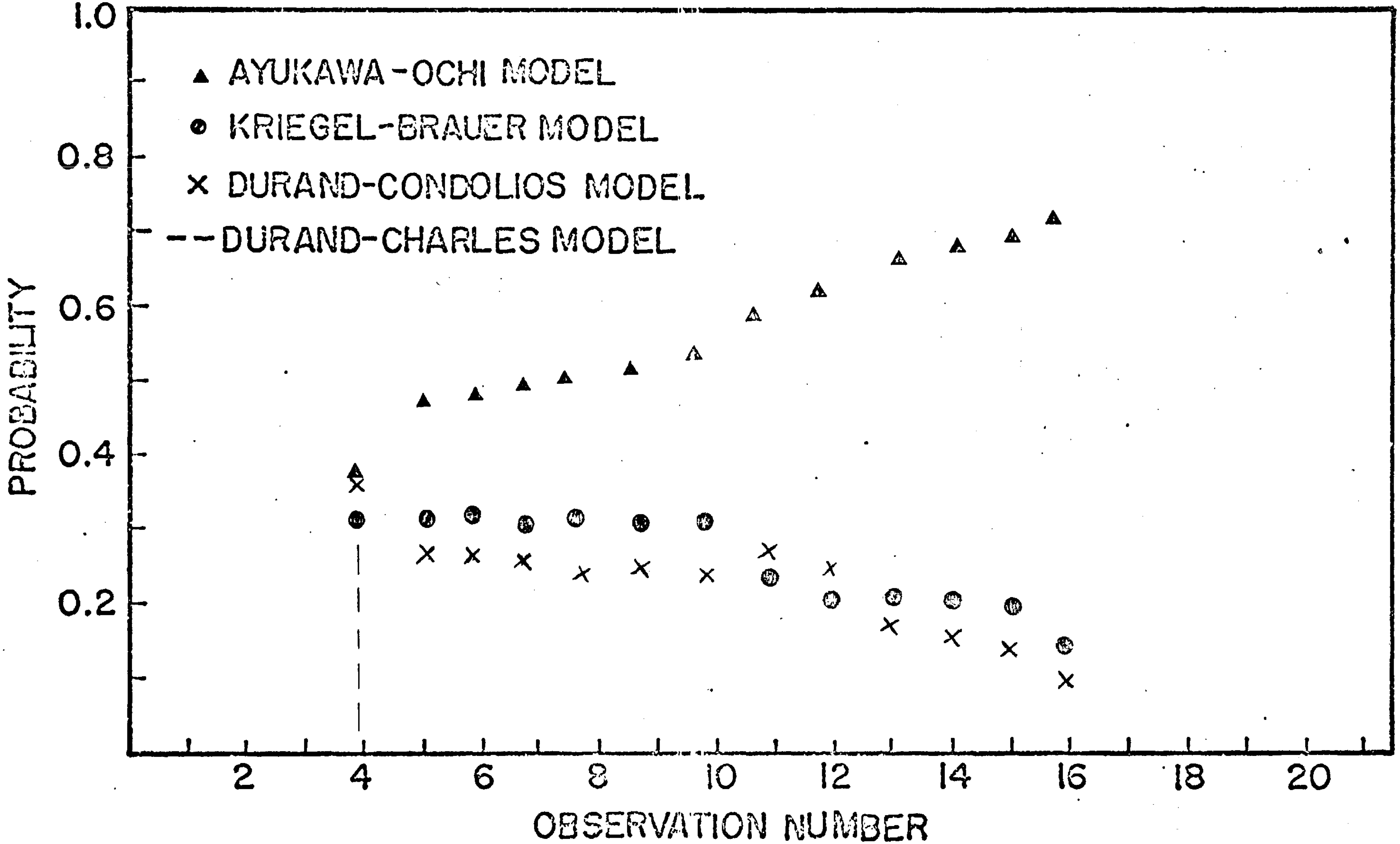

FIG. 1.12 Model discrimination by sequential design.

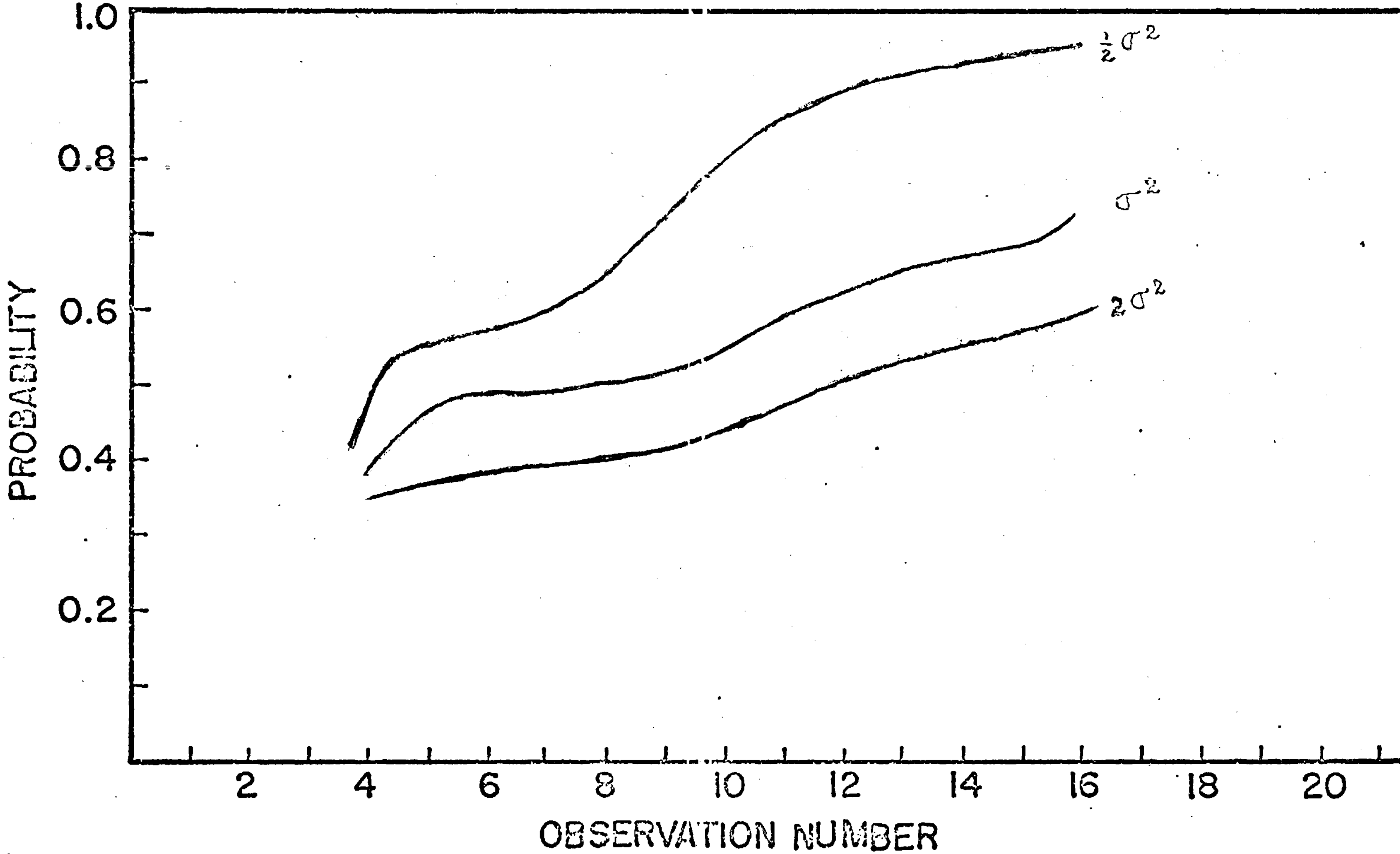

Fig. 1.12.a. Posterior probabilities for Ayukawa-Ochi model considering different values for the variance of errors.

the conditions indicated by the Roth Criterion, and the nearest experimental conditions were taken (for some of the cases) from experimental data that had been previously collected when the boundaries and the general operation curves of this regime were determined. This fact is frequently encountered in the practical design of experiments but the final result is not altered, only a few more iterations are necessary. The design of experiments was terminated at sequence 16 because of the evidence that one of the models (Ayukawa-Ochi) gave the best correlation of the data. This fact can be readily appreciated by figure 1.12 where the tendency of the probability curve for model 1 is steadily increasing and significantly better than thh curves of other models. Figure 1.12.a shows the posterior probabilities of Ayukawa-Ochi model for different values of the error variance. Asdexpected, when the error variance increases the posterior probabilities decrease. However, the initial estimate of the error variance appears to be correct: the ratio of the error variance to the residual variance (for Ayukawa-Ochi model) is approximately 1.4. The experimental points indicated by sequence 17 to 27 were ramdomly chosen (not considered in the design of experiments) and they are representative of those level of concentration not considered of significant importance in the general design of experiments. See table 1.5.

The equation proposed by Ayukawa-Ochi correlates the experimental data well and for high concentrations of solid and low velocities it can predict the hydraulic gradient with an error no greater than 6% (using the parameters here estimated) while Durand's equation predicts the data with an error no lower than 10% for these conditions. The region around 13 ft./sec. is correlated well by any of the models with exception of the one proposed by Charles. The separation in the responses of the models increases again when velocity is high, 15-16 ft./sec. This fact points out the importance of the design of experiments because if measurements had been carried out over equally spaced intervals, including high and low levels of concentrations, the result would have been significantly different.

The coefficient ϕ has been plotted versus the Froude number in figure 1.13, using a double logarithmic scale. The responses of different models are also shown, with exception of the one due to Kriegel and Brauer in order to reduce congestion. Experimental points tend to be ordered in two straight lines, one following the other, with a slight inflexion point around ϕ = s-1 = 4.17. The model proposed by Ayukawa-Ochi gives a dependency of ϕ on the Froude number and the friction factor, the same for Kriegel and Brauer, while Durand's model does not consider the effect of change of the friction factor with the velocity. For these reasons, Durand's model gives a straight line on this plane and consequently cannot fit those points at high velocities. The response of the Ayukawa-Ochi model, and the same for Kriegel-Brauer, is slightly curved, with slope directly dependent on the value of the friction factor for clear water at a given Froude number. However, the effect of the friction factor may not be significant for large pipes, when the Reynolds number is large and the friction factor is practically constant. Figure 1.13 also indicates that differences in the responses between Ayukawa-Ochi and Durand equations are significant at high or low Froude numbers, while at intermediate flow rates, say 13 ft./sec., both models correlates the data well. Since the presentation of data on the ϕ-F_r plane is presented here for first time, it is not possible to make comparisons with other references.

The equations due to Durand and Charles are always represented on the ϕ-ψ plane (figure 1.14). Durand's equation appears to fit the experimental data better on the ϕ-ψ plane than in the ϕ-F_r one,

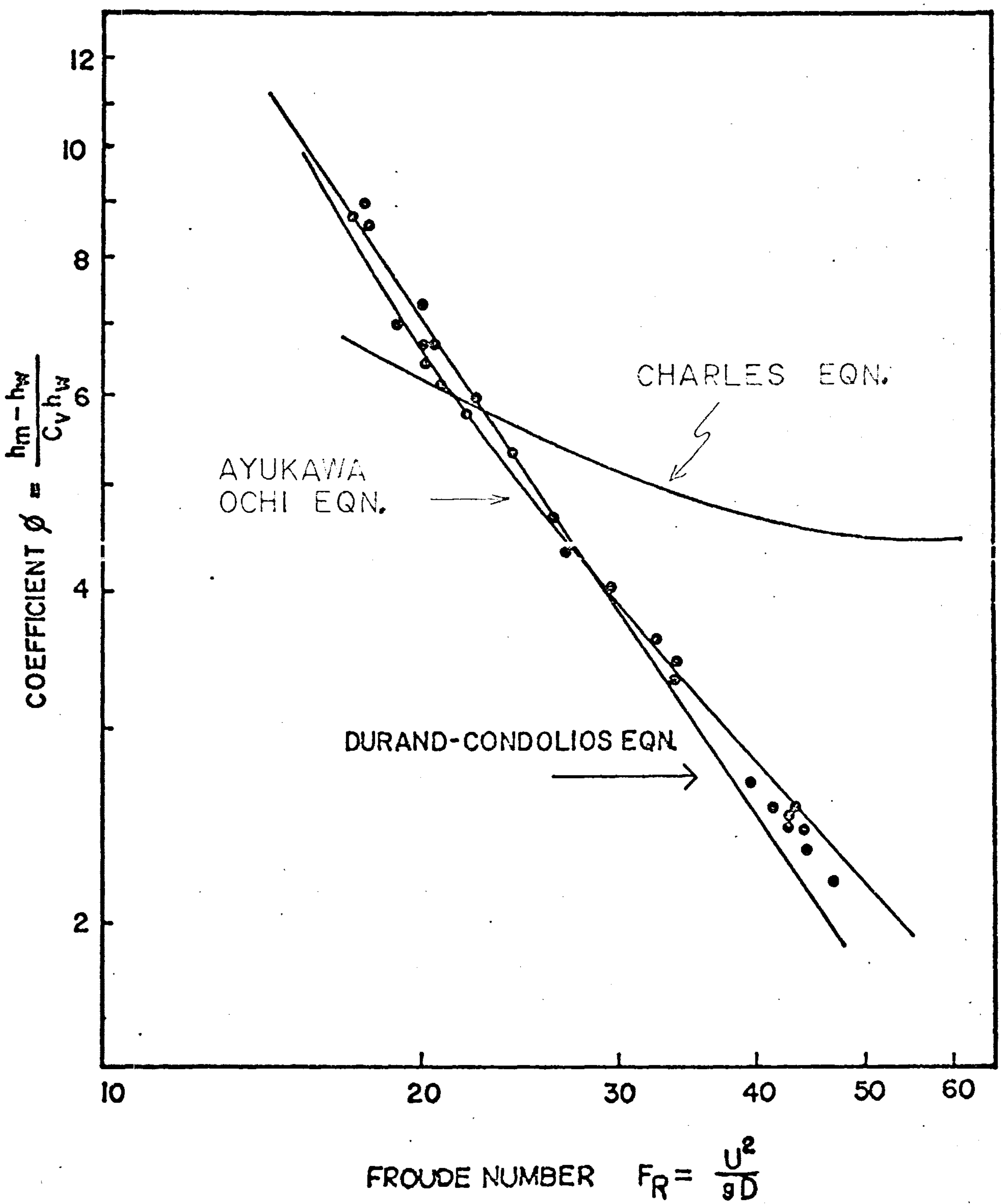

FIG. 1.13 Comparison of different models on ϕ-F_r plane.

This has been noted by Babcock (1970), who has shown, using Durand's original data, how the experimental data looks when it is plotted in different coordinate systems. However, the ϕ-F_r plane is completely general while the ϕ-ψ one is only valid for Durand or Durand-Charles equations. From figure 1.13 it would seem that the Durand-Charles model in no way represents the experimental data. Charles (1970) indicated that the intersection of Durand's equation and equation 1.2 suggests that there is a sudden transition from a regime in which Durand's equation applies to one in which equation 1.2 applies. He also pointed-out that this sharp transition is physically unrealistic and is not supported by experimental data. However, this statement of Professor Charles does not appear entirely correct. Indeed, the data presented by Round (1963), Newitt (1955), Nora Blatch (1902), Durand (1952), Babcock (1970), Hayden (1970) etc., do not show the tendency indicated by Charles. On the other hand, some data (Babcock, 1970) indicates that when specific gravity of particles is not large, say 2, then the systems appear to behave as stated by Charles. Positively, the modification of Durand's equation proposed by Charles is not a good alternative for the present data.

The fact that the Ayukawa-Ochi equation does not fit the lower concentration data as well as it does the higher concentration data could be interpreted in the following manner: the parameter in this model represents the friction factor due to a friction between particles and the pipe wall; it is correct to assume that this effect of friction becomes significant when the volume occupied by particles also becomes

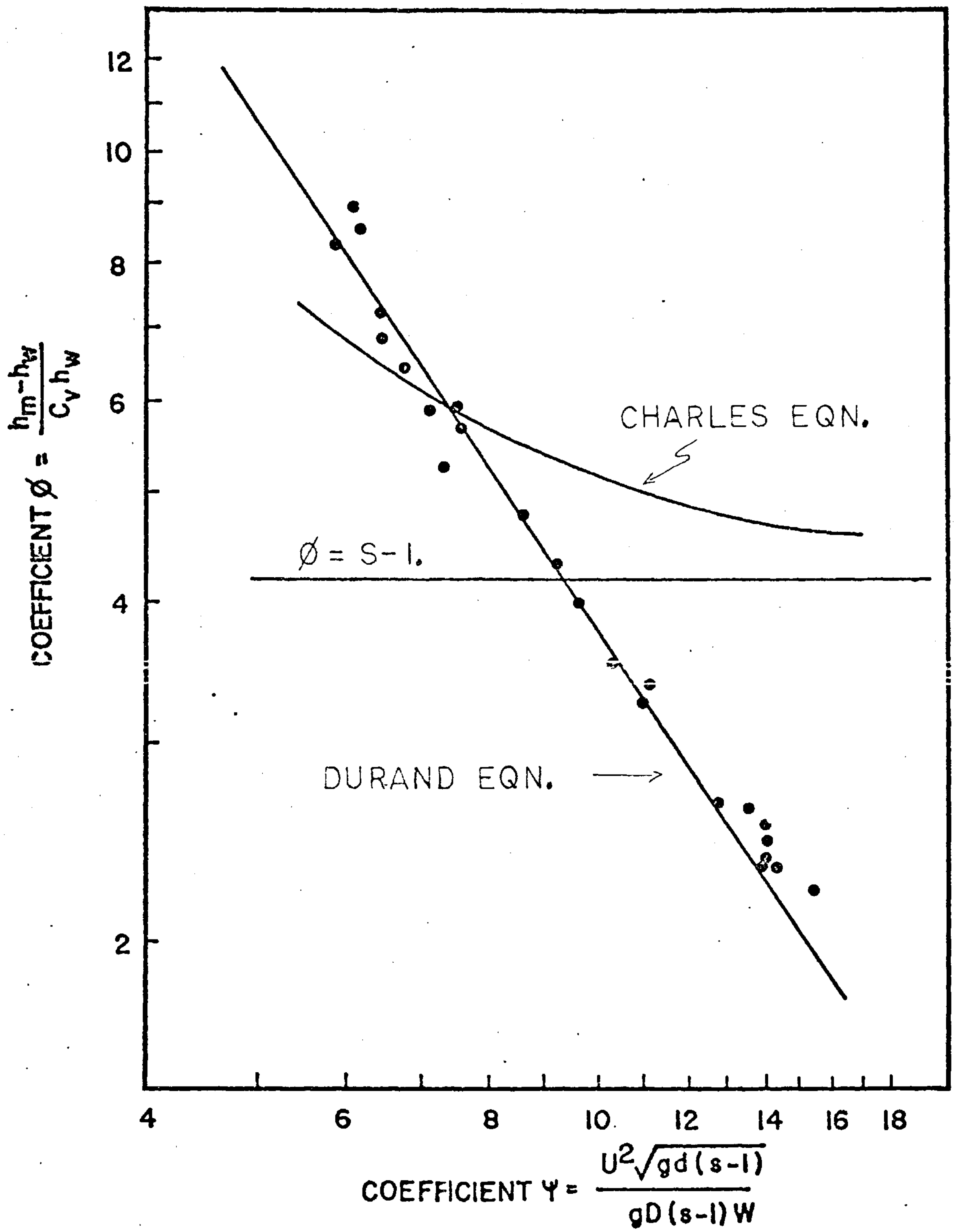

FIG. 1.14 Comparison of Durand-Condolios and Charles equations on ϕ-ψ plane.

large, i.e., when concentration of solids is large and/or the velocity of the mixture is low.

Durand's equation has been widely used since it was proposed in 1952 and apparently the most representative value of its parameter is 121. The Ayukawa-Ochi model, proposed in 1968, has been used only by its authors and its parameter depends directly on the kind of pipe and material to be transported. However, this equation takes into account the factors that govern the mechanism of transport in a more detailed form. While Durand's equation is valid at any velocity greater than the limit deposit velocity, the Ayukawa-Ochi model does not predict the pressure gradient at high velocities well, as indicated by its authors, who have suggested as the upper limiting velocity;

$$U \approx 2.9 \sqrt{gD(s-1)} \tag{1.39}$$

For the present system this velocity is approximately 14 ft./sec. but the correlation was extended up to 15.5 ft./sec. without detriment to the model. However, this fact is not important because from the practical point of view it would not be economic to transport hematite at 14 ft./sec.

The equation proposed by Kriegel-Brauer represents a good alternative when its parameter is fitted by experimental data, otherwise it is advisable to use Durand's equation.

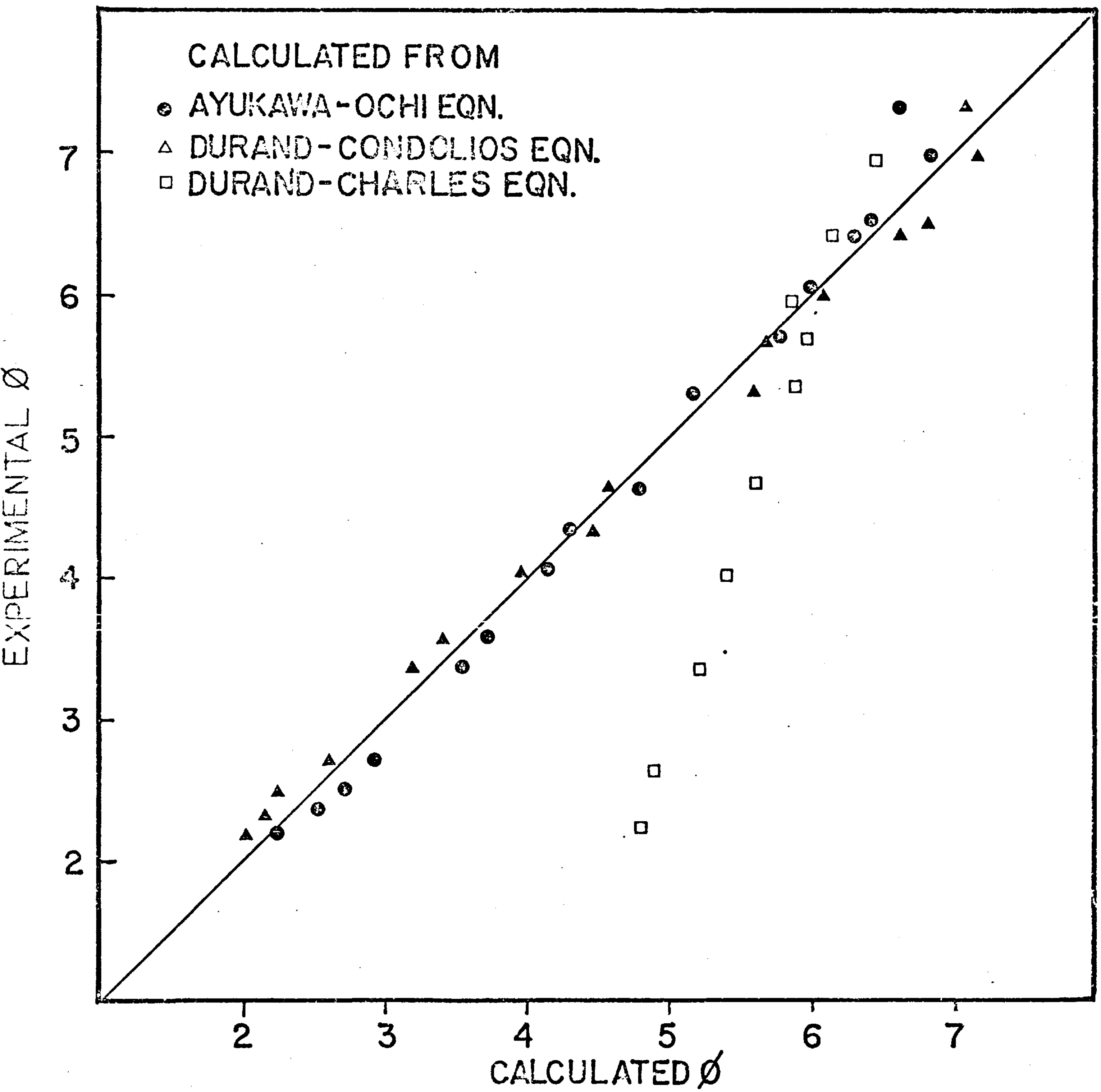

FIG. 1.15 Experimental ø vs. predicted ø

1.7 CONCLUSIONS

- The studies on the turbulent flow of hematite-water suspensions indicated that this mixture behaves as "settling slurries".

- The hematite mineral can be slurried and conveyed in a 2 inch-diameter and horizontal duct. Three flow regimes were observed:

  (a) stationary bed with saltation at velocities below 7.0 ft./sec., depending on concentration of solids.

  (b) intermediate flow regime with unstable tendency of bed formation. (7. - 10. ft./sec.)

  (c) heterogeneous flow regime with full suspension of particles at velocities greater than 10.5 ft./sec. when the delivered concentration of solids is lower than 25% by volume.

The limit deposit velocity shows dependency on the delivered concentration of solids.

- A sequential discrimination of model using the Bayesian Approach and a design of experiments using the Roth Criterion indicated that the best model to correlate hydraulic gradients for these suspensions in the heterogeneous flow regime is the one proposed by Ayukawa-Ochi (1968). These experiments also showed that the difference between experimental and predicted data increase with the increasing concentration of solids and are significant at velocities near the limit deposit velocity.

1.8 BIBLIOGRAPHY PART I.

Ayukawa, K. and J. Ochi,
Memoirs of the Ehime University.
Sect. III (Engineering) Vol. VI, 1, (1968).

Babcock, H.A.,
Paper presented to Int. Symp. on solid-liquid flow.
Univ. of Pennsylvania, Philadelphia (1968).

Blatch, N.S.,
Trans. A.S.C.E., 57, (1902).

Bonnington, S.T.,
B.H.R.A., RR 637, (1958).

Box, G.E.P. and W.J. Hill,
Technometrics, 9, 57 (1967).

Brebner, A.,
C.E. Research Report # 21 (1962).
Queen's University.

Castro, L.O., Carniero, B.P. and Tavares, H.L.,
Engenh. Miner. Metal., 39, (1964).

Carstens, M.R.,
Proc. A.S.C.E., 95, HY1, (1969).

Charles, M.E.,
Proc. Canadian Transportation Research Forum,
Toronto (1969).

-Proc. 1st Int. Conf. Hydraul. Transp. Solids in Pipes
(HYDROTRANSPORT 1), B.H.R.A., (1970).

Clarke, B.,
Trans. Inst. Chem. Eng., 45, 6, (1967).

Condolios, E. and E. Chapus,
Chemical Engineering, July, (1963).

Durand, R. and E. Condolios,
Paper presented to the 2nd Conference of the Soc. Hyd.
de France, Grenoble, (1952).

-Proc. Int. Assn for Hydr. Research,
Minneapolis (1953).

-La Houille Blanche, 9, 3, (1954).

Gay, E.C., Nelson, P.A. and W.P. Armstrong,
AIChE Journal, 15, 6, (1969).

Kriegel, E. and H. Brauer,
VDI-Forschungsheft, 515, (1966).

Linford, A. and D.H. Saunders,
B.H.R.A., RR 1015, (1969).

Nardi, J.,
Pipeline News, Aug., (1959).

Newitt, D.M., Richardson, J.F., Abbott, M., and R.N. Turtle,
Trans. Inst. Chem. Eng., 33, (1955).

Newitt, D.M., Richardson, J.F. and C.A. Shook,
Proc. 3rd Congress of the European Federation of Chemical Engineering, London. (1962).

Reilly, P.M.,
Can. Journal of Chem. Eng., 48, (1970).

Roth, P.M.,
Ph.D. Thesis, Princeton University (1965).

Round, G.F. and H.S. Ellis,
Trans. Can. Inst. Min. Met., 66, (1963).

Spells, K.E.,
Trans. Inst. Chem. Eng., 33, (1955).

Streeter, V.L.,
Fluid Mechanics.
McGraw-Hill Book Co. (1966).

Sinclair, G.C.,
Ph.D. Thesis. Univ. of Sydney. (1960).

Tchen, C.M.,
Ph.D. Thesis, Delft Univ. (1947).

Toda M., Konno, H., Saito, S.,Maeda,S.,
Int. Chem. Eng., 9, 3, (1969).

Thomas, D.G.,
AIChE Journal, 7, (1961).

Watanabe, Y.,
Jnl. Coal Res. Inst., 9, (1958).

Wayment, W.R., Wilhelm, G.L. and J.D. Bardill.
U.S. Dept. of the Interior, Rep 6065 (1962).

Wilson, W.E.,
Trans. A.S.C.E., 107, (1942).

Williams, P.S.,
J. Appl. Chem., 3, 120, (1953).

Worster, R.C.,
3rd Annual Conference, B.H.R.A., (1954).

Zandi, I.,
J. Am. W.W. Ass., 59, 2, (1967).

1.9 SYMBOLS.

A	Posterior mean estimate of Θ.
B	Least square estimate of parameter Θ.
C_D	Drag coefficient.
C_v	Delivered volumetric concentration of solids.
d	Particle diameter
D	Pipe diameter.
D_f	likelihood density function.
f	Friction factor.
F_r	Froude Number.
g	Acceleration of gravity.
h_m	Hydraulic gradient due to suspension.
h_w	Hydraulic gradient for clear water.
Re	Reynolds Number.
s	specific gravity.
P_r	Probability.
U	Mean velocity.
U_c	Limit deposit velocity.
U_j	Covariance parameter matrix.
w	particle settling velocity.
v	Kinematic viscosity.
x	Independent variable.
X	differential matrix.
y	Dependent variable.
Z	Auxiliar variable (Roth Criterion).

α Prior estimate of parameter θ.

μ Difference between experimental and predicted value of the dependent variable.

σ^2 Variance.

ρ Density of clear water.

ω Fraction by weight.

θ Parameter to be determined by experiments.

TABLE 1.1

EXPERIMENTAL DATA UNDER STEADY STATE CONDITIONS.

FLOW USGPM	U FEET/SEC	ΔP PSI	GRAD. Ft. WATER/100 Ft. Pipe.
68.17	6.9670	1.2997	9.4677
68.17	6.9670	1.3175	9.5974
68.62	7.0133	1.3068	9.5196
68.62	7.0133	1.3140	9.5714
68.62	7.0133	1.3175	9.5974
68.62	7.0133	1.3104	9.5455
70.43	7.1984	1.3353	9.7271
70.43	7.1984	1.3442	9.7919
70.43	7.1984	1.3531	9.8568
74.96	7.6611	1.5134	11.0240
74.96	7.6611	1.5045	10.9592
74.96	7.6611	1.5045	10.9592
74.96	7.6611	1.5525	11.3093
74.96	7.6611	1.5668	11.4131
74.96	7.6611	1.5597	11.3612
74.96	7.6611	1.5312	11.1537
74.96	7.6611	1.5241	11.1018
81.00	8.2781	1.7359	12.4452
81.00	8.2781	1.6825	12.2561
81.00	8.2781	1.7270	12.5803
81.00	8.2781	1.7377	12.6581
81.00	8.2781	1.7448	12.7101
81.00	8.2781	1.8089	13.1769
81.00	8.2781	1.7947	13.0732
81.00	8.2781	1.7377	12.6581
90.05	9.2035	2.0475	14.9148
90.05	9.2035	2.0030	14.5906
90.05	9.2035	2.0920	15.2391
90.05	9.2035	2.0297	14.7851
90.05	9.2035	2.0226	14.7332
90.05	9.2035	2.0297	14.7852
90.05	9.2035	2.0795	15.1483
90.05	9.2035	2.0653	15.0445
90.05	9.2035	2.0938	15.2520
96.09	9.8205	2.2700	16.5360
96.09	9.8205	2.2344	16.2766
96.09	9.8205	2.2612	16.4711
96.09	9.8205	2.2362	16.2896
96.09	9.8205	2.2220	16.1858
96.09	9.8205	2.2932	16.7046
96.09	9.8205	2.2790	16.6009
96.09	9.8205	2.2647	16.4971
105.14	10.7460	2.6261	19.1299
105.14	10.7460	2.5727	18.7408
105.14	10.7460	2.6261	19.1299
105.14	10.7460	2.5994	18.9353

105.14	10.7460	2.5567	18.6241
105.14	10.7460	2.5638	18.6760
105.14	10.7460	2.6564	19.3504
105.14	10.7460	2.6706	19.4541
105.14	10.7460	2.6635	19.4022
111.18	11.3629	2.8487	20.7510
111.18	11.3629	2.7686	20.1674
111.18	11.3629	2.8309	20.6214
111.18	11.3629	2.8416	20.6992
111.18	11.3629	2.7775	20.2323
111.18	11.3629	2.8131	20.4917
111.18	11.3629	2.8487	20.7511
111.18	11.3629	2.7917	20.3360
120.24	12.2884	3.2493	23.6692
120.24	12.2884	3.2582	23.7340
120.24	12.2884	3.1692	23.0855
120.24	12.2884	3.2048	23.3449
120.24	12.2884	3.2333	23.5525
120.24	12.2884	3.1692	23.0855
120.24	12.2884	3.3401	24.3307
120.24	12.2884	3.2190	23.4487
120.24	12.2884	3.2333	23.5525
129.29	13.2139	3.6588	26.6521
129.29	13.2139	3.5164	25.6146
129.29	13.2139	3.7122	27.0412
129.29	13.2139	3.6463	26.5614
129.29	13.2139	3.5609	25.9388
129.29	13.2139	3.7033	26.9764
129.29	13.2139	3.7389	27.2356
135.33	13.8308	3.9971	29.1163
135.33	13.8308	3.8279	27.8842
135.33	13.8308	4.0950	29.8297
135.33	13.8308	4.0060	29.1812
135.33	13.8308	3.9098	28.4809
135.33	13.8308	3.8457	28.0140
135.33	13.8308	3.9098	28.4809
135.33	13.8308	4.0594	29.5703
135.33	13.8308	4.0238	29.3109
141.36	14.4478	4.3621	31.7750
141.36	14.4478	4.3264	31.5156
141.36	14.4478	4.0950	29.8297
141.36	14.4478	4.2303	30.8153
141.36	14.4478	4.4796	32.6310
141.36	14.4478	4.4155	32.1642
141.36	14.4478	4.4084	32.1123
150.42	15.3733	4.6576	33.9280
150.42	15.3733	4.6291	33.7205
150.42	15.3733	4.8517	35.3416
150.42	15.3733	4.8161	35.0822
150.42	15.3733	4.5401	33.0720
150.42	15.3733	4.5401	33.0720

TABLE 1.2

FRICTION FACTORS.

	PRANDTL MODEL		BLAUSIUS MODEL		
f EXP.	f	DIF.	f	DIF.	Re
.020923	.020988	-.000065	.020972	-.000049	69520.84
.021210	.020988	.000222	.020972	.000238	69520.84
.020761	.020932	-.000171	.020919	-.000157	69982.58
.020875	.020932	-.000056	.020919	-.000044	69982.58
.020931	.020932	-.000001	.020919	.000012	69982.58
.020818	.020932	-.000114	.020919	-.000101	69982.58
.020137	.020714	-.000577	.020710	-.000573	71829.54
.020271	.020714	-.000443	.020710	-.000439	71829.54
.020405	.020714	-.000309	.020710	-.000305	71829.54
.020148	.020205	-.000056	.020220	-.000072	76446.96
.020030	.020205	-.000175	.020220	-.000190	76446.96
.020030	.020205	-.000175	.020220	-.000190	76446.96
.020670	.020205	.000465	.020220	.000450	76446.96
.020859	.020205	.000655	.020220	.000639	76446.96
.020765	.020205	.000560	.020220	.000544	76446.96
.020385	.020205	.000181	.020220	.000165	76446.96
.020290	.020205	.000086	.020220	.000070	76446.96
.019795	.019595	.000199	.019627	.000167	82603.51
.019186	.019595	-.000410	.019627	-.000442	82603.51
.019693	.019595	.000098	.019627	.000066	82603.51
.019815	.019595	.000220	.019627	.000188	82603.51
.019896	.019595	.000301	.019627	.000269	82603.51
.020627	.019595	.001032	.019627	.001000	82603.51
.020465	.019595	.000869	.019627	.000837	82603.51
.019815	.019595	.000220	.019627	.000188	82603.51
.018888	.018803	.000085	.018844	.000044	91838.33
.018478	.018803	-.000325	.018844	-.000366	91838.33
.019299	.018803	.000496	.018844	.000455	91838.33
.018724	.018803	-.000079	.018844	-.000120	91838.33
.018658	.018803	-.000144	.018844	-.000185	91838.33
.018724	.018803	-.000079	.018844	-.000120	91838.33
.019184	.018803	.000381	.018844	.000340	91838.33
.019052	.018803	.000250	.018844	.000209	91838.33
.019315	.018803	.000513	.018844	.000472	91838.33
.018393	.018339	.000053	.018380	.000013	97994.88
.018104	.018339	-.000235	.018380	-.000275	97994.88
.018320	.018339	-.000019	.018380	-.000059	97994.88
.018119	.018339	-.000221	.018380	-.000261	97994.88
.018003	.018339	-.000336	.018380	-.000376	97994.88
.018580	.018339	.000241	.018380	.000201	97994.88
.018465	.018339	.000125	.018380	.000085	97994.88
.018349	.018339	.000010	.018380	-.000030	97994.88
.017771	.017723	.000048	.017754	.000016	107229.71
.017409	.017723	-.000313	.017754	-.000345	107229.71
.017771	.017723	.000048	.017754	.000016	107229.71
.017590	.017723	-.000133	.017754	-.000164	107229.71

.017301	.017723	-.000422	.017754	-.000454	107229.71
.017349	.017723	-.000374	.017754	-.000405	107229.71
.017975	.017723	.000253	.017754	.000221	107229.71
.018072	.017723	.000349	.017754	.000318	107229.71
.018024	.017723	.000301	.017754	.000269	107229.71
.017240	.017355	-.000115	.017377	-.000137	113386.26
.016755	.017355	-.000600	.017377	-.000622	113386.26
.017132	.017355	-.000222	.017377	-.000245	113386.26
.017197	.017355	-.000158	.017377	-.000180	113386.26
.016809	.017355	-.000546	.017377	-.000568	113386.26
.017025	.017355	-.000330	.017377	-.000353	113386.26
.017240	.017355	-.000115	.017377	-.000137	113386.26
.016895	.017355	-.000459	.017377	-.000482	113386.26
.016814	.016857	-.000043	.016862	-.000048	122621.08
.016860	.016857	.000003	.016862	-.000002	122621.08
.016399	.016857	-.000457	.016862	-.000463	122621.08
.016584	.016857	-.000273	.016862	-.000278	122621.08
.016731	.016857	-.000126	.016862	-.000131	122621.08
.016400	.016857	-.000457	.016862	-.000463	122621.08
.017284	.016857	.000427	.016862	.000422	122621.08
.016657	.016857	-.000199	.016862	-.000205	122621.08
.016731	.016857	-.000126	.016862	-.000131	122621.08
.016374	.016413	-.000039	.016398	-.000024	131855.91
.015737	.016413	-.000676	.016398	-.000662	131855.91
.016613	.016413	.000200	.016398	.000215	131855.91
.016318	.016413	-.000095	.016398	-.000080	131855.91
.015936	.016413	-.000477	.016398	-.000462	131855.91
.016573	.016413	.000160	.016398	.000175	131855.91
.016733	.016413	.000320	.016398	.000334	131855.91
.016328	.016142	.000186	.016113	.000215	138012.45
.015637	.016142	-.000505	.016113	-.000476	138012.45
.016728	.016142	.000586	.016113	.000615	138012.45
.016364	.016142	.000222	.016113	.000251	138012.45
.015971	.016142	-.000171	.016113	-.000142	138012.45
.015709	.016142	-.000433	.016113	-.000404	138012.45
.015971	.016142	-.000171	.016113	-.000142	138012.45
.016582	.016142	.000440	.016113	.000469	138012.45
.016437	.016142	.000295	.016113	.000324	138012.45
.016329	.015889	.000440	.015845	.000484	144169.00
.016196	.015889	.000307	.015845	.000351	144169.00
.015329	.015889	-.000560	.015845	-.000516	144169.00
.015836	.015889	-.000053	.015845	-.000009	144169.00
.016769	.015889	.000880	.015845	.000924	144169.00
.016529	.015889	.000640	.015845	.000684	144169.00
.016502	.015889	.000613	.015845	.000658	144169.00
.015399	.015539	-.000139	.015471	-.000072	153403.83
.015305	.015539	-.000233	.015471	-.000166	153403.83
.016041	.015539	.000503	.015471	.000570	153403.83
.015923	.015539	.000385	.015471	.000452	153403.83
.015011	.015539	-.000528	.015471	-.000460	153403.83
.015011	.015539	-.000528	.015471	-.000460	153403.83

TABLE 1.3

PARTICLE SIZE DISTRIBUTION OF HEMATITE.

U.S. STANDARD MESH	WEIGHT %	CUMULATIVE %
+ 18	16.24	16.24
+ 25	16.92	33.16
+ 40	28.67	61.83
+ 50	13.96	75.79
+ 70	9.28	85.07
+ 100	7.24	92.31
+ 140	4.44	96.75
+ 170	1.13	97.88
+ 200	1.32	99.20
+ 270	0.35	99.55
+ 325	0.34	99.99
- 400	0.ol	-

TABLE 1.4

SETTLING VELOCITY AND MEAN PARTICLE DIAMETER.

w (feet/sec)	d_i (inches)
0.7690	0.0501
0.5944	0.0336
0.4250	0.0215
0.2905	0.0141
0.1985	0.0100
0.1349	0.0071
0.1100	0.0050
0.0761	0.0038
0.0634	0.0032
0.05357	0.0025
0.044	0.0019

TABLE 1.5

EXPERIMENTAL COORDINATES.

SEQ.	C_v	U	h_m
1	.1120	11.360	.3249
2	.0710	15.370	.3891
3	.2530	12.280	.4841
4	.1960	15.980	.5090
5	.2416	10.520	.4615
6	.2510	10.520	.4735
7	.2500	10.520	.4729
8	.2490	10.256	.4701
9	.2530	10.830	.4736
10	.2530	11.050	.4752
11	.2480	15.090	.5238
12	.2480	15.380	.5321
13	.2500	13.210	.4950
14	.1910	15.010	.4782
15	.1900	13.520	.4439
16	.1880	10.570	.4008
17	.1520	15.340	.4541
18	.1500	12.570	.3864
19	.1480	11.000	.3612
20	.1080	10.350	.3127
21	.1110	13.390	.3643
22	.1140	14.860	.4081
23	.0685	9.950	.2642
24	.0700	11.890	.2901
25	.0710	13.260	.3231
26	.0700	14.490	.3598
27	.0720	15.660	.3987

TABLE 1.6

PREDICTED PRESSURE GRADIENTS USING LEAST SQ. ESTIMATES.*

SEQ.	EXP.	M-1	M-2	M-3	M-4
1	.3249	.3304	.3072	.3194	.3203
2	.3891	.3865	.4356	.3933	.3928
3	.4841	.4893	.4928	.4802	.4811
4	.5090	.4953	.6557	.5174	.5157
5	.4615	.4738	.4241	.4507	.4526
6	.4735	.4813	.4481	.4649	.4664
7	.4729	.4783	.4539	.4659	.4670
8	.4701	.4783	.4475	.4638	.4651
9	.4736	.4762	.4769	.4738	.4742
10	.4752	.4747	.4856	.4761	.4761
11	.5238	.5041	.7129	.5459	.5426
12	.5321	.5108	.7324	.5519	.5487
13	.4950	.4805	.5977	.5028	.5013
14	.4782	.4625	.6186	.4904	.4883
15	.4439	.4332	.5330	.4509	.4497
16	.4008	.4066	.3914	.3921	.3934
17	.4541	.4421	.5761	.4652	.4634
18	.3864	.3820	.4329	.3895	.3891
19	.3612	.3615	.3631	.3547	.3553
20	.3127	.3085	.2944	.2978	.2987
21	.3643	.3624	.4184	.3722	.3716
22	.4081	.4015	.4915	.4172	.4160
23	.2642	.2535	.2384	.2439	.2447
24	.2901	.2906	.3048	.2915	.2915
25	.3231	.3242	.3582	.3300	.3296
26	.3598	.3572	.4075	.3661	.3654
27	.3987	.3943	.4623	.4057	.4048

* The models are presented in figure 1.5

TABLE 1.7

PREDICTED PRESSURE GRADIENTS USING POSTERIOR MEAN ESTIMATES.

SEQ.	EXP.	M-1	M-2	M-3	M-4
1	.3249	.3304	.3072	.3194	.3203
2	.3891	.3865	.4356	.3933	.3928
3	.4841	.4893	.4928	.4802	.4811
4	.5090	.4953	.6557	.5174	.5157
5	.4615	.4847	.3822	.4435	.4466
6	.4735	.4820	.4398	.4651	.4664
7	.4729	.4768	.4548	.4678	.4685
8	.4701	.4773	.4493	.4663	.4671
9	.4736	.4735	.4857	.4774	.4772
10	.4752	.4720	.4925	.4788	.4783
11	.5238	.5018	.7146	.5492	.5452
12	.5321	.5119	.7324	.5515	.5481
13	.4950	.4854	.5963	.4991	.4980
14	.4782	.4662	.6170	.4878	.4860
15	.4439	.4390	.5306	.4469	.4463
16	.4008	.4158	.3867	.3866	.3886
17	.4541	.4456	.5746	.4630	.4616
18	.3864	.3876	.4318	.3860	.3861
19	.3612	.3679	.3627	.3507	.3519
20	.3127	.3130	.2935	.2954	.2966
21	.3643	.3656	.4189	.3715	.3710
22	.4081	.4042	.4929	.4160	.4150
23	.2642	.2566	.2404	.2424	.2434
24	.2901	.2935	.3078	.2916	.2917
25	.3231	.3265	.3598	.3300	.3297
26	.3598	.3590	.4082	.3657	.3651
27	.3987	.3961	.4623	.4050	.4043

* The models are presented in figure 1.5

TABLE 1.8

ESTIMATED VALUES OF PARAMETERS AFTER EACH ITERATION.*

DURAND		CHARLES		KRIEGEL		AYUKAWA	
A	B	A	B	A	B	A	B
122.91	122.91	9.16	9.16	54.43	54.43	.05124	.05124
117.28	113.59	28.39	41.04	56.67	58.14	.05296	.05409
115.71	113.98	34.60	41.43	57.44	58.34	.05357	.05427
115.13	114.20	37.34	41.65	57.82	58.45	.05387	.05438
114.23	112.40	39.92	45.18	58.06	58.57	.05405	.05442
114.24	114.26	38.57	35.10	57.85	57.29	.05386	.05338
114.55	115.54	36.83	31.47	57.68	57.12	.05372	.05328
117.44	128.65	35.74	31.47	56.35	51.20	.05266	.04856
119.78	130.71	34.98	31.47	55.44	51.34	.05195	.04874
120.59	124.88	34.42	31.47	55.28	54.49	.05185	.05131
121.98	130.50	34.01	31.47	54.82	52.12	.05150	.04942
122.43	125.52	33.69	31.47	54.70	53.89	.05141	.05081
121.50	114.63	34.56	41.04	55.16	58.48	.05177	.05441

A Posterior mean estimate.

B Least Squares estimate.

* The models are presented in figure 1.5

TABLE 1.9

PREDICTED COEFFICIENTS Ø USING THE POSTERIOR MEAN ESTIMATES.*

SEQ.	EXP.	M-1	M-2	M-3	M-4
1	5.3675	5.6103	4.5882	5.1247	5.1643
2	2.3736	2.2652	4.3389	2.5529	2.5315
3	4.3515	4.4415	4.5011	4.2847	4.2999
4	2.2127	2.0155	4.3203	2.3330	2.3087
5	6.5288	7.0644	4.6966	6.1127	6.1852
6	6.5513	6.7413	5.8020	6.3636	6.3927
7	6.5641	6.6508	6.1587	6.4504	6.4663
8	6.9723	7.1414	6.4861	6.8825	6.9025
9	6.0193	6.0177	6.2731	6.0998	6.0942
10	5.7307	5.6658	6.0828	5.8037	5.7936
11	2.5055	2.2310	4.8873	2.8225	2.7723
12	2.4043	2.1602	4.8273	2.6386	2.5978
13	3.6253	3.4772	5.1855	3.6886	3.6709
14	2.5823	2.3863	4.8512	2.7389	2.7093
15	3.3988	3.3030	5.0909	3.4576	3.4447
16	6.4956	6.9376	6.0788	6.0763	6.1366
17	2.4219	2.2525	4.8107	2.5988	2.5697
18	4.0942	4.1269	5.3579	4.0838	4.0860
19	5.9185	6.1534	5.9715	5.5511	5.5935
20	7.3445	7.3609	6.3268	6.4236	6.4886
21	3.3532	3.3988	5.2067	3.5986	3.5818
22	2.5926	2.4839	4.9538	2.8136	2.7860
23	8.9814	8.3014	6.8529	7.0370	7.1237
24	4.6737	4.8929	5.8300	4.7687	4.7765
25	3.3329	3.5172	5.3117	3.7049	3.6890
26	2.7223	2.6866	5.0079	2.9999	2.9737
27	2.2370	2.1300	4.8077	2.4931	2.4623

* The models are presented in figure 1.5

TABLE 1.10

PREDICTED COEFFICIENTS Ø USING LEAST SQ. ESTIMATES

SEQ.	EXP.	M-1	M-2	M-3	M-4
1	5.3675	5.6103	4.5882	5.1247	5.1643
2	2.3736	2.2652	4.3389	2.5529	2.5315
3	4.3515	4.4415	4.5011	4.2847	4.2999
4	2.2127	2.0155	4.3203	2.3330	2.3087
5	6.5288	6.8133	5.6651	6.2781	6.3237
6	6.5513	6.7253	5.9870	6.3601	6.3927
7	6.5641	6.6850	6.1399	6.4069	6.4323
8	6.9723	7.1637	6.4446	6.8257	6.8552
9	6.0193	6.0738	6.0883	6.0238	6.0309
10	5.7307	5.7198	5.9431	5.7493	5.7499
11	2.5055	2.2591	4.8662	2.7815	2.7397
12	2.4043	2.1461	4.8276	2.6439	2.6046
13	3.6253	3.4026	5.2078	3.7458	3.7223
14	2.5823	2.3264	4.8774	2.7814	2.7466
15	3.3988	3.1906	5.1380	3.5350	3.5113
16	6.4956	6.6660	6.2189	6.2405	6.2786
17	2.4219	2.1842	4.8403	2.6421	2.6067
18	4.0942	3.9726	5.3883	4.1811	4.1695
19	5.9185	5.9276	5.9851	5.6887	5.7128
20	7.3445	7.1205	6.3741	6.5547	6.6031
21	3.3532	3.2891	5.1879	3.6229	3.6001
22	2.5926	2.4078	4.9147	2.8457	2.8126
23	8.9814	8.0288	6.6768	7.1726	7.2420
24	4.6737	4.7050	5.6322	4.7658	4.7664
25	3.3329	3.3919	5.2242	3.7058	3.6848
26	2.7223	2.5997	4.9779	3.0185	2.9875
27	2.2370	2.0600	4.8100	2.5214	2.4853

TABLE 1.11

POSTERIOR MODEL PROBABILITIES AFTER EACH ITERATION.*

SEQ.	M-1	M-2	M-3	M-4
4	.3415	.0000	.3063	.3522
5	.2580	.0000	.3159	.4261
6	.2506	.0000	.3119	.4376
7	.2519	.0000	.3088	.4393
8	.2337	.0000	.3139	.4524
9	.2391	.0000	.3108	.4500
10	.2394	.0000	.3093	.4513
11	.2565	.0000	.2243	.5192
12	.2043	.0000	.1938	.6019
13	.1736	.0000	.1982	.6281
14	.1482	.0000	.1925	.6593
15	.1428	.0000	.1924	.6648
16	.1241	.0000	.1769	.6990

---

* The models are presented in figure 1.5

APPENDIX 1.10.1

COMPUTER PROGRAM FOR DISCRIMINATION OF MODELS.

```
      COMMON/UNO/RHO,VIS,DIA,D,S,W
      COMMON/DOS/HM(30),U(30),CV(30),FR(30),FI(30),PSI(30),HW(30)
      COMMON/CUATRO/UU(5,30),X(5,30),V(5,5,5),Y(5,30)
      COMMON/CINCO/ NMODEL,ALPHA(5),BETA(5),PRPRE(5),PRPOST(5),SU(5),
     1PHI1,PHI3,PHI4
      COMMON/OCHO/PHI(4,30),SSQ(5),RATIO(4,30),R(30)


      READ(5,10) RHO,VIS,DIA,D,S,W
      READ(5,20)(SU(M),M=1,5)
      READ(5,30) SIGMA
      READ(5,35)(PRPRE(M), M=1,5)

      DO 40  M=1,4
      DO 40  J=1,4
      DO 40  I=1,4
 40   V(M,J,I) = 0.0
      DO 50  M=1,4
      DO 50  J=1,4
 50   V(M,J,J) = SIGMA

      NORMALIZATION OF AUXILIAR CONSTANTS
      D = D/12.
      PHI1 = (W/SQRT(32.174*D))**1.5
      PHI3 = W
      PHI4 = (D/DIA)**(-0.707)*(SQRT(32.174*D*(S-1.)))**(2.72)/W**2

 60   READ(5,70)NEXP,NINIT,NTOTAL,NCOUNT,NMODEL
      ITER = 1
      IF(NTOTAL.NE.NINIT) ITER=NTOTAL
      READ(5,80)(CV(I),U(I),HM(I), I=ITER,NTOTAL)

 85   CONTINUE
      IF(NTOTAL.GT.30) GO TO 150

      SUBROUTINE LEASQ RETURNS THE BEST ESTIMATES OF THE PARAMETERS.
      CALL LEASQ(NINIT,NEXP,NTOTAL)

      SUBROUTINE GRAD RETURNS VECTORS X AND UU.
      CALL GRAD(NTOTAL,NEXP,NINIT)

      WRITE(6,100)
     1*M5*,//)
      WRITE(6,110)(BETA(M), M=1,NMODEL)
      WRITE(6,111)(ALPHA(M), M=1,NMODEL)
      WRITE(6,114)(SU(M), M=1,NMODEL)
      WRITE(6,112)(PRPRE(M), M=1,NMODEL)

      SUBROUTINE BAYES PERFORMS BAYESIAN ANALYSIS.
      CALL BAYES(NTOTAL,NEXP,NINIT,SIGMA)

      WRITE(6,113)(PRPOST(M), M=1,NMODEL)
      WRITE(6,120)
      WRITE(6,130)(CV(I),U(I),HM(I), (Y(M,I),UU(M,I), M=1,NMODEL),
     1I=1,NTOTAL)

      SUBROUTINE ROTH RETURNS THE NEW EXPERIMENTAL COORD NATES.
      CALL ROTH(NINIT,NEXP,CVEXP,UEXP)
```

```
      WRITE(6,140) CVEXP, UEXP
      IF(NCOUNT.EQ.1)GO TO 60

150 CONTINUE

10    FORMAT(6F10.0)
20    FORMAT(5F10.0)
30    FORMAT(F10.0)
35    FORMAT(5F10.0)
70    FORMAT(5I5)
80    FORMAT(3F10.0)
100 FORMAT(1H1,///,53X, *M1*, 13X, *M2*, 13X, *M3*, 13X, *M4*, 13X,
110 FORMAT(/,X,*BETA*,36X, 5E15.5)
111 FORMAT(/,X,*ALPHA*,35X,5E15.5)
114 FORMAT(/,X,*SU*,38X, 5E15.5)
112 FORMAT(/,X,*PRPRE*, 35X, 5E15.5)
113 FORMAT(/,X,*PRPOST*, 35X, 5E15.5)
120 FORMAT(/,8X,*CV*,9X,*U*,8X,*HM*)
130 FORMAT(3F10.4, 8X, 4(2F8.4, 4X))
140 FORMAT(//,2X,*NEW EXPERIMENTAL COORDINATES*, 10X, *CV*, F10.4,
     110X, *U*, F10.4)

      STOP
      END




      SUBROUTINE GRAD(NTOTAL,NEXP,NINIT)

      COMMON/UNO/RHO,VIS,DIA,D,S,W
      COMMON/DOS/HM(30),U(30),CV(30),FR(30),FI(30),PSI(30),HW(30)
      COMMON/CUATRO/UU(5,30),X(5,30),V(5,5,5),YMODEL(5,30)
      COMMON/CINCO/ NMODEL,ALPHA(5),BETA(5),PRPRE(5),PRPOST(5),SU(5),
     1PHI1,PHI3,PHI4
      COMMON/OCHO/PHI(4,30),SSQ(5),RATIO(4,30),R(30)
      DIMENSION F(30)

      IF(NTOTAL.GT.NINIT) GO TO 15
      DO 10  M=1,NMODEL
      ALPHA(M) = BETA(M)
      SSQ(M) = 0.
10    CONTINUE

15    ITER = NTOTAL
      IF(NEXP.EQ.NINIT) ITER = 1
      DO 20  I=ITER,NTOTAL
      YMODEL(1,I) = HW(I) + ALPHA(1)*CV(I)*HW(I)*((S-1.0)**0.75)*PHI1/
     1FR(I)**1.5
      UU(1,I) = HM(I) - YMODEL(1,I)
      X(1,I) = CV(I)*HW(I)*((S-1.)**0.75)*PHI1/FR(I)**1.5
      PHI(1,I) = ALPHA(1)*((S-1.)**0.75)*PHI1/FR(I)**1.5
      SSQ(1) = SSQ(1) + UU(1,I)*UU(1,I)

      YMODEL(2,I) = HW(I) + ALPHA(2)*CV(I)*HW(I)*((S-1.0)**0.75)*PHI1/
```

```
   1FR(I)**1.5 + CV(I)*HW(I)*(S-1.0)
    UU(2,I) = HM(I) -YMODEL(2,I)
    X(2,I) = X(1,I)
    PHI(2,I) = ALPHA(2)*PHI(1,I)/ALPHA(1) + S-1.
    SSQ(2) = SSQ(2) + UU(2,I)*UU(2,I)

    YMODEL(3,I) = HW(I) + ALPHA(3)*0.282*(S-1.)*CV(I)*((PHI3**3/
   1(32.174*VIS))**(1./3.))*(FR(I)**(-4./3.))*(U(I)**2)/(2.0*32.174*
   2DIA)
    UU(3,I) = HM(I) - YMODEL(3,I)
    X(3,I) = 0.282*(S-1.)*CV(I)*((PHI3**3/(32.174*VIS))**(1./3.))*
   1(FR(I)**(-4./3.))*U(I)**2/(2.0*32.174*DIA)
    CALL FRIC(F(I),U(I))
    PHI(3,I) = ALPHA(3)*0.282*(S-1.)*(PHI3**3/(32.174*VIS))**(1./3.)*
   1FR(I)**(-4./3.)
    PHI(3,I) = PHI(3,I)/F(I)
    SSQ(3) = SSQ(3) + UU(3,I)*UU(3,I)

    YMODEL(4,I) = HW(I) + ALPHA(4)*1.80*32.174*(S-1.)*DIA*CV(I)*
   1(U(I)**(-2.72))*PHI4*U(I)**2/(2.0*32.174*DIA)
    UU(4,I) = HM(I) - YMODEL(4,I)
    X(4,I) = 1.80*32.174*(S-1.)*DIA*CV(I)*(U(I)**(-2.72))*PHI4*
   1U(I)**2/(2.0*32.174*DIA)
    PHI(4,I) = ALPHA(4)*1.80*32.174*(S-1.)*DIA*U(I)**(-2.72)*PHI4
    PHI(4,I) = PHI(4,I)/F(I)
    SSQ(4) = SSQ(4) + UU(4,I)*UU(4,I)
20  CONTINUE
    RETURN
    END




    SUBROUTINE BAYES(NTOTAL,NEXP,NINIT,SIGMA)

    COMMON/CUATRO/ UU(5,30),X(5,30),V(5,5,5),YMODEL(5,30)
    COMMON/CINCO/ NMODEL,ALPHA(5), BETA(5), PRPRE(5), PRPOST(5),SU(5)
    DIMENSION AUX(5,5), AUX1(5,5,5), VAR(5,5,5), AUX2(5,5,5),
   1AUX3(5,5,5), DETVAR(5), DETAUX(5), DF(5), AUX4(5,30), AUX5(5),
   2VAR1(5,30)


    IF(NEXP.NE.NINIT) GO TO 65
    DO 10  M=1,NMODEL
    DO 10  I=1,NINIT
    AUX(M,I) = SU(M)*X(M,I)
10  CONTINUE
    DO 20  M=1,NMODEL
    DO 20  I=1,NINIT
    DO 20  J=1,NINIT
    AUX1(M,I,J) = AUX(M,I)*X(M,J)
20  CONTINUE
    DO 30  M= 1,NMODEL
    DO 30  I=1,NINIT
    DO 30  J=1,NINIT
    VAR(M,I,J) = V(M,I,J) + AUX1(M,I,J)
```

```
30   CONTINUE
     DO 40   M=1,NMODEL
     DO 40   I=1,NINIT
     DO 40   J=1,NINIT
     AUX2(M,I,J) = UU(M,I)*UU(M,J)
40   CONTINUE

     DO 50   M=1,NMODEL
     DO 50   I=1,NINIT
     DO 50   J=1,NEXP
     AUX3(M,I,J) = VAR(M,I,J) + AUX2(M,I,J)
50   CONTINUE

     SUBROUTINE DETER RETURNS THE DETERMINANTS OF VAR AND AUX3
     DO 60   M=1,NMODEL
     CALL DETER(NINIT,DETAUX(M),AUX3,M)
     CALL DETER(NINIT,DETVAR(M),VAR,M)
60   CONTINUE
     GO TO 66
65   CONTINUE
     DO 66 M=1,NMODEL
     VAR1(M,NTOTAL) = X(M,NTOTAL)*SU(M)*X(M,NTOTAL) + SIGMA
     DETVAR(M) = VAR1(M,NTOTAL)
     DETAUX(M) = VAR1(M,NTOTAL) + UU(M,NTOTAL)*UU(M,NTOTAL)
66   CONTINUE

     CALCULATION OF THE LIKELIHOOD FUNCTIONS.
     DO 70   M=1,NMODEL
     Z = -0.5*(DETAUX(M)/DETVAR(M) - 1.0)
     DF(M) = EXP(Z)/SQRT(DETVAR(M))
70   CONTINUE
     EVALUATION OF UNORMALIZED POSTERIOR MODEL PROBABILITIES.
     ANORM = 0.
     DO 80   M=1,NMODEL
     PRPOST(M) = PRPRE(M)*DF(M)
     ANORM = ANORM + PRPOST(M)
80   CONTINUE

     NORMALIZED POSTERIOR MODEL PROBABILITIES
     DO 90   M=1,NMODEL
     PRPOST(M) = PRPOST(M)/ANORM
     PRPRE(M) = PRPOST(M)
90   CONTINUE

     POSTERIOR PARAMETERS DISTRIBUTION.
     DO 100  M=1,NMODEL
     DO 100  I=1,NTOTAL
     AUX4(M,I) = X(M,I)/SIGMA
100  CONTINUE

     DO 110  M=1,NMODEL
     AUX5(M) = 0.0
     DO 110  I=1,NTOTAL
     AUX5(M) = AUX5(M) + X(M,I)*AUX4(M,I)
110  CONTINUE

     DO 120  M=1,NMODEL
```

```
      Z = 1.0/(AUX5(M) + 1.0/SU(M))
      ALPHA(M) = Z*(AUX5(M)*BETA(M) + ALPHA(M)/SU(M))
      SU(M) = Z
  120 CONTINUE
      RETURN
      END




      SUBROUTINE ROTH(NINIT,NEXP,CVEXP,UEXP)

      COMMON/UNO/RHO,VIS,DIA,D,S,W
      COMMON/CINCO/NMODEL,ALPHA(5),BETA(5),PRPRE(5),PRPOST(5),SU(5),
     1PHI1,PHI3,PHI4
      DIMENSION GRADW(30),F(30),YMODEL(5,30,30),CV(30),U(30),C(5),
     1Z(30,30),ZMAX(30,30)
      DIMENSION FR(30)

      IF(NEXP.NE.NINIT) GO TO 20
      CVMIN = 0.03
      CVMAX = 0.25
      UMIN = 10.
      UMAX = 16.0

      IDELTA = IFIX(100*(CVMAX-CVMIN))
      JDELTA = 2*IFIX(UMAX-UMIN)
      DO 10  I=1,IDELTA
      CV(I) = CVMIN + FLOAT(I)/100.0
   10 CONTINUE
      DO 20  I=1,JDELTA
      U(I) = UMIN + 0.5*FLOAT(I)
      CALL WATER(U(I),GRADW(I))
      FR(I) = U(I)**2/(2.0*32.174*DIA)
   20 CONTINUE

      DO 30  L=1,IDELTA
      DO 30  K=1,JDELTA
      YMODEL(1,K,L) = GRADW(K) + BETA(1)*CV(L)*GRADW(K)*((S-1.)**0.75)*
     1PHI1/FR(K)**1.5

      YMODEL(2,K,L) = GRADW(K) + BETA(2)*CV(L)*GRADW(K)*((S-1.)**0.75)*
     2PHI1/FR(K)**1.5 + CV(L)*GRADW(K)*(S-1.)

      YMODEL(3,K,L) = GRADW(K) + BETA(3)*0.282*(S-1.)*CV(L)*((PHI3**3/
     3(32.174*VIS))**(1./3.))*(FR(K)**(-4./3.))*(U(K)**2)/(2.0*32.174*
     4DIA)

      YMODEL(4,K,L) = GRADW(K) + BETA(4)*1.80*32.174*(S-1.)*DIA*CV(L)*
     5(U(K)**(-2.72))*PHI4*U(K)**2/(2.0*32.174*DIA)

      DO 25  I=1,NMODEL
      C(I) = 1.
      DO 25 J=1,NMODEL
      IF(J.EQ.I) GO TO 25
```

```
25   CONTINUE
     Z(K,L) = PRPOST(1)*C(1) + PRPOST(2)*C(2) + PRPOST(3)*C(3) +
    1PRPOST(4)*C(4)
30   CONTINUE

     ZMAX(1,1) = Z(1,1)
     L = 1
     J = 1
     DO 40  K=1,IDELTA
     DO 40  I=1,JDELTA
     IF(Z(I,K).GT.ZMAX(J,L)) GO TO 35
     GO TO 40
35   J=I
     L=K
     ZMAX(J,L) = Z(I,K)
40   CONTINUE

     CVEXP = CV(L)
     UEXP = U(J)
     RETURN
     END




     SUBROUTINE DETER(N,DET,A,M)

     THIS SUBROUTINE CALCULATES THE DETERMINANT OF A SQ ARE MATRIX OF
     ORDER N BY THE METHOD OF PIVOTAL CONDENSATION.

     DIMENSION A(5,5,5)

     K = 2
     L = 1
5    DO 10  I=K,N
     RATIO = A(M,I,L)/A(M,L,L)
     DO 10  J=K,N
10   A(M,I,J) = A(M,I,J) - A(M,L,J)*RATIO
     IF(K-N)15,20,20
15   L=K
     K = K + 1
     GO TO 5
20   DET = 1.0
     DO 25  L=1,N
     DET = DET*A(M,L,L)
25   CONTINUE
     RETURN
     END




     SUBROUTINE FRIC(F,U)
```

```
THIS SUBROUTINE WILL COMPUTE THE FRICTION FACTOR F R A PURE FLUID
UNDER LAMINAR OR TURBULFNT REGIMF.  FOR TURBULENT  LOW THE FRICTION
FACTOR IS FVALUATED ACCORDING WITH VON-KARMAN-PRAN TL FQUATION AND
THE NEWTON-RAPHSON ITERATION METHOD IS USED FOR FI DING THE ROOT
OF THIS EQUATION.

REFERENCES.  V.L. STREETER. FLUID MECHANICS. CHAPT R 5. MC GRAW-HILL
             BOOK COMPANY. $OURTH EDITION (1966).

             B. CARNAHAN ET. AL..  APPLIED NUMERIC L METHODS. CHAP-
             TER 3.  JOHN WILEY AND SONS INC. (197 ).


GLOSSARY OF PRINCIPAL SYMBOLS.

A,B = EMPIRICAL COEFFICIENTS IN VON-KARMAN-PRANDTL EQUATION.
C,D = EMPIRICAL COEFFICIENTS IN BLAUSIUS EQUATION.
VIS = FLUID VISCOSITY, LBM/FT.SEC.
DVIS = DYNAMIC FLUID VISCOSITY, LB.SEC./CU.FT.
U = MEAN FLUID VELOCITY, FEET/SEC.
F = FRICTION FACTOR, DIMENSIONLESS.
DIA = PIPELINE INTERNAL DIAMETER, FEET.
RHO = FLUID DENSITY, LBM/CU.FT.
RE = REYNOLDS NUMBER, DIMENSIONLESS.



DATA DIA,RHO,DVIS/0.1667, 62.4, 0.0000300/
DATA A,B,C,D/-9.1947749, 4.0212147, 1.523312, -0.3843671/

TRANSFORMATION OF DYNIMIC VISCOSITY (LB.SEC/CU.FT.  INTO THE ENGLISH
ENGINEERIN7 UNIT SYSTEM (LB/FT.SEC)
VIS = DVIS*32.174

FVALUATION OF REYNOLDS NUMBER.
RE = DIA*U*RHO/VIS

CHECK FOR TURBULENT FLOW
IF(RE.GT.2000.0) GO TO 10
F = 64.0/RE
RETURN

THE BLAUSIUS EQUATION IS USED TO GET A FIRST ESTIM TE OF F.
10 F = C*RE**D

BEGIN NEWTON-RAPHSON ITERATION.
DO 20  I=1,50
PRO = RE*SQRT(F)
FNEW = F - (1.0/SQRT(F) - B*ALOG10(PRO) - A)*(2.0*F*SQRT(F))/
1(-1.0 - 0.4342944819*B*SQRT(F))

CHECK FOR CONVERGENCE.
IF(ABS(F-FNEW).LT.1.0E-6) GO TO 40
F = FNEW
20 CONTINUE
```

```
      WRITE(6,30)
30    FORMAT(//, 5X, *NO CONVERGENCE FOR FRICTION FACTOR )
      CALL EXIT

40    RETURN
      END



      SUBROUTINE WATER(U, GRADW)

      THIS SUBROUTINE WILL CALCULATE THE HYDRAULIC GRADI NT FOR PURE WATER
      ACCORDING WITH DARCY-WEISBACH EQUATION.

      REFERENCE.   V.L. STREETER.  FLUID MECHANICS. CHAP ER 5. MC GRAW-HILL
                   BOOK COMPANY. FOURTH EDITION (1966).

      GLOSSARY OF PRINCIPAL SYMBOLS.

      DIA = PIPELINE DIAMETER, FEET.
      F = FRICTION FACTOR, DIMENSIONLESS.
      GRADW = HYDRAULIC GRADIENT FOR PURE WATER, FEET OF WATER PER FT. OF PIPE.
      U = AVERAGE FLUID VELOCITY, FEET/SEC.


      DATA DIA,RHO,DVIS/0.1667, 62.4, 0.0000167/

      SUBROUTINE FRICTION RETURNS THE FRICTION FACTOR.
      CALL FRIC(F,U)
      GRADW = (F/DIA)*U**2/(2.0*32.174)
      RETURN
      END
```

APPENDIX 1.10.2 Calibration of Electromagnetic Flowmeter.

Figure 1.16 represents the calibration curve for the electromagnetic flowmeter (see 1.5.1). The electronic calibration given by the maker (also indicated on figure 1.16) certifies an error no greater than 1.05 % on the flow rate. The water displacement of the pump (as percent of maximum flow) as a function of the pump speed is given in table 1.12.

TABLE 1.12

Percent of maximum flow	Pump speed (r.p.m.)
31	188
36	228
41	256
45	280
51	314
56	352
61	386
67	423
73	458
78	480
84	515
90	549

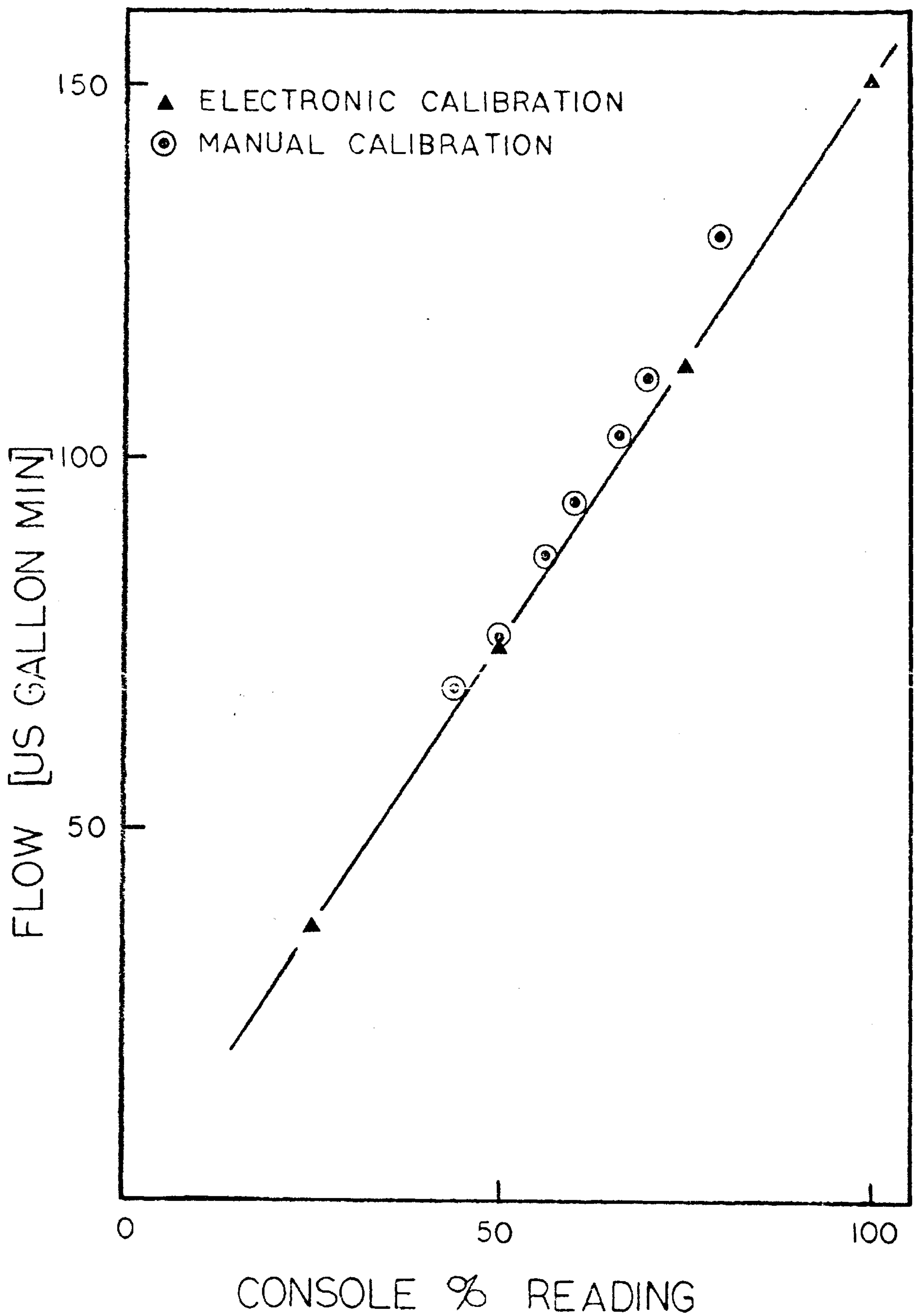

FIG. 1.16 CALIBRATION CURVE FOR ELECTROMAGNETIC FLOWMETER.

PART II OSCILLATORY FLOW STUDIES

2.1 INTRODUCTION

Part II of this thesis deals with the behaviour of clear water under pulsed turbulent flow. Some preliminary observations on the behaviour of settling mixtures under oscillatory flow conditions are also included.

The behaviour of particles in pulsating flows is of interest in such diverse fields as fluidized-bed technology, atmospheric dispersion, transport of solids, etc. When pulsations were applied to solid-fluid systems, increases of up to 13-fold were reported in the mass-transfer coefficients (Lemlich, 1961) and up to 4-fold in the heat transfer coefficients (Hogg, 1966). But the enhancement of heat and mass transfer are not the only advantages gained by the application of pulsations to particulate systems. It was reported that pulsations enhance the stability of fluidized beds (Massimilla, 1964), decrease the viscosity of dispersed systems (Mikhailov, 1964) and increase the settling rate of flocculated suspensions (Obiakor, 1965). It has also been discovered that under the influence of pulsations it is possible to force bubbles to move downwards against the net buoyant force (Buchanan, 1962, Jameson, 1966) and to suspend particles against gravity in liquids (Houghton, 1963).

Pulsations are not necessarily externally superimposed on the system. Many solid-fluid systems will themselves generate macroscopic pulsations which otherwise will not exist in the fluid alone. This was reported during the hydraulic transport of solids (Lamb, 1932) and in fluidized beds (Kang, 1967, Klein, 1971).

2.2 THE BEHAVIOUR OF CLEAR WATER UNDER PULSED TURBULENT FLOW

Theory, results and comments on pressure drop, air consumption, fluid velocity and power dissipation for clear water under pulsatile flow are presented in appendix 2.5.1. Some complementary results are presented in appendix 2.5.2. The computer program listing for determining Fourier coefficients by numerical integration is included in appendix 2.5.3.

2.3 COMMENTS ON THE BEHAVIOUR OF SETTLING MIXTURES UNDER PULSATILE FLOW

When a solid-liquid mixture flows in a horizontal pipeline under steady state conditions at velocities below the minimum deposit velocity, partial or total deposition of solids will occur, depending on concentration of solids and mean velocity of the mixture. The objective of these observations was to estimate the effect of including an oscillatory component in the liquid flow when partial or total deposition of solids exists.

The apparatus used was the same indicated in appendix 2.5.1 and the slurry was prepared by adding a determined amount of hematite to the system, obtaining an overall concentration of solids of about 10% by volume.

Three flow regimes were visually observed when pulsations are applied to the system above mentioned:

1. At low amplitudes a stationary bed exists on the bottom of the pipe at all times.
2. At intermediate amplitudes a transition region exists, in which a stationary bed of solids exists for part of the time only.
3. At large amplitudes all particles are moving in water at all times.

Figure 2.1 gives some indication of the effect of pulsations on the flow regimes involved when the mean velocity of the mixture is changed. It would appear that the pulsatile component of velocity is as effective as the mean flow velocity in keeping particles in suspension. Thus, in pulsed flow a high solid concentration can be transported by a relatively small flow of water.

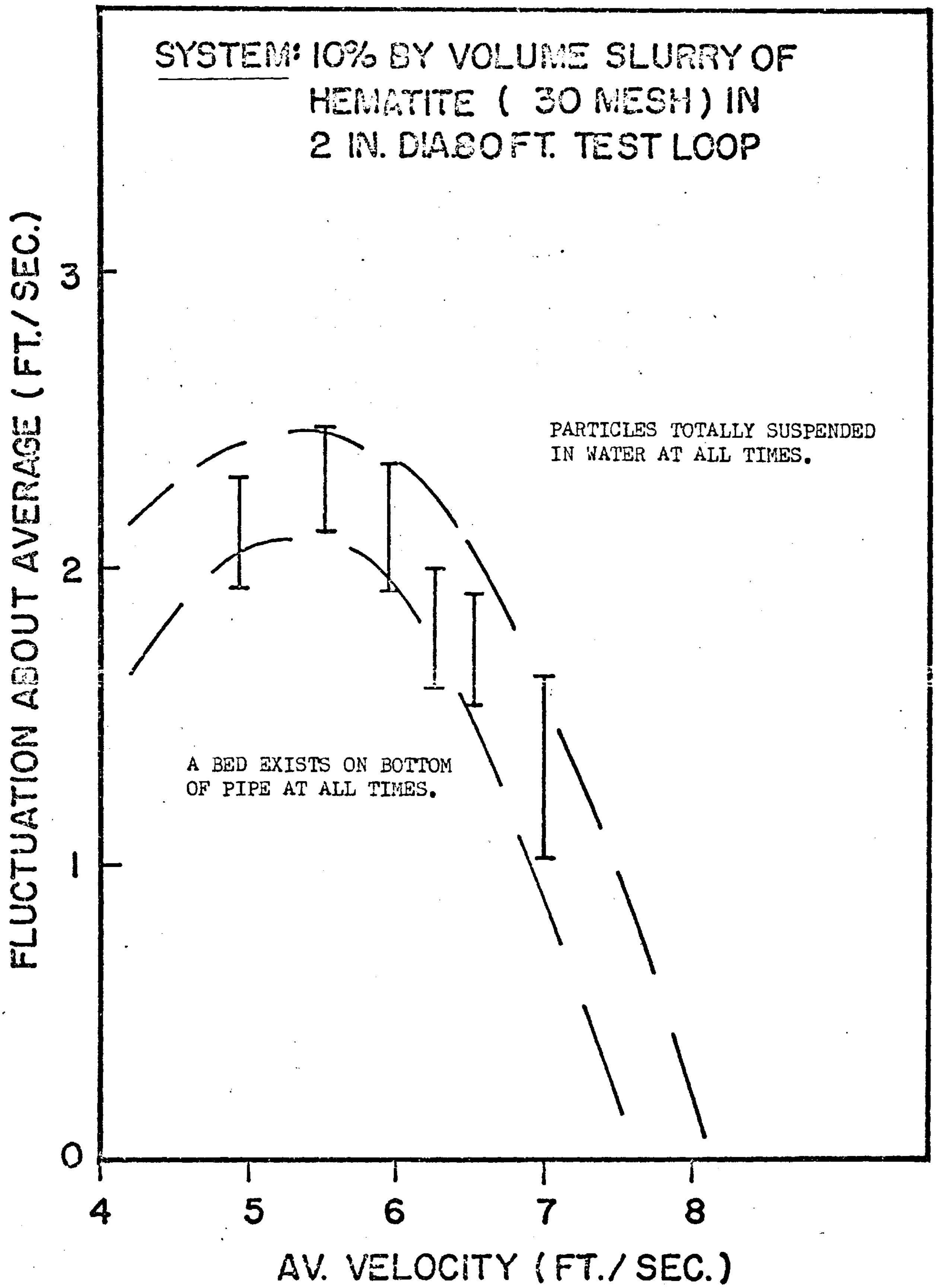

SYSTEM: 10% BY VOLUME SLURRY OF HEMATITE (30 MESH) IN 2 IN. DIA 80 FT. TEST LOOP
PARTICLES TOTALLY SUSPENDED IN WATER AT ALL TIMES.
A BED EXISTS ON BOTTOM OF PIPE AT ALL TIMES.
FLUCTUATION ABOUT AVERAGE (FT./ SEC.)
0
1
2
3
4
5
6
7
8
AV. VELOCITY (FT./ SEC.)

FIGURE 2.1

2.4 REFERENCES*

1. Buchanan, R.H., G. Jameson and D. Oedjoe, I.E.C. (Fundamentals), 1, 82 (1962)

2. Hogg, G.W. and E.S. Grimmet, Chem. Eng. Prog. Symp. Series, 67, 62 (1966)

3. Houghton, G., Proc. Roy. Soc., A272, 33 (1963)

4. Jameson, G.J., Chem. Eng. Sci., 21, 35 (1966)

5. Kang, W.K., J.P. Sutherland and G.L. Osberg, I.E.C. (Fundamentals), 6, 499 (1967)

6. Klein, A., M. Eng. Report, McMaster University (1971)

7. Lamb, H., Hydrodynamics, Dover, New York (1932)

8. Lemlich, R. and M.R. Levy, A.I.Ch.E. J., 7, 240 (1961)

9. Massimilla, L., and G. Volpicelli, Paper presented at the 57th Annual A.I.Ch.E. meeting, Boston (1964)

10. Mikhailov, N.V., Dokl. Akad. Nausk. SSSR, 155 (4), 920 (1964)

11. Obiakor, E.K., Nature, 205, 385 (1965)

*SEE ALSO APPENDIX 2.5.1

APPENDIX 2.5.1

THE BEHAVIOUR OF CLEAR WATER UNDER PULSED TURBULENT FLOW.

Friction Factors in Pulsed Turbulent Flow

M. H. I. BAIRD, G. F. ROUND and J. N. CARDENAS
McMaster University, Hamilton, Ontario

Reprinted in Canada from The Canadian Journal of Chemical Engineering
49:220-223:, April, 1971.
A Publication of The Canadian Society for Chemical Engineering, 151 Slater Street, Ottawa, Ontario K1P 5H3.

Friction Factors in Pulsed Turbulent Flow

M. H. I. BAIRD[2], *G. F. ROUND*[1] *and J. N. CARDENAS*[2]
McMaster University, Hamilton, Ontario

An apparatus for investigating pulsed turbulent liquid flow in a 2 in. diameter, 80 ft. pipeline is described. The pulsation unit was powered by compressed air with a consumption of up to 2.7 std. cu.ft./min. at 35 lb/in^2 gauge. The pressure drop for water flowing at mean velocities of 7.66 to 12.28 ft./sec. has been measured, both for steady flow and for pulsed flow, at frequencies between 0.48 and 0.82 Hz. The experimentally measured pressure versus time curves for pulsed flow can be matched fairly closely by a solution of Euler's equation employing the friction factors measured under steady flow conditions.

On décrit un appareil pour étudier un courant liquide turbulent et pulsatoire dans un pipeline de 80 pieds de longueur et 2 pouces de diamètre. On a actionné le dispositif de pulsation avec de l'air comprimé à raison de 2.7 std. pieds cubes à la minute à une pression de 35 livres au pouce carré. On a mesuré la chute de pression de l'eau qui coule à des vélocités moyennes de 7.66 à 12.28 pieds à la seconde et ce dans les cas d'un courant stable et d'un courant pulsatoire et à des fréquences variant entre 0.48 et 0.82 Hz. Les graphiques reproduisant les mesures expérimentales de la pression vs le temps, dans le cas d'un écoulement pulsatoire, s'harmonisent assez bien avec la solution d'une équation d'Euler où l'on emploie les facteurs de frottement mesurés dans des conditions correspondant à celles d'un écoulement stable.

Pulsating flow of fluids occurs widely, both in nature and industry. One area that has interested chemical engineers for many years is the improvement of processes by the deliberate application of pulsed flow[1]. The present authors have begun a program of research on pipeline conveying of slurries in a pulsed flow of water, using an air pulsation technique[2,3,4]. Such a technique has an advantage over pistons or flow interrupters which would be adversely affected by suspended solids.

The equipment, which is described in detail following, has first been operated with pure water alone. The objective of this work has been to obtain data on instantaneous pressure drops and friction losses in pulsed turbulent flow. The operating characteristics of the pulsation unit are also given.

[1]Department of Mechanical Engineering.
[2]Department of Chemical Engineering.

Pulsed laminar flow in pipes has been quite thoroughly investigated[5,6,7] and it has been found that above a certain limiting frequency friction factors are greater than the values for steady flow. Consequently the energy losses are greater than would be expected using a quasi-steady model[7]. In the case of turbulent flow, Schultz-Grunow[8] found that a quasi-steady state model was satisfactory, i.e., the instantaneous frictional pressure drop could be predicted from the instantaneous velocity using the steady-flow friction factor values. This early work[8] was at frequencies up to only 0.25 Hz, but more recently Streeter and Wylie[9] have successfully used the quasi-steady model in analyzing the hydraulic transients from a reciprocating pump at frequencies in the order of 10 Hz.

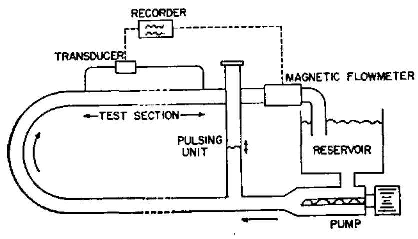

Figure 1 – Schematic diagram of test loop.

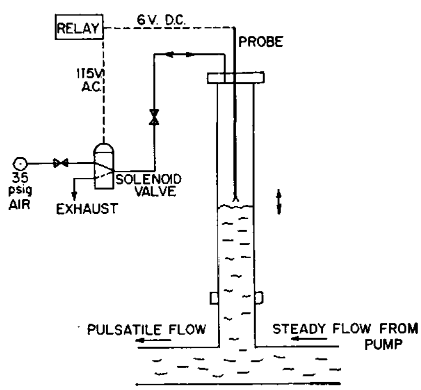

Figure 2 – Pulsation unit.

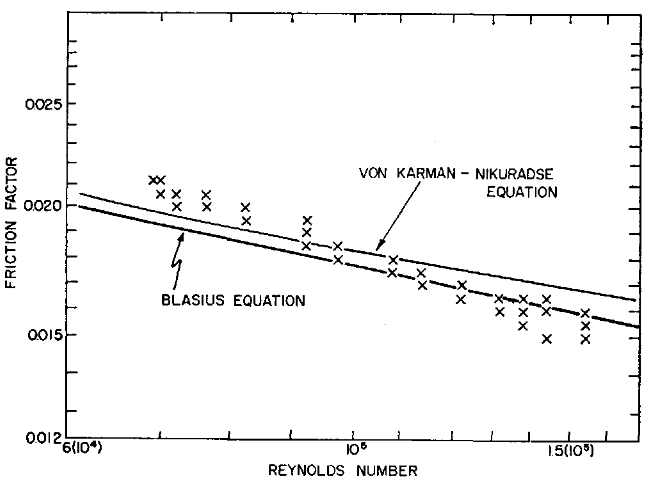

Figure 3 – Friction factor under steady flow conditions.

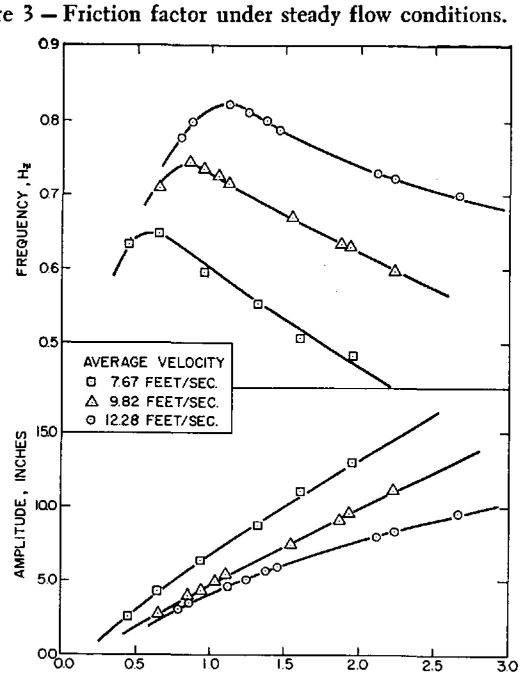

Figure 4 – Effect of air consumption on frequency and amplitude at different average velocities.

However this analysis was valid for flows with only a relatively small oscillatory component. Recently, Brown and others[10] studied the response of turbulent flows to small-amplitude oscillations at acoustic frequencies (50 - 3000 Hz). At these high frequencies, the observed attenuation agreed with calculation based on "constant turbulence", i.e. the flow pattern and turbulence did not have time to adjust to the rapid fluctuations in velocity. The present investigation concerns pulsed turbulent flows at frequencies of 0.48-0.82 Hz with flow fluctuations of up to $\pm 50\%$ of the mean flow.

Apparatus

The circulation loop used is shown schematically in Figure 1. Water from the reservoir was pumped at a steady rate to the 80-ft. loop of 2-in. internal diameter steel pipe by a rotary, positive displacement pump (Moyno, type CDR). The pump speed could be varied to give a flow range from 6.7 - 20-cu.ft./min.

Shortly downstream of the pump, the water line was connected to the pulsation unit, the purpose of which was to impose an oscillatory component on the flow. The pulsation unit, which is shown in detail in Figure 2, operated on the self-triggering principle[2,3,4]. This principle has been useful in pulsing gas absorbers[2], extraction columns[3] and hydraulic test tanks[4]. The present investigation deals with a new application of the principle to a continuous turbulent flow system. The water rising into the vertical section of 2-in. bore glass tubing activated a conductivity probe which operated a solenoid valve, supplying compressed air (normally 35 psi). As the water level receded past the probe, the solenoid switched to the "exhaust" position and the air space was connected to atmosphere. In this way the cycle repeated itself, with the water level oscillating about the probe. Previous investigations[2,3,4] have shown that such a pulsator tends to operate at the natural frequency of the system, giving a smooth waveform and a relatively efficient use of compressed air. The pulsation frequency could be altered by adjusting the probe vertically, and the amplitude could be adjusted by varying the air supply. An air shut-off valve was also provided to permit unpulsed operation of the loop.

The water flow continued along the lower part of the loop, then via a U-section with a radius of curvature 1.33-ft. to the upper part of the loop in which the pressure-drop test section was situated. The test section began 3-ft. from the U-Section. The pressure-drop between two points 31.66 ft. apart was measured by a diaphragm transducer (Pace Engineering Co., type P7D) and transmitted to a high-speed recorder. Downstream of the test section, an electromagnetic flowmeter (Brooks Instruments, model 7300) measured the fluid velocity which was recorded on the same chart as the pressure drop signal.

The measurements taken in a typical pulsed-flow test included the pressure drop and velocity as functions of time, the frequency of pulsation (by stopwatch timing of ten cycles), the stroke (amplitude) of the water level in the pulsation unit, and the air consumption. This latter measurement was made by connecting the exhaust air line to an inverted water-filled measuring cylinder for a known number of cycles. The air consumption was obtained as the volume collected per cycle multiplied by the frequency.

Friction in steady flow

The friction factor in steady flow was calculated from the experimental pressure and velocity data using the well-known Darcy-Weisbach equation:

$$\triangle P = f \cdot \left(\frac{L}{D}\right) \cdot \left(\rho \frac{U^2}{2g_c}\right) \qquad (1)$$

The experimental values of f are shown in Figure 3. Also shown are the Blasius equation and the von Karman-Nikuradse equation for the friction factor in smooth pipes:

Blasius: $$f = 0.316\, Re^{-0.25} \qquad (2)$$

Von Karman-Nikuradse: $$1/\sqrt{f} = 0.86\, ln\, [Re\sqrt{f}] - 0.8 \qquad (3)$$

The scatter of the data points on Figure 3 is consistent with the experimental accuracy of the individual determinations of f. Although the measured values of f are in reasonable agreement with Equations (2) and (3), the effect of Reynolds number appears to be slightly greater than expected; no definite reason for this effect can be advanced.

In interpreting pulsed-flow data, it was necessary to consider a Reynolds number range greater than that over which data (Figure 3) could be obtained in steady flow. The Blasius-type equation for f, though simple, should not be applied at Reynolds numbers greater than 10^5. Accordingly it was decided to use a form of Equation (3) with coefficients adjusted to fit the data on Figure 3.

$$1/\sqrt{f} = 1.746\, ln\, [Re\sqrt{f}] - 9.195 \qquad (4)$$

Pulsed flow operation

Figure 4 shows the effect of air flow rate upon frequency and amplitude, at three different liquid flow velocities and a single position of the probe. A volumetric efficiency may be defined[2] as the ratio of the volume of liquid displaced per cycle, divided by the volume of air (standard conditions) supplied per cycle:

$$\eta = \frac{2\pi\, A\omega S}{Q} \qquad (5)$$

The values of n obtained in the present work are between 0.25 and 0.4, a range somewhat lower than that obtained[2] in pulsing systems with no net flow. The friction due to turbulent flow undoubtedly contributes heavily to damping effects.

The negative effect of air consumption upon frequency, shown in Figure 4, is also characteristic of heavily damped systems. The curves resemble the curve obtained by Baird and Garstang[11] for the pulsing of water through a bed of Raschig rings.

Quasi steady state model

If the velocity u as a function of time is known, and assuming the dependence of f upon u given by Equation (4), the pressure gradient variation may be calculated.

The equation of motion may be written in terms of the instantaneous flow velocity u (averaged across the pipe section), taking a length of pipe as the control volume. Incompressible flow and rigid pipe walls are assumed.

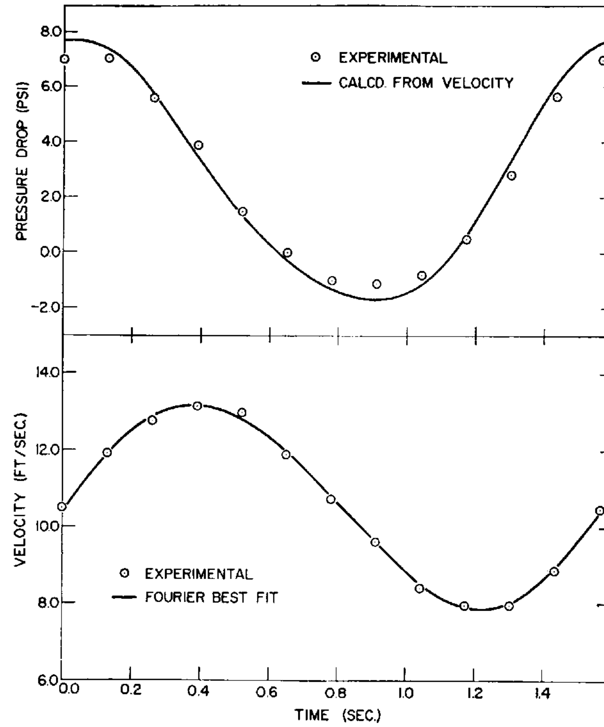

Figure 5 — Velocity and pressure drop variation.
U = 10.5 ft/s A = 9.1 in.
frequency = 0.64 Hz

$$\frac{1}{\rho} \cdot \frac{\partial P}{\partial x} + \frac{\partial u}{\partial t} + \frac{fu^2}{2D} = 0 \qquad (6)$$

It was apparent from chart records of the velocity and pressure gradient that a simple sinusoidal approximation was not sufficient to describe the velocity variation. However it was found that the velocity-time curves could be empirically fitted in any particular case by a five-term Fourier series:

$$u(t) = A_o + A_1 sin\omega t + A_2 sin2\omega t + B_1 cos\omega t + B_2 cos2\omega t \qquad (7$$

The lower portion of Figure 5 shows a typical curve of this type, fitted to experimental points taken from the chart. The pressure drop, calculated from Equations (6), (4) and (7), is shown in the upper portion of Figure 5. According to the quasi steady state hypothesis, the experimental pressure drop points should lie on the calculated curve. The agreement is not very good at the peaks and troughs of the pressure curve which correspond to the maximum acceleration (at $t \cong 0$ and 1.5 sec.) and deceleration (at $t \cong 0.9$ sec.) repectively.

The deviations are consistent with a response time τ of about 0.1 sec., based on a velocity measurement lag of $\tau(du/dt)$. This corresponds closely with the manufacturers' estimates for the magnetic flowmeter response. In other words, this investigation leads to the conclusion that the fluid behavior at the frequencies and amplitudes studied is "quasi-steady".

Brown et al[10] found that at frequencies of 50 - 3000 Hz the behavior was not quasi-steady, as the turbulence level and flow pattern did not have time to adjust to the rapid fluctuations. They suggested tentatively a relationship for the transition between quasi steady and non-quasi steady behavior:

$$\omega R^2/\nu \simeq 0.025\, Re$$

i.e. $$\omega \simeq 0.1\, U/D \qquad (8)$$

TABLE 1

POWER DISSIPATION IN TEST SECTION

Velocity U, ft/s	Amplitude A, inches	Frequency Hz	Power dissipation $\bar{J}$, $ft\ lb/s$ (observed)	Power dissipation $\bar{J}$, $ft\ lb/s$ (calculated)
7.67	2.5	0.621	12.52	12.49
	5.0	0.650	12.77	12.78
	7.95	0.580	13.35	13.21
	10.55	0.541	14.08	13.94
	12.8	0.482	14.29	14.28
9.82	2.8	0.701	23.49	23.41
	4.2	0.741	24.47	24.35
	8.0	0.662	25.33	25.16
	9.55	0.629	25.92	25.77
	11.5	0.588	26.80	26.70
12.28	2.9	0.759	42.88	42.76
	3.95	0.799	42.98	42.80
	5.0	0.815	43.44	43.22
	7.9	0.741	44.88	44.75
	9.55	0.692	46.23	56.66

Thus for the present conditions the transition frequency would be in the order of 6 radians/sec or 1 Hz.

Although the frequencies used in this work were of the order of 1 Hz, the response lag was no more than may be expected from the magnetic flowmeter, so the transition frequency must be somewhat greater than that given by Equation (8).

Further support for the contention of a higher transition frequency is given by the success[9] of the quasi-steady model for frequencies up to 10 Hz in a 3-in. pipe.

Power dissipation

The power dissipation averaged over a cycle is an important factor in the design of pulsed flow equipment. It is given by:

$$\bar{J} = \frac{\omega}{2\pi} \int_0^{\frac{2\pi}{\omega}} \frac{\pi}{4} D^2 u \triangle P \, dt \quad \ldots\ldots\ldots\ldots (9)$$

Experimental values of this quantity are obtained from the values of u and $\triangle P$ on the chart record. The value of $\bar{J}$ may also be estimated from the experimental measurement of u and a value of $\triangle P$ calculated from u using Equation (6) in conjunction with the steady flow friction relationship of Equation (4). In both these calculations of J, due attention is paid in the integration to that period in which $\triangle P$ has a negative sign, in which case there is a net recovery of energy from the water as it decelerates.

The results of the tests are summarised in Table 1, and it will be seen that the observed and calculated values of $\bar{J}$ agree within 1%. The small error due to velocity measurement lag, apparent on Figure 5, is largely cancelled out when integration over the complete oscillation cycle is performed.

Conclusions

This investigation has confirmed that the quasi-steady state hypothesis (i.e., fully developed flow assumption) applied to pulsatile turbulent flow in the conditions studied. The air-pulsing principle[2,3,4] can be applied for turbulent water flow in a 2-in. pipeline.

Acknowledgments

We are grateful to the Department of Energy, Mines and Resources (Mines Branch) and the National Research Council of Canada for financial support. One of us (J..N.C.) acknowledges the support of an Interamerican Development Bank scholarship.

Nomenclature

A	=	amplitude (stroke) measured at pulsation unit
$A_{0, 1} \ldots$	=	Fourier coefficients
$B_{0, 1} \ldots$	=	Fourier coefficients
D	=	pipe diameter
f	=	friction factor
g_c	=	gravitational constant
J	=	power dissipation (average over 1 cycle)
L	=	length of test section
P	=	pressure
Q	=	volume of air supplied per cycle
R	=	radius of pipe
S	=	cross-sectional area of pipe
t	=	time
u	=	velocity (instantaneous)
U	=	velocity (average over 1 cycle)
x	=	axial distance
$\triangle P$	=	pressure drop
ρ	=	water density
τ	=	time constant
ω	=	angular frequency
η	=	volumetric efficiency
ν	=	kinematic viscosity
Re	=	Reynolds number $= UD/\nu$

References

(1) Baird, M. H. I., Brit. Chem. Eng., 11, 20 (1966).
(2) Baird, M. H. I., Proc. IChemE/AIChE Joint Symposium, p. 6:53, London (1965).
(3) Vermijs, W. J. W., ibid. p. 6:98.
(4) Carstens, M. R., J. Hydraulics Div., ASCE, 92, (HY3), Proc. Paper 4818, 13 (1966).
(5) Womersley, J. R., J. Physiol., 127, 553 (1955).
(6) Hershey, D. and Song, G., AIChE Journal, 13, 491 (1967).
(7) Linke, W. and Hufschmidt, W., Chem.-Ing.-Techn., 30, 159 (1958).
(8) Schultz-Grunow, F., Forsch. Gebiete Ing.-Wes., 11, 170 (1940).
(9) Streeter, V. L. and Wylie, E. B., J. Eng. Power, Trans. ASME Ser. A, 89, 615 (1967).
(10) Brown, F. T., Margolis, D. L. and Shah, R. P., J. Basic Eng., Trans. A.S.M.E. Ser. D, 91, 678 (1969).
(11) Baird, M. H. I. and Garstang, J. H., Chem. Eng. Sci., 22, 1663 (1967).

Manuscript received November 23, 1970; accepted January 19, 1971.

★ ★ ★

APPENDIX 2.5.2

RESULTS OF RUN NUMBER 271

EXPERIMENTAL CONDITIONS

AMPLITUDE (FEET) = .27083
FRECUENCY (1/SEC) = .66666
AVERAGE VELOCITY (FEET/SEC) = 13.21000
NUMBER OF EXPERIMENTAL POINTS = 11

FACTOX = 1.00000 FACTOY = .40000 FACTOZ = .35609

INDEPENDENT COEFFICIENT A0 = 13.1245006

COEFFICIENTS CORRESPONDING TO SINE SERIE AND VELOCITIES CALCULATED WITH THEM

A1 = B(1,1) = 1.0696591 A2 = B(1,2) = .0801216

A3 = B(1,3) = -.0086353 A4 = B(1,4) = .3891010

TIME	UEXP	U(1,1,I)	D(1,1,I)	U(1,2,I)	D(1,2,I)	U(1,3,I)	D(1,3,I)	U(1,4,I)	D(1,4,I)
0.00000	13.21000	13.12450	.08550	13.12450	.08550	13.12450	.08550	13.12450	.08550
.15000	13.66201	13.75323	-.09122	13.82943	-.16742	13.82122	-.15920	14.04993	-.38791
.30000	13.87732	14.14181	-.26448	14.18890	-.31158	14.19398	-.31665	13.82392	.05340
.45000	13.91744	14.14181	-.22436	14.09471	-.17727	14.09979	-.18235	14.46985	-.55240
.60001	13.91611	13.75323	.16287	13.67703	.23907	13.66882	.24729	13.44011	.47599
.75001	13.80511	13.12450	.68061	13.12450	.68061	13.12450	.68061	13.12450	.68061
.90001	12.96028	12.49577	.47351	12.57197	.38731	12.58018	.38910	12.80889	.15139
1.05001	11.89943	12.10719	-.20777	12.15429	-.25486	12.14921	-.24979	11.77916	.12027
1.20001	11.77907	12.10719	-.32813	12.06010	-.28103	12.05502	-.27596	12.42508	-.64601
1.35001	12.27388	12.49577	-.22189	12.41957	-.14569	12.42778	-.15391	12.19908	.07480
1.50002	13.21000	13.12450	.08550	13.12450	.08550	13.12450	.08550	13.12450	.08550

SUM ABS VALUE OF DIFFERENCE = 2.82585 2.82585 2.82585 3.32277

MEAN DEVIATION = .25690 .25690 .25690 .30207

STANDARD DEVIATION = .31002 .30370 .30324 .38447

COEFFICIENTS CORRESPONDING TO COSINE SERIE AND VELOCITIES CALCULATED WITH THEM

B1 = B(2,1) = -.2951035   B2 = B(2,2) = .3504604

B3 = B(2,3) = -.1473822   B4 = B(2,4) = .1317640

TIME	UEXP	U(2,1,I)	D(2,1,I)	U(2,2,I)	D(2,2,I)	U(2,3,I)	D(2,3,I)	U(2,4,I)	D(2,4,I)
0.00000	13.21000	12.82940	.38060	13.17986	.03014	13.03248	.17752	13.16424	.04576
.15000	13.66201	12.88576	.77626	12.99406	.66796	13.03960	.62242	12.93300	.72902
.30000	13.87732	13.03331	.84401	12.74978	1.12754	12.86902	1.00831	12.90973	.96759
.45000	13.91744	13.21569	.70175	12.93216	.98526	12.81293	1.10451	12.85365	1.06380
.60001	13.91611	13.36324	.55286	13.47154	.44456	13.42600	.49011	13.31940	.59671
.75001	13.80511	13.41960	.38550	13.77006	.03504	13.91745	-.11234	14.04921	-.24410
.90001	12.96928	13.36324	-.39396	13.47154	-.50226	13.42600	-.45672	13.31940	-.35012
1.05001	11.89943	13.21569	-1.31627	12.93216	-1.03274	12.81293	-.91350	12.85365	-.95422
1.20001	11.77907	13.03331	-1.25424	12.74978	-.97071	12.86901	-1.08995	12.90973	-1.13067
1.35001	12.27388	12.88576	-.61188	12.99405	-.72018	13.03960	-.76572	12.93300	-.65912
1.50002	13.21000	12.82940	.38060	13.17986	.03014	13.03248	.17752	13.16424	.04576
SUM ABS VALUE OF DIFFERENCE =			7.59795		6.54656		6.91863		6.78586
MEAN DEVIATION =			.69072		.59514		.62897		.61699
STANDARD DEVIATION =			.76197		.71787		.72346		.72395

RESULTS OF RUN NUMBER 272

EXPERIMENTAL CONDITIONS

AMPLITUDE (FEET) = .42708
FRECUENCY (1/SEC) = .71000
AVERAGE VELOCITY (FEET/SEC) = 13.21000
NUMBER OF EXPERIMENTAL POINTS = 11

FACTOX = 1.00000 FACTOY = .38350 FACTOZ = .35609

INDEPENDENT COEFFICIENT A0 = 13.1952125

COEFFICIENTS CORRESPONDING TO SINE SERIE AND VELOCITIES CALCULATED WITH THEM

A1 = B(1,1) = 1.6390574 A2 = B(1,2) = .0685331

A3 = B(1,3) = .0199063 A4 = B(1,4) = .5591421

TIME	UEXP	U(1,1,I)	D(1,1,I)	U(1,2,I)	D(1,2,I)	U(1,3,I)	D(1,3,I)	U(1,4,I)	D(1,4,I)
0.00000	13.21000	13.19521	.01479	13.19521	.01479	13.19521	.01479	13.19521	.01479
.14085	14.03058	14.15863	-.12805	14.22380	-.19322	14.24274	-.21216	14.57139	-.54081
.28169	14.39599	14.75405	-.35805	14.79433	-.39834	14.78263	-.38664	14.25085	.14514
.42254	14.52421	14.75405	-.22984	14.71377	-.18956	14.70207	-.17786	15.23384	-.70963
.56338	14.54088	14.15863	.38225	14.09345	.44743	14.11238	.42850	13.78373	.75715
.70423	13.90108	13.19521	.70587	13.19521	.70587	13.19521	.70587	13.19521	.70587
.84507	12.77535	12.23180	.54355	12.29698	.47837	12.27805	.49730	12.60670	.16865
.98592	11.46627	11.63638	-.17011	11.67666	-.21039	11.68836	-.22209	11.15659	.30968
1.12676	11.22907	11.63638	-.40731	11.59609	-.36702	11.60779	-.37873	12.13957	-.91050
1.26761	11.96631	12.23180	-.26549	12.16662	-.20031	12.14769	-.18138	11.81903	.14728
1.40845	13.21000	13.19521	.01479	13.19521	.01479	13.19521	.01479	13.19521	.01479
JM ABS VALUE OF DIFFERENCE =			3.22009		3.22009		3.22009		4.42429
MEAN DEVIATION =			.29274		.29274		.29274		.40221
STANDARD DEVIATION =			.35713		.35404		.35437		.51027

COEFFICIENTS CORRESPONDING TO COSINE SERIE AND VELOCITIES CALCULATED WITH THEM

B1 = B(2,1) = -.3696078   B2 = B(2,2) = .3647568

B3 = B(2,3) = -.1194170   B4 = B(2,4) = .1107392

TIME	UEXP	U(2,1,I)	D(2,1,I)	U(2,2,I)	D(2,2,I)	U(2,3,I)	D(2,3,I)	U(2,4,I)	D(2,4,I)
0.00000	13.21000	12.82560	.38440	13.19036	.01964	13.07094	.13906	13.18168	.02832
.14085	14.03058	12.89619	1.13439	13.00891	1.02167	13.04581	.98477	12.95622	1.07436
.28169	14.39599	13.08100	1.31500	12.78590	1.61009	12.88251	1.51348	12.91673	1.4792[illegible]
.42254	14.52421	13.30943	1.21478	13.01433	1.50988	12.91772	1.60649	12.95194	1.57227
.56338	14.54088	13.49423	1.04665	13.60695	.93393	13.57004	.97083	13.48045	1.[illegible]42
.70423	13.90108	13.56482	.33626	13.92958	-.02849	14.04899	-.14791	14.15973	-.25865
.84507	12.77535	13.49423	-.71888	13.60695	-.83160	13.57005	-.79470	13.48046	-.70511
.98592	11.46627	13.30943	-1.84316	13.01433	-1.54807	12.91772	-1.45146	12.95194	-1.48559
1.12676	11.22907	13.08100	-1.85193	12.78590	-1.55683	12.88251	-1.65344	12.91673	-1.68767
1.26761	11.96631	12.89619	-.92989	13.00891	-1.04260	13.04581	-1.07950	12.95622	-.95991
1.40845	13.21000	12.82560	.38440	13.19036	.01964	13.07094	.13906	13.18168	.02832
SUM ABS VALUE OF DIFFERENCE =			11.15972		10.12244		1[illegible].48069		[illegible]
MEAN DEVIATION =			1.01452		.92022		.95279		.94272
STANDARD DEVIATION =			1.13635		1.10324		1.107[illegible]7		1.1[illegible]

[illegible] COMPUTER [illegible]

RESULTS OF RUN NUMBER 273

EXPERIMENTAL CONDITIONS

AMPLITUDE (FEET) = .63541
FRECUENCY (1/SEC) = .70500
AVERAGE VELOCITY (FEET/SEC) = 13.21000
NUMBER OF EXPERIMENTAL POINTS = 11

FACTOX = 1.00000 FACTOY = .37710 FACTOZ = .35609

INDEPENDENT COEFFICIENT A0 = 13.1539382

COEFFICIENTS CORRESPONDING TO SINE SERIE AND VELOCITIES CALCULATED WITH THEM

A1 = B(1,1) = 2.2831967 A2 = B(1,2) = .2153013

A3 = B(1,3) = .1551513 A4 = B(1,4) = .7737687

TIME	UEXP	U(1,1,I)	D(1,1,I)	U(1,2,I)	D(1,2,I)	U(1,3,I)	D(1,3,I)	U(1,4,I)	D(1,4,I)
0.00000	13.21000	13.15394	.05606	13.15394	.05606	13.15394	.05606	13.15394	.05606
.14184	14.28417	14.49597	-.21180	14.70073	-.41656	14.84829	-.56412	15.30311	-1.01894
.28369	14.88681	15.32539	-.43858	15.45194	-.56513	15.36074	-.47393	14.62483	.26198
.42553	15.20830	15.32539	-.11708	15.19884	.00947	15.10764	.10066	15.84356	-.63525
.56738	14.94354	14.49597	.44758	14.29120	.65234	14.43876	.50478	13.98394	.95960
.70922	13.94376	13.15394	.78982	13.15394	.78982	13.15394	.78982	13.15394	.78982
.85106	12.45354	11.81191	.64163	12.01667	.43687	11.86912	.58443	12.32394	.12960
.99291	11.17387	10.98249	.19138	11.10904	.06483	11.20024	-.02636	10.46432	.70956
1.13475	10.47415	10.98249	-.50834	10.85594	-.38179	10.94713	-.47298	11.68305	-1.20890
1.27660	11.06041	11.81191	-.75150	11.60714	-.54674	11.45959	-.39918	11.00477	.05564
1.41844	13.21000	13.15394	.05606	13.15393	.05607	13.15397	.05607	13.15393	.05607
SUM ABS VALUE OF DIFFERENCE =			4.20984		3.97567		4.02840		5.88144
MEAN DEVIATION =			.38271		.36142		.36622		.53468
STANDARD DEVIATION =			.46249		.44603		.44346		.67731

COEFFICIENTS CORRESPONDING TO COSINE SERIE AND VELOCITIES CALCULATED WITH THEM

B1 = B(2,1) = -.5735996   B2 = B(2,2) = .2697001

B3 = B(2,3) = .0392804   B4 = B(2,4) = .2755242

TIME	UEXP	U(2,1,I)	D(2,1,I)	U(2,2,I)	D(2,2,I)	U(2,3,I)	D(2,3,I)	U(2,4,I)	D(2,4,I)
0.00000	13.21000	12.58034	.62966	12.85004	.35996	12.88932	.32068	13.16484	.04516
.14184	14.28417	12.68989	1.59428	12.77323	1.51094	12.76109	1.52308	12.53819	1.74598
.28369	14.88681	12.97669	1.91012	12.75849	2.12832	12.72672	2.16009	12.81186	2.07495
.42553	15.20830	13.33119	1.87711	13.11300	2.09531	13.14478	2.06353	13.22992	1.97838
.56738	14.94354	13.61799	1.32555	13.70133	1.24221	13.71347	1.23007	13.49057	1.45298
.70922	13.94376	13.72754	.21622	13.99724	-.05348	13.95796	-.01420	14.23348	-.28972
.85106	12.45354	13.61799	-1.16445	13.70133	-1.24779	13.71347	-1.25993	13.49057	-1.03702
.99291	11.17387	13.33119	-2.15732	13.11300	-1.93913	13.14478	-1.97090	13.22992	-2.05604
1.13475	10.47415	12.97669	-2.50253	12.75849	-2.28434	12.72672	-2.25256	12.81186	-2.33771
1.27660	11.06041	12.68989	-1.62948	12.77323	-1.71282	12.76109	-1.70068	12.53819	-1.47778
1.41844	13.21000	12.58034	.62966	12.85004	.35996	12.88932	.32068	13.16484	.04516
SUM ABS VALUE OF DIFFERENCE =			15.63640		14.93425		14.81641		14.54088
MEAN DEVIATION =			1.42149		1.35766		1.34695		1.32190
STANDARD DEVIATION =			1.57360		1.55146		1.54923		1.54974

RESULTS OF RUN NUMBER 274

EXPERIMENTAL CONDITIONS

AMPLITUDE (FEET) = .83200
FRECUENCY (1/SEC) = .66660
AVERAGE VELOCITY (FEET/SEC) = 13.21000
NUMBER OF EXPERIMENTAL POINTS = 11

FACTOX = 1.00000 FACTOY = .38350 FACTOZ = .35609

INDEPENDENT COEFFICIENT A0 = 13.1134109

COEFFICIENTS CORRESPONDING TO SINE SERIE AND VELOCITIES CALCULATED WITH THEM

A1 = B(1,1) = 2.9095313 A2 = B(1,2) = .0439549

A3 = B(1,3) = .0011266 A4 = B(1,4) = .9497416

TIME	UEXP	U(1,1,I)	D(1,1,I)	U(1,2,I)	D(1,2,I)	U(1,3,I)	D(1,3,I)	U(1,4,I)	D(1,4,I)
0.00000	13.21000	13.11341	.09659	13.11341	.09659	13.11341	.09659	13.11341	.09659
.15002	14.72936	14.82359	-.09424	14.86539	-.13604	14.86647	-.13711	15.42471	-.69535
.30003	15.56660	15.88054	-.31394	15.90638	-.33977	15.90571	-.33911	15.00245	.56415
.45005	15.89612	15.88054	.01558	15.85470	.04141	15.85404	.04208	16.75730	-.86118
.60006	15.08836	14.82359	.26477	14.78179	.30657	14.78286	.30550	14.22462	.86374
.75008	13.27283	13.11341	.15941	13.11341	.15941	13.11341	.15941	13.11341	.15942
.90009	11.75475	11.40323	.35152	11.44504	.30972	11.44397	.31079	12.00221	-.24746
1.05011	10.43029	10.34628	.08400	10.37212	.05817	10.37278	.05750	9.46952	.96076
1.20012	9.89947	10.34628	-.44681	10.32045	-.42097	10.32111	-.42163	11.22436	-1.32489
1.35014	11.26240	11.40323	-.14082	11.36142	-.09902	11.36035	-.09795	10.80211	.46029
1.50015	13.21000	13.11341	.09659	13.11341	.09659	13.11341	.09659	13.11340	.09660
SUM ABS VALUE OF DIFFERENCE =			2.06426		2.06427		2.06427		6.33043
MEAN DEVIATION =			.18766		.18766		.18766		.57549
STANDARD DEVIATION =			.22802		.22564		.22568		.69315

COEFFICIENTS CORRESPONDING TO COSINE SERIE AND VELOCITIES CALCULATED WITH THEM

B1 = B(2,1) = -.1863762   B2 = B(2,2) = .1219837

B3 = B(2,3) = .1186688   B4 = B(2,4) = .0164770

TIME	UEXP	U(2,1,I)	D(2,1,I)	U(2,2,I)	D(2,2,I)	U(2,3,I)	D(2,3,I)	U(2,4,I)	U(2,4,I)
0.00000	13.21000	12.92703	.28297	13.04902	.16098	13.16769	.04231	13.18416	.02584
.15002	14.72936	12.96263	1.76673	13.00032	1.72903	12.96365	1.76570	12.95032	1.77903
.30003	15.56660	13.05582	2.51079	12.95713	2.60947	12.86113	2.70548	12.86622	2.70039
.45005	15.89612	13.17100	2.72511	13.07232	2.82380	13.16832	2.72780	13.17341	2.72271
.60006	15.08836	13.26419	1.82417	13.30189	1.78647	13.33856	1.74980	13.32523	1.76313
.75008	13.27283	13.29979	-.02696	13.42177	-.14895	13.30310	-.03028	13.31958	-.04675
.90009	11.75475	13.26419	-1.50944	13.30189	-1.54714	13.33856	-1.58381	13.32523	-1.57048
1.05011	10.43029	13.17100	-2.74072	13.07232	-2.64203	13.16832	-2.73804	13.17341	-2.74313
1.20012	9.89947	13.05582	-3.15635	12.95713	-3.05766	12.86113	-2.96165	12.86622	-2.96675
1.35014	11.26240	12.96263	-1.70022	13.00032	-1.73792	12.96365	-1.70125	12.95032	-1.68792
1.50015	13.21000	12.92703	.28297	13.04902	.16098	13.16769	.04231	13.18416	.02584

	D(2,1,I)	D(2,2,I)	D(2,3,I)	U(2,4,I)
SUM ABS VALUE OF DIFFERENCE =	18.52641	18.40443	18.04842	18.03195
MEAN DEVIATION =	1.68422	1.67313	1.64077	1.63927
STANDARD DEVIATION =	1.97676	1.97212	1.96828	1.96848

APPENDIX 2.5.3

PROGRAM R-10

PIPELINE CONEYING PROJECT. MCMASTER UNIVERSITY, HAMILTON, CANADA.
SUPERVISORS DR. M. BAIRD, CH. ENG., AND DR. G. ROUND, MECH. ENG.
PROGRAMMER GEORGE CARDENAS. CHEMICAL ENGINEERING DEPARTMENT.

THIS PROGRAM WILL EVALUATE IN PART ONE THE FOURIERS COEFFICIENTS AND VELOCITIES FROM AN EXPERIMENTAL SET OF VELOCITY AND TIME VALUES. IN PART TWO WILL CALCULATE VELOCITIES ACCORDING WITH THE SINOUSOIDAL MODEL. IN PART THREE WIL COMPUTE PRESSURE DROPS ACCORDING WITH DIFFERENT MODELS. IN PART FOUR WILL PLOT THE EXPERIMENTAL DATA. EVENTUALLY A FIFTH PART CAN BE ADDED IN ORDER TO PUNCH THE DATA CALCULATED.

EACH EXPERIMENTAL POINT IS EXPRESSED IN TERMS OF VELOCITY, TIME AND PRESSURE DROP RESPECTIVELY. THE NUMBER OF EXPERIMENTAL POINTS OF EACH SET OF DATA MUS CORRESPOND TO A COMPLETE PERIOD AND MUST ALWAYS BE AN ODD NUMBER (THE MAXIMU NUMBER CAN BE 91). THE TIME INTERVAL BETWEEN SUCCESIVE TIME VALUES MUST BE CONSTANT.
THE ARRANGEMENT OF EACH SET OF DATA IS AS FOLLOW
1.- ONE CARD WITH THE CONDITIONS OF THE RUN
2.- THE SET OF EXPERIMENTAL POINTS
3.- THE IDENTIFICATION CARDS OF THE GRAPHS
4.- A CONTROL CARD. IF IT IS EQUALS ONE ANOTHER COMPLETE SET OF DATA MUST FOLLOW. IF IT IS NOT EQUALS ONE THE PROGRAM WILL EXIT.

GLOSSARY OF PRINCIPAL SYMBOLS.
AREA = TRANSVERSAL SECTION OF THE PIPE, SQ.FEET.
ALENGT = LENGTH OF THE PIPE, FEET.
AMPL = AMPLITUDE, FEET.
DP = PRESSURE DROP, PSI.
DIA = DIAMETER OF PIPE, FEET.
DPEXP = EXPERIMENTAL PRESSURE DROP, PSI.
DVIS = DYNAMIC VISCOSITY OF THE FLUID, POUND.SEC/SQ.FEET.
DERIV = DERIVATE OF VELOCITY RESPECT TO TIME.
FACTOY, FACTOX, FACTOZ = CONVERSION FACTORS FOR VELOCITY, TIME AND PRESSURE DRP FROM EXPERIMENTAL UNITS TO FEET/SEC, SEC AND PSI.
FRE = FRECUENCY, 1/SEC.
F = FRICTION FACTOR
N = NUMBER OF EXPERIMENTAL POINTS.
RHO = DENSITY OF FLUID, POUND/CU.FEET.
RN = NUMBER OF THE EXPERIMENTAL RUN.
T = TIME, SEC.
UAVER = AVERAGE VELOCITY, FEET/SEC.
UEXP = EXPERIMENTAL VELOCITY, FEET/SEC.
USIN = VELOCITY CALCULATED ACCORDING WITH SINOUSOIDAL MODEL, FEET/SEC.
U(L,M,I) = VELOCITY CALCULATED ACCORDING WITH FOURIERS MODEL, FEET/SEC.
XI, YI, ZI = EXPERIMENTAL COORDINATES FOR TIME, VELOCITY AND PRESSURE DROP.

```
    DIMENSION XI(51), YI(51), ZI(51), T(51), UEXP(51), DPEXP(51),
   1XX(51), FT(51), B(5,5), SDI(5,5), DIFSQ(5,5), AMEAN(5,5),
   1STAND(5,5), U(5,5,51), D(5,5,51)
    DIMENSION USIN(21), DIFER(21)
    DIMENSION SDIFF(10), SDIFFS(5), UAUX(10,21), DERIV(100), DP(10,21)
   1, DIFF(10,21), ZMEAN(10), ZSTAND(10)
```

```
      DIMENSION  TT(100), UA(100), DPB(100)
      READ EXPERIMENTAL DATA. CONVERSION TO CONVENTIONAL UNITS.
    1 READ(5,10) N, RN, FRE, AMPL, UAVER, FACTOX, FACTOY, FACTOZ
   10 FORMAT(I5, F5.0, 6F10.0)
      K = N - 1
      DO  30  I = 1,N
      READ(5,20) XI(I), YI(I), ZI(I)
   20 FORMAT(3F15.0)
      T(I) = FACTOX*(1.0/(FRE*FLOAT(K)))*XI(I)
      UEXP(I) = FACTOY*(0.70876/2.12)*YI(I) + UAVER
      DPEXP(I) = FACTOZ*ZI(I)
   30 CONTINUE
      WRITE(6,40) RN
      WRITE(6,50)
      WRITE(6,60)
      WRITE(6,70)
      WRITE(6,80) AMPL
      WRITE(6,90) FRE
      WRITE(6,95) UAVER
      WRITE(6,100) N
      WRITE(6,110) FACTOX, FACTOY, FACTOZ
      WRITE(6,120)
   40 FORMAT(1H1, 35X, * RESULTS OF RUN NUMBER*, 1X, F4.0)
   50 FORMAT(1H , 34X,                                    ,////)
   60 FORMAT(1H , 14X, *EXPERIMENTAL CONDITIONS*)
   70 FORMAT(1H , 14X,                               ,/)
   80 FORMAT(1H , 31X, *AMPLITUDE (FEET) = *, F7.5)
   90 FORMAT(1H , 31X, *FRECUENCY (1/SEC) = *, F7.5)
   95 FORMAT(1H , 31X, *AVERAGE VELOCITY (FEET/SEC) = *, F9.5)
  100 FORMAT(1H , 31X, *NUMBER OF EXPERIMENTAL POINTS = *, I3, /)
  110 FORMAT(1H , 14X, 9HFACTOX = , F9.5, 6X, 9HFACTOY = , F9.5, 6X,
     19HFACTOZ = , F9.5)
  120 FORMAT(1H , ///, 9X,


      ************************************************************************
      PART ONE.- EVALUATION OF FOURIERS COEFFICIENTS FOR THE FOLLOWING MODEL

      U = AO + A1*SIN(X) + A2*SIN(2X) + A3*SIN(3X) + A4*SIN(4X) + B1*COS(X)
           + B2*COS(2X) + B3*COS(3X) + B4*COS(4X)

      EVALUATION OF THE INDEPENDENT COEFFICIENT AO. THE SIMPSONS RULE IS USED
      IN ORDER TO EVALUATE THE CORRESPONDING INTEGRAL.
      SUM4 = 0.0
      SUM2 = 0.0
      J = N - 3
      H IS THE CONSTANT TIME INTERVAL
      H = (T(N) - T(1))/FLOAT(K)
      DO 200  I = 2,J,2
      SUM4 = SUM4 + UEXP(I)
      SUM2 = SUM2 + UEXP(I+1)
  200 CONTINUE
      AO = FRE*((H/3.0)*(UEXP(1) + 4.0*(SUM4 + UEXP(K)) + 2.0*SUM2 +
     1UEXP(N)))
      EVALUATION OF COEFFICICIENTS CORRESPONDING TO SINE AND COSINE SERIES.
      M IS THE SUBSCRIPT OF THE FOURIERS COEFFICIENT.
      L = 1
  210 M = 1
```

```
220 SUM4 = 0.0
    SUM2 = 0.0
    DO 240  I = 1,N
    XX(I) = FLOAT(M)*2.0*3.141592*FRE*T(I)
    IF(L.EQ.2) GO TO 230
    FT(I) = UEXP(I)*SIN(XX(I))
    GO TO 240
230 FT(I) = UEXP(I)*COS(XX(I))
240 CONTINUE
    DO 250  I = 2,J,2
    SUM4 = SUM4 + FT(I)
    SUM2 = SUM2 + FT(I+1)
250 CONTINUE
    B(L,M) = 2.0*FRE*((H/3.0)*(FT(1) + 4.0*(SUM4 + FT(N)) + 2.0*SUM2
   1+ FT(N)))

    EVALUATION OF VELOCITIES.
    DIFSQ(L,M) = 0.0
    SDI(L,M) = 0.0
    DO 300  I = 1,N
    IF(L.EQ.2) GO TO 260
    UTRANS = B(L,M)*SIN(XX(I))
    GO TO 270
260 UTRANS = B(L,M)*COS(XX(I))
270 IF(M.EQ.1) GO TO 280
    U(L,M,I) = U(L,M-1,I) + UTRANS
    GO TO 290
280 U(L,M,I) = AO + UTRANS
290 D(L,M,I) = UEXP(I) - U(L,M,I)
    SDI(L,M) = SDI(L,M) + ABS(D(L,M,I))
    DIFSQ(L,M) = DIFSQ(L,M) + (D(L,M,I))**2
300 CONTINUE
    AMEAN(L,M) = (SDI(L,M))/FLOAT(N)
    STAND(L,M) = SQRT((DIFSQ(L,M))/FLOAT(N))
    IF(M.EQ.4) GO TO 310
    M = M + 1
    GO TO 220
310 L = L + 1
    IF(L.EQ.3) GO TO 320
    GO TO 210
320 M = 1
330 SDI(L,M) = 0.0
    DIFSQ(L,M) = 0.0
340 DO 350  I = 1,N
    U(L,M,I) = U(L-2,M,I) + U(L-1,M,I) - AO
    D(L,M,I) = UEXP(I) - U(L,M,I)
    SDI(L,M) = SDI(L,M) + ABS(D(L,M,I))
    DIFSQ(L,M) = DIFSQ(L,M) + (D(L,M,I))**2
350 CONTINUE
    AMEAN(L,M) = (SDI(L,M))/FLOAT(N)
    STAND(L,M) = SQRT((DIFSQ(L,M))/FLOAT(N))
    IF(M.EQ.4) GO TO 360
    M = M + 1
    GO TO 330
360 WRITE(6,370) AO
    WRITE(6,380)
    WRITE(6,390)
    WRITE(6,400)
```

```
      WRITE(6,410) B(1,1), B(1,2)
      WRITE(6,420) B(1,3), B(1,4)
      WRITE(6,430)
      WRITE(6,440)
      DO 460  I= 1,N
      WRITE(6,450) T(I), UEXP(I), U(1,1,I), D(1,1,I), U(1,2,I), D(1,2,I)
     1, U(1,3,I), D(1,3,I), U(1,4,I), D(1,4,I)
  460 CONTINUE
      WRITE(6,470) SDI(1,1), SDI(1,2), SDI(1,3), SDI(1,4)
      WRITE(6,480) AMEAN(1,1), AMEAN(1,2), AMEAN(1,3), AMEAN(1,4)
      WRITE(6,490) STAND(1,1), STAND(1,2), STAND(1,3), STAND(1,4)
      WRITE(6,500)
      WRITE(6,400)
      WRITE(6,510) B(2,1), B(2,2)
      WRITE(6,520) B(2,3), B(2,4)
      WRITE(6,530)
      WRITE(6,440)
      DO 540  I = 1,N
      WRITE(6,450) T(I), UEXP(I), U(2,1,I), D(2,1,I), U(2,2,I), D(2,2,I)
     1,U(2,3,I), D(2,3,I), U(2,4,I), D(2,4,I)
  540 CONTINUE
      WRITE(6,470) SDI(2,1), SDI(2,2), SDI(2,3), SDI(2,4)
      WRITE(6,480) AMEAN(2,1), AMEAN(2,2), AMEAN(2,3), AMEAN(2,4)
      WRITE(6,490) STAND(2,1), STAND(2,2), STAND(2,3), STAND(2,4)
      WRITE(6,550)
      WRITE(6,400)
      WRITE(6,560)
      WRITE(6,440)
      DO 570  I = 1,N
      WRITE(6,450) T(I), UEXP(I), U(3,1,I), D(3,1,I), U(3,2,I), D(3,2,I)
     1, U(3,3,I), D(3,3,I), U(3,4,I), D(3,4,I)
  570 CONTINUE
      WRITE(6,470) SDI(3,1), SDI(3,2), SDI(3,3), SDI(3,4)
      WRITE(6,480) AMEAN(3,1), AMEAN(3,2), AMEAN(3,3), AMEAN(3,4)
      WRITE(6,490) STAND(3,1), STAND(3,2), STAND(3,3), STAND(3,4)
  370 FORMAT(1H ,///, X, *INDEPENDENT COEFFICIENT          A0 = *, F12.7)
  380 FORMAT(1H , X,                                      , ///)
  390 FORMAT(1H , *COEFFICIENTS CORRESPONDING TO SINE SERIE AND VELOCITI
     1ES CALCULATED WITH THEM*)
  400 FORMAT(1H ,

  410 FORMAT(1H ,/, 5X, *A1 = B(1,1) = *, F15.7, 15X, *A2 = B(1,2) = * ,
     1F15.7)
  420 FORMAT(1H , /, 5X, *A3 = B(1,3) = *, F15.7, 15X, *A4 = B(1,4) = *
     1, F15.7)
  430 FORMAT(1H ,//, 7X, *TIME          UEXP      U(1,1,I)    D(1,1,I)    U(1,2
     1,I)    D(1,2,I)    U(1,3,I)    D(1,3,I)    U(1,4,I)    D(1,4,I)*)
  440 FORMAT(1H , 6X,

  450 FORMAT(1H , 10F11.5)
  470 FORMAT(1H ,/,X, *SUM ABS VALUE OF DIFFERENCE = *, 2X, F11.5, 3F22.
     15)
  480 FORMAT(1H , /, 11X, *MEAN DEVIATION = *, 6X, F11.5( 3F22.5)
  490 FORMAT(1H ,/, 7X, *STANDARD DEVIATION = *, 6X, F11.5, 3F22.5)
  500 FORMAT(1H1, /,X, *COEFFICIENTS CORRESPONDING TO COSINE SERIE AND V
     1ELOCITIES CALCULATED WITH THEM*)
  510 FORMAT(1H ,/, 5X, *B1 = B(2,1) = *, F15.7, 15X, *B2 = B(2,2) = *,
     1F15.7)
```

```
520 FORMAT(1H , //, 5X, *B3 = B(2,3) = *, F15.7, 15X, *B4 = B(2,4) = *
   1, F15.7)
530 FORMAT(1H , //, 7X, *TIME          UEXP     U(2,1,I)    D(2,1,I)    U(2,
   12,I)    D(2,2,I)    U(2,3,I)    D(2,3,I)    U(2,4,I)    D(2,4,I)*)
550 FORMAT(1H1, //, X, *VELOCITIES CALCULATED USING TERMS OF BOTH COSI
   1NE AND SINE SERIES*)
560 FORMAT(1H ,/, 6X, *TIME          UEXP     U(3,1,I)    D(3,1,I)    U(3,2,
   1I)    D(3,2,I)    U(3,3,I)    D(3,3,I)    U(3,4,I)    D(3,4,I)*)

    PART TWO.-  ****************************************************************
    CALCULATION OF VELOCITY ACCORDING WITH SINOUSOIDAL MODEL AND EXPERIMENTAL
    CONDITIONS OF THE RUN.
600 SDIFER = 0.0
    SDIFSQ = 0.0
    W = 2.0*3.141592*FRE
    DO 610  I = 1,N
    USIN(I) = UAVER + W*AMPL*SIN(W*T(I))
    DIFER(I) = UEXP(I) - USIN(I)
    SDIFER = SDIFER + ABS(DIFER(I))
    SDIFSQ = SDIFSQ + (DIFER(I))**2
610 CONTINUE
    XMEAN = SDIFER/FLOAT(N)
    XSTAND = SQRT(SDIFSQ/FLOAT(N))

    COMPARATION BETWEEN EXPERIMENTAL FACTOR A1 AND UPRIM.
    UPRIM = W*AMPL
    XDIF = UPRIM - B(1,1)
    WRITE(6,620)
    WRITE(6,630)
    WRITE(6,640) UPRIM, XDIF
    WRITE(6,650)
    WRITE(6,660)
    DO 680  I = 1,N
    WRITE(6,670) UEXP(I), T(I), USIN(I), DIFER(I)
680 CONTINUE
    WRITE(6,690) SDIFER
    WRITE(6,700) XMEAN
    WRITE(6,710) XSTAND
620 FORMAT(1H1, *  CALCULATION OF VELOCITY ACCORDING WITH SINOUSOIDAL
   1MODEL AND EXPERIMENTAL CONDITIONS OF THE RUN*)
630 FORMAT(1H ,

640 FORMAT(1H , 2X, *UPRIM = *, F8.5, 10X, *XDIF = UPRIM - A1 = *,
   1F8.6, //)
650 FORMAT(1H ,
   1 USIN
660 FORMAT(1H ,                                                          -

670 FORMAT(1H , 4F20.5)
690 FORMAT(1H ,/, 40X, *SUM ABS VALUE OF DIFFERENCE = *, F11.5)
700 FORMAT(1H , /, 52X, *MEAN DEVIATION = *, F11.5)
710 FORMAT(1H ,/,48X, *STANDARD DEVIATION = *, F11.5)

    PART THREE. ****************************************************************
    EVALUATION OF PRESSURE DROP USING EULERS EQUATION AND THE FOLLOWING VELOC
    TY MODELS.
       A.-  EXPERIMENTAL VELOCITY (K=1)
       B.- U = A0 + A1*SIN(X) + A2*SIN(2X) + B1*COS(X) + B2*COS(2X)   (K=2)
```

```
        C.- U = AO + A1*SIN(X)      (K=3)
        D.- U = UAVER + UPRIM*SIN(X)    (K=4)
      K = 1
  800 SDIFF(K) = 0.0
      SDIFFS(K) = 0.0
      DO 850  I = 1,N
      IF(K.EQ.1) UAUX(K,I) = UEXP(I)
      IF(K.EQ.2) UAUX(K,I) = U(3,2,I)
      IF(K.EQ.3) UAUX(K,I) = U(1,1,I)
      IF(K.EQ.4) UAUX(K,I) = USIN(I)
      DIMENSION OF APPARATUS AND PROPERTIES OF THE FLUID.
      DIA = 0.1667
      ALENGT = 31.6666
      RHO = 62.4
      DVIS = 0.0000324
      REYNOLDS NUMBER EVALUATION.
      RE = ABS(DIA*UAUX(K,I)*RHO/(DVIS*32.174))
      EVALUATION OF INSTANTANEOUS FRICTION FACTOR ACCORDING WITH EQUATION DETER-
      MINED EXPERIMENTALLY (VON KARMAN-PRANDTL MODEL). THE RAPHSON-NEWTON INTE
      ATION METHOD IS USED FOR SOLVE THE EQUATION.
      AA = -19.0226202
      BB = 2.8236854
      F = 0.000800
      R IS A COUNT OF THE NUMBER OF INTERATIONS
      R = 1.0
  810 PRO = RE*SQRT(F)
      FNEW = F - (1.0/SQRT(F) - BB*ALOG(PRO) - AA)*(2.0*F*SQRT(F))/
     1(-1.0 - BB*SQRT(F))
      IF(ABS(F-FNEW).LT.1.E-6.OR.R.GT.50.0) GO TO 820
      R = R + 1.0
      F = FNEW
      GO TO 810
  820 IF(K.GT.2) GO TO 830
      DERIV(I) = B(1,1)*W*COS(W*T(I)) + B(1,2)*2.0*W*COS(2.0*W*T(I))
     1- B(2,1)*W*SIN(W*T(I)) - B(2,2)*2.0*W*SIN(2.0*W*T(I))
      GO TO 840
  830 IF(K.EQ.4) B(1,1) = UPRIM
      DERIV(I) = B(1,1)*W*COS(W*T(I))
  840 DP(K,I) = (DERIV(I) + F*(UAUX(K,I))**2/(2.0*DIA))*(ALENGT*RHO)/
     1(32.174*144.0)
      DIFF(K,I) = DPEXP(I) - DP(K,I)
      SDIFF(K) = SDIFF(K) + ABS(DIFF(K,I))
      SDIFFS(K) = SDIFFS(K) + (DIFF(K,I))**2
  850 CONTINUE
      ZMEAN(K) = (SDIFF(K))/FLOAT(N)
      ZSTAND(K) = SQRT((SDIFFS(K))/FLOAT(N))
      K = K + 1
      IF(K.EQ.5) GO TO 860
      GO TO 800
  860 WRITE(6,870)
      WRITE(6,890)
      WRITE(6,900)
      WRITE(6,910)
      WRITE(6,920)
      WRITE(6,930)
      WRITE(6,940)
      WRITE(6,950)
      DO 970  I = 1,N
```

```
      WRITE(6,960) T(I), DPEXP(I), DP(1,I), DIFF(1,I), DP(2,I), DIFF(2,I
     1), DP(3,I), DIFF(3,I), DP(4,I), DIFF(4,I)
  970 CONTINUE
      WRITE(6,980) SDIFF(1), SDIFF(2), SDIFF(3), SDIFF(4)
      WRITE(6,990) ZMEAN(1), ZMEAN(2), ZMEAN(3), ZMEAN(4)
      WRITE(6,999) ZSTAND(1), ZSTAND(2), ZSTAND(3), ZSTAND(4)
  870 FORMAT(1H1, 2X, *PRESSURE DROP (DP) RESULTS USING EULERS EQUATION
     1AND THE FOLLOWING VELOCITY MODELS*)
  890 FORMAT(1H ,

  900 FORMAT(1H ,//,4X, * A.- EXPERIMENTAL VELOCITY*)
  910 FORMAT(1H ,3X, * B.- U = A0 + A1SIN(X) + A2SIN(2X) + B1COS(X) + B2
     1COS(2X)*)
  920 FORMAT(1H ,3X, * C.- U = A0 + A1SIN(X)*)
  930 FORMAT(1H ,3X, * D.- U = UAVER + UPRIMSIN(X)*)
  940 FORMAT(1H ,///, *          TIME       DPEXP          DP(A)     DIF(A)
     1    DP(B)        DIF(B)         DP(C)        DIF(C)         DP(D)         DIF
     1(D)*)
  950 FORMAT(1H ,5X,

  960 FORMAT(1H , 2F11.5, 8F12.5)
  980 FORMAT(1H ,/,X, *SUM ABS VALUE OF DIFFERENCE = *, F14.5, 12X,
     1F12.5, 12X, F12.5, 12X, F12.5)
  990 FORMAT(1H ,/,14X, *MEAN DEVIATION = *,F14.5, 12X, F12.5, 12X,
     1F12.5, 12X, F12.5)
  999 FORMAT(1H ,/,10X, *STANDARD DEVIATION = *, F14.5, 12X, F12.5, 12X,
     1F12.5, 12X, F12.5)

C
C     PART FOUR.- PLOTING THE DIFFERENT PARAMETERS.- ***********************
C     STORING 50 POINTS FOR A CONTINUOUS CURVE USING THE FOURIERS 4 TERMS VELOCI
C     MODEL. (MODEL B).
      PERIOD = 1.0/FRE
      DT = PERIOD/50.0
      I = 1
      TT(I) = 0.0
 1000 X = W*TT(I)
      UA(I) = A0 + B(1,1)*SIN(X) + B(1,2)*SIN(2.0*X) + B(2,1)*COS(X) +
     1B(2,2)*COS(2.0*X)
      DERIV(I) = B(1,1)*W*COS(X) + B(1,2)*2.0*W*COS(2.0*X) - B(2,1)*W*
     1SIN(X) - B(2,2)*2.0*W*SIN(2.0*X)
      RE = ABS(DIA*UA(I)*RHO/(DVIS*32.174))
      F = 0.000800
 1010 PRO = RE*SQRT(F)
      FNEW = F - (1.0/SQRT(F) - BB*ALOG(PRO) - AA)*(2.0*F*SQRT(F))/
     1(-1.0 - BB*SQRT(F))
      IF(ABS(F-FNEW).LT.1.E-6) GO TO 1020
      F = FNEW
      GO TO 1010
 1020 DPB(I) = (DERIV(I) + F*(UA(I))**2/(2.0*DIA))*(ALENGT*RHO)/(32.174
     1*144.0)
      IF(TT(I).GT.PERIOD) GO TO 1030
      I = I + 1
      TT(I) = TT(I-1) + DT
      GO TO 1000
C
C     FIGURE ONE. VELOCITY VS. TIME
 1030 DO 1040  I = 1,50
```

```
      CALL PLOTPT(TT(I), UA(I), 4)
 1040 CONTINUE
      DO 1050  I = 1,N
      CALL PLOTPT(T(I), UEXP(I), 44)
      CALL PLOTPT(T(I), U(1,1,I), 23)
      CALL PLOTPT(T(I), USIN(I), 24)
 1050 CONTINUE
      CALL OUTPLT
      CALL COPYCD
C
C     FIGURE TWO.  PRESSURE DROP VS. TIME.
      DO 1060  I = 1,50
      CALL PLOTPT(TT(I), DPB(I), 4)
 1060 CONTINUE
      DO 1070  I = 1,N
      CALL PLOTPT (T(I), DPEXP(I), 44)
      CALL PLOTPT (T(I), DP(3,I), 23)
      CALL PLOTPT (T(I), DP(4,I), 24)
 1070 CONTINUE
      CALL OUTPLT
      CALL COPYCD
C
C     FIGURE THREE. PRESSURE DROP VS. VELOCITY.
      DO 1080  I = 1,50
      CALL PLOTPT (UA(I), DPB(I), 4)
 1080 CONTINUE
      DO 1090  I = 1,N
      CALL PLOTPT (UEXP(I), DPEXP(I), 44)
      CALL PLOTPT (U(1,1,I), DP(3,I), 23)
      CALL PLOTPT(USIN(I), DP(4,I), 24)
 1090 CONTINUE
      CALL OUTPLT
      CALL COPYCD
C
C     FIGURE FOUR.  EXPERIMENTAL PRESSURE DROP VS. CALCULATED PRESSURE DROP.
      DO 1100  I = 1,N
      CALL PLOTPT (DP(2,I), DPEXP(I), 4)
      CALL PLOTPT (DP(3,I), DPEXP(I), 23)
      CALL PLOTPT (DP(4,I), DPEXP(I), 24)
 1100 CONTINUE
      CALL OUTPLT
      CALL COPYCD
C
C     FIGURE FIVE. EXPERIMENTAL VELOCITY VS. CALCULATED VELOCITY.
      DO 1110  I = 1,N
      CALL PLOTPT (U(3,2,I), UEXP(I), 4)
      CALL PLOTPT (U(1,1,I), UEXP(I), 23)
      CALL PLOTPT (USIN(I), UEXP(I), 24)
 1110 CONTINUE
      CALL OUTPLT
      CALL COPYCD
C
C     FIGURE SIX.  DU/DT VS. TIME.
      DO 1120  I = 1,50
      CALL PLOTPT (TT(I), DERIV(I), 2)
 1120 CONTINUE
      CALL OUTPLT
      CALL COPYCD
```

```
C
C       END IS A CONTROL CARD.
        READ(5,1200) END
 1200   FORMAT(F5.0)
        IF(END.EQ.1.0) GO TO 1
        END
```